HEINRICH HEINE
UNIVERSITÄT DÜSSELDORF

The role of the PsbS protein in high light acclimation of the
green alga *Chlamydomonas reinhardtii*

Inaugural-Dissertation

For attaining the title of Doctor (Dr. rer. nat.)
in the Faculty of Mathematics and Natural Sciences
at Heinrich-Heine-Universität Düsseldorf

Presented by

Petra Redekop

From Bielefeld, Germany

Düsseldorf, January 2019

From the Institute of Plant Biochemistry,
Heinrich-Heine-Universität Düsseldorf

Printed with permission from the Faculty of Mathematics and Natural Sciences,
Heinrich Heine University Düsseldorf

Supervisor: apl. Prof. Dr. Peter Jahns

Co-Supervisor: Prof. Dr. Andreas Weber

Date of Oral Examination: March 8th, 2019

STATEMENT OF DECLARATION

I, Petra Redekop, hereby declare that I have fully and independently written the submitted dissertation without additional unauthorized support and consultation beyond that permitted and specified in the dissertation to include the necessary and appropriate cited literary resources. The dissertation in its present or similar form has not been previously submitted under the same or otherwise specified institution and department name. Previous unsuccessful oral examinations have not been registered or attempted.

Düsseldorf, January 28th, 2019

Table of Contents

1 Introduction

1.1 The model organism *Chlamydomonas reinhardtii*

The unicellular algae *Chlamydomonas reinhardtii* (*C. reinhardtii*) represents an ideal model organism for research on photosynthesis and chloroplast biogenesis (Rochaix, 1995) as it goes through a simple life cycle, allows easy generation of mutants and offers a fast reproduction rate. The alga belongs to the division of Chlorophyta (class: Chlorophyceae), whose arrangement of cilia further defines it as being part of the order of Chlamydomonadales. The average cell length of the elliptic body is approximately 10µm (Rochaix, 2001), and two anterior located cilia are responsible for motility. The direction of movement is controlled by the carotenoid-containing eyespot that mediates phototaxis (Harris, 2001). A single cup-shaped chloroplast, which occupies about 40% of the cell (Hummel et al., 2012), signifies the center of oxygenic photosynthesis. The green alga cannot only grow photoautotrophically but also heterotrophically, e.g. in presence of acetate as the only carbon source. The carbon-concentrating mechanism (Wang et al., 2015) guarantees optimal CO_2 fixation at CO_2-limiting conditions by accumulating inorganic carbon inside the pyrenoid, where it is converted into CO_2 – the substrate for ribulose-1,5-bisphosphate carboxylase/oxygenase (RuBisCO), which is also located in the pyrenoid (Park et al., 1999).

1.2 The thylakoid membranes of the chloroplast

The chloroplast is a semi-autonomous organelle which is apparently derived from cyanobacteria (Cavalier-Smith, 2000). About 95% of chloroplast genes are nucleus encoded (Schleiff and Becker, 2011), but many multi-protein complexes such as the two photosystems contain both chloroplast and nucleus encoded subunits. The reactions of carbon fixation take place in the stroma and the pyrenoid, with carbon being actively transported and accumulated at the side of RubisCO. In contrast, light reactions and photosynthetic electron transport are catalyzed by protein complexes located in and at the thylakoid membrane. The chloroplast consists of two outer membranes that are remnants of endosymbiosis (McFadden and Gilson, 1995) and an inner thylakoid membrane system, which separates the inner thylakoid lumen from the outer stroma region. The thylakoid membrane can be arranged in stacked grana regions consisting of multiple thylakoid discs, and unstacked single lamellae regions (Fig. 1, Yamamoto, 2016). Depending on environmental light conditions, the membrane structure can be dynamically re-organized, so that grana stacks appear tightly stacked in the dark or lower light conditions and undergo unstacking and swelling as a result of light exposure. Embedded in the thylakoid membrane are multi-protein complexes which are running the photosynthetic electron and proton transport chain in order to synthesize ATP and NADPH through linear and cyclic electron flow (LEF and CEF, respectively) across the thylakoid membrane. The primary

light capturing reaction centers of photosystem II (PSII) and photosystem I (PSI) are physically separated as PSII and its light-harvesting complexes (LHCII) are located in the grana regions, while PSI is favorably located at the grana margins and stroma lamellae alongside with the ATP synthase, which are both excluded from the grana stacks due to their voluminous shape (Fig. 1, Andersson and Anderson, 1980; Danielsson et al., 2004). Exclusively the cytochrome b_6f (Cyt b_6f) complex is homogeneously distributed among grana and stroma lamellae (Anderson, 1992). Recent studies provided new insights into the interplay between dynamic thylakoid stacking, organization of protein complexes in the thylakoid membrane and its effects on balancing LEF and CEF during changing light environments in vascular plants and algae. Light exposure has particular impact on the macromolecular membrane organization and thylakoid membrane stacking through light-induced phosphorylation of PSII and LHCII (Puthiyaveetil et al., 2017; Wood et al., 2018). Wood and colleagues further proposed that light exposure of vascular plants results in a decrease of the grana diameter and a lower number of membrane layers per grana, while a higher number of grana stacks per chloroplast abets a larger contact area between stroma lamellae and grana (Fig. 1, Wood et al., 2018). Contrarily, in *C. reinhardtii*, a transient increase of grana thickness was observed during HL acclimation with a maximum of about 120nm after 10h HL exposure. Other effects of HL acclimation and resulting photoinhibition were found, including enhanced formation of palmelloids, with one palmelloid consisting of 5 cells. Additionally, increasing duration of HL exposure was found to lead to a rising number of non- functional cells. Cell death is known to be a result of the complete inhibition of the function of photosystems and their turnover (Yamamoto, 2016).

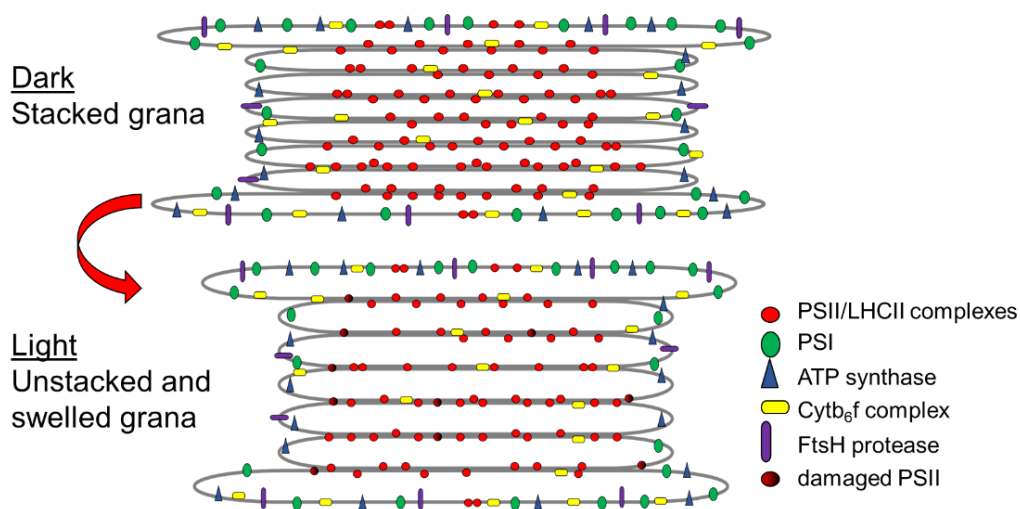**Figure 1: Unstacking of thylakoid grana as a result of light exposure.** PSII and LHCII (red circles) are localized in the grana stacks, Cyt b_6f complexes (yellow symbols) are equally distributed among grana and stroma region, whereas PSI, ATP synthase and FtsH proteases (green, blue and purple symbols respectively) are exclusively located at the stroma-exposed grana margins. Adapted from (Yamamoto et al., 2016).

1.3 Photosynthesis and the photosynthetic electron transport chain

The thylakoid membrane-localized photosynthetic electron transport chain drives electron transfer through three major transmembrane protein complexes: PSII, Cyt b_6f and PSI (Fig. 2). Plastoquinone (PQ) and plastocyanin (PC) are mobile electron carriers, which link the protein complexes (Hervás et al., 2003). Light-harvesting complexes (LHC) of PSII (LHCII) and PSI (LHCI) (Minagawa and Tokutsu, 2015) funnel photons into the luminal exposed reaction centers of PSII (P680) and PSI (P700). Excitation of P680 and P700 induces charge separation, which initiates stromal directed electron transfer from water to $NADP^+$ (Krauß et al., 1996). The electron gap at PSII is compensated by electrons originating from water oxidation at the lumen-localized oxygen-evolving complex (OEC) which is accompanied by proton release into the lumen (Fig. 2). Electrons from PSII are transferred from plastohydroquinone (PQH_2) – which is formed at the PSII acceptor side along with proton uptake from the stroma – to the lumen-localized PC. This reaction, which further releases protons into the lumen is catalyzed by Cyt b_6f. Charge separation in PSI enforces electron transfer from P700 to the stroma localized ferredoxin (Fd) at the PSI acceptor side. The electron gap in $P700^+$ is compensated by electrons transferred from PC to PSI. Electrons are finally funneled to ferredoxin-NADP reductase (FNR) which reduces $NADP^+$ to NADPH (Fig. 2). Coupled electron and proton transfer generates the proton motive force (pmf) across the thylakoid membrane, which is the driving force for the synthesis of ATP by the ATP synthase (Choquet and Vallon, 2000; Nelson and Junge, 2015). Electron transfer from water (lumen-localized donor side of PSII) to $NADP^+$ (stroma-localized acceptor side of PSI) is defined as LEF, which results in the generation of NADPH and ATP. Aside from LEF, another pathway termed CEF is defined as the recycling of electrons from Fd to PQ and thus only contributes to the generation of ATP, but not to the reduction of $NADP^+$ to NADPH (Joliot and Johnson, 2011). CEF is supposedly balancing the ATP/NADPH ratio by further accumulating protons in the lumen and hence driving ATP synthesis (Avenson et al., 2005). Moreover, CEF has been shown to contribute to the photoprotection of PSI (Suorsa et al., 2012). CEF is known to be accompanied by the dissociation of LHCA2 and LHCA9 from PSI-LHCI, when stromal electron carriers are reduced (Steinbeck et al., 2018). Hence, PSI-LHCI and Cyt b_6f may move closer together, which favors the formation of CEF supercomplexes (Fig. 4 C) and finally promoting CEF. The complete CEF supercomplex in *C. reinhardtii* consists of PSI, Cyt b_6f, ferredoxin–NADP–oxidoreductase (FNR), Anaerobic Response 1 (ANR1), Proton Gradient Regulation-Like 1 (PGRL1) and Calcium Sensor (CAS) (Steinbeck et al., 2018).
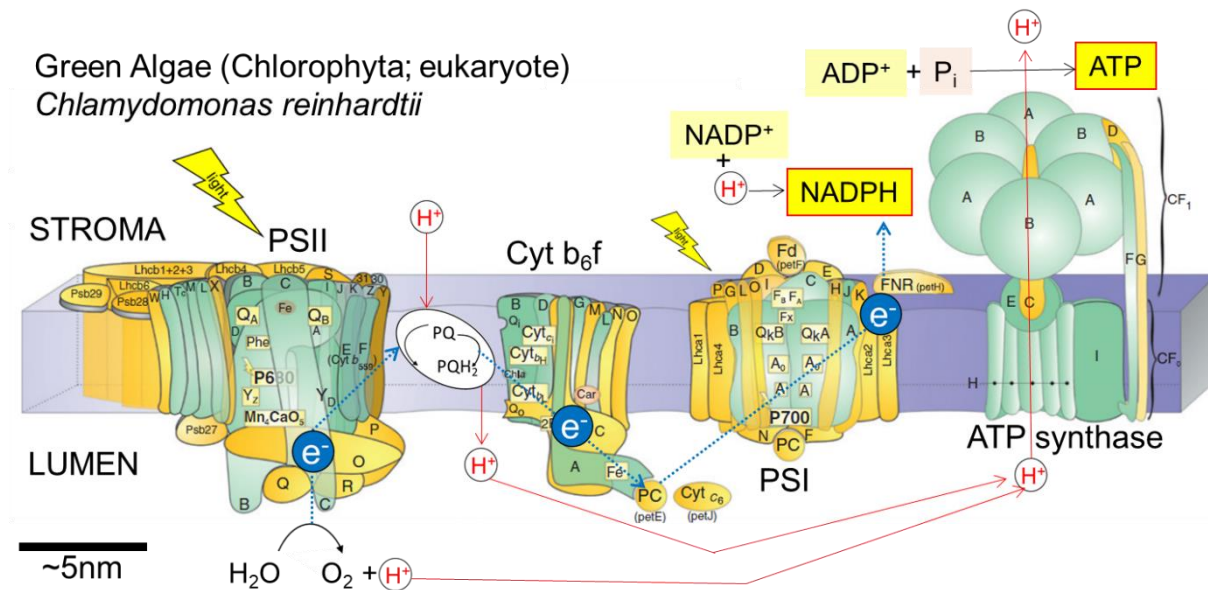
Figure 2: Photosynthetic electron and proton transport along the thylakoid membrane. Electrons are passing PSII, plastoquinone (PQ), Cyt b$_6$f, plastocyanin (PC) and PSI. PQ is reduced to plastohydroquinone (PQH$_2$) once electrons pass the electron carrier. Electrons are transferred from PSI to ferredoxin (Fd) and finally to the stromal located ferredoxin-NADP reductase (FNR). The electron acceptor NADP$^+$ is finally reduced to NADPH. Luminal directed proton flux generates a proton gradient required for ATP synthesis. Adapted after (Allen et al., 2011).

1.3.1 The PSII supercomplex

The functional PSII unit is organized as a 700kDa dimer. Each monomer consists of a reaction center (RC) heterodimer D1 (PSBA)/D2 (PSBD). 20 transmembrane and peripheral subunits, at least 20 lipids (Guskov et al., 2009), 35 chlorophylls, 11 β-carotenes (Telfer, 2002), 2 pheophytins, 2 plastoquinones, 1 heme iron, 1 non-heme iron, 4 manganese atoms, 1 bicarbonate ion, 4 calcium atoms and 3 Cl$^-$ ions are bound to one monomer (Umena et al., 2011). Furthermore, small subunits are associated with the PSII RC namely: PsbH/I/J/K/L/M/N/T/X/Z and the subunits PsbO/P/Q further stabilize the luminal localized OEC (Fig. 3, Ferreira et al., 2004; Barber, 2012). The PSII RC is surrounded by internal antenna proteins (CP43 and CP47) and external minor (monomer) and major (trimer) LHC antenna (Lhcb1-6). In chlorophyta like *C. reinhardtii*, the LHC proteins are differentiated in two minor and nine major LHC proteins whose function is to harvest light energy and to funnel the energy into the PSII RC. All LHCII proteins are nuclear encoded chlorophyll a/b binding proteins (Green et al., 1991). The minor LHCII proteins CP29 and CP26 are encoded by the genes *Lhcb4* and *Lhcb5*, respectively, whereas most vascular plants contain an additional minor antenna protein, CP24 (Lhcb6), which is missing in green algae (Minagawa and Takahashi, 2004), but also in some gymnosperms (Kouřil et al., 2016). The nine major LHC proteins are encoded by *LhcbM1–9* and are classified into the distinct types I-IV (Elrad and Grossman,

2004). Type I proteins are encoded by *LhcbM3/4/6/8/9*, type II is encoded by *LhcbM5* (Takahashi et al., 2006), *LhcbM2/7* encode for type III proteins and *LhcbM1* encodes for type IV proteins (Drop et al., 2014) with each protein having specific functions in light-harvesting (Teramoto et al., 2002). The organization of LHC proteins around the dimeric PSII reaction center (C_2) is well described. The binding characteristics of *C. reinhardtii* LHCII trimers to the PSII core define them as strongly (S) and moderately (M) bound trimers. Whereas in vascular plants another trimer is named loosely (L) bound, in *C. reinhardtii* an additional intrinsic component has been termed LHCII-N trimer and is supposed to substitute CP24 (Fig. 3, Drop et al., 2014). Typical PSII-LHCII supercomplexes are organized supposedly in a dimeric PSII reaction core center, which are associated with two LHCII-S trimers, two LHCII-M and two LHCII-N ($C_2S_2M_2N_2$), but other organizational forms such as C_2S_2MN, and/or C_2SMN supercomplexes have been described as well (Dekker and Boekema, 2005; Drop et al., 2014; Pagliano et al., 2014).
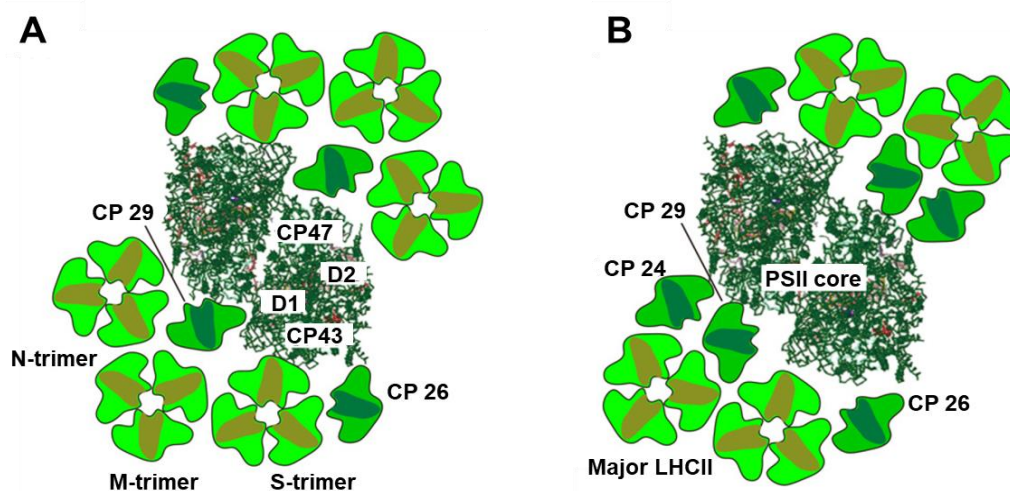

Figure 3: Organization of PSII–LHCII supercomplex. The model shows the top view from the luminal side of the complex in green algae (**A**) and vascular plants (**B**). Adapted after (Drop et al., 2014; Minagawa and Tokutsu 2015).

1.3.2 The PSI supercomplex

The current model of the PSI-LHCI SC in *C. reinhardtii* suggests an overall mass of about 700 kDa for this complex (Ozawa et al., 2010). It is organized as a monomer with two central proteins PsaA and PsaB forming a heterodimer. The RC contains a total of ten LHCI subunits (LHCA1-9), each binding 10 chlorophylls (Kargul et al., 2003), with two copies of LHCA1 and one copy each of the other subunits LHCA2-9 (Ozawa et al., 2018). The organization is probably as follows: four subunits (LHCA1/8/7/3) form the inner layer in contact with PsaG to PsaK which is strongly bound to PSI-LHCI at the side of PsaF (Fig. 4, Moseley et al., 2002; Ozawa et al., 2018). This organization is similar to that of LHCI in vascular plants, which, however, bind in total only four LHCI subunits, whereas a second layer of LHCI (LHCA1/4/6/5)

is arranged on top of the first layer in *C. reinhardtii*. This suggests a duplication of LHC proteins in PSI-LHCI in green algae in order to increase the antenna size (Ozawa et al., 2018). LHCA2 and LHCA9 localize between PsaH and PsaG, which are neither included in the first, nor in the second layer, but are located at the other side of the PSI core. The organization of LHCA2 and LHCA9 at PSI-LHCI SC is conserved in red algae (PSI-LHCR) as well, suggesting that it represents an early form of PSI-LHCI (Ozawa et al., 2018). This particular position of LHCA2 and LHCA9 is likely required to control the switch from LEF to CEF (Steinbeck et al., 2018). The proposed organization of the PSI-LHCI SC was recently supported by the 3D structure obtained from cryo EM analysis (Fig. 4 A, Kubota-Kawai et al., 2019).
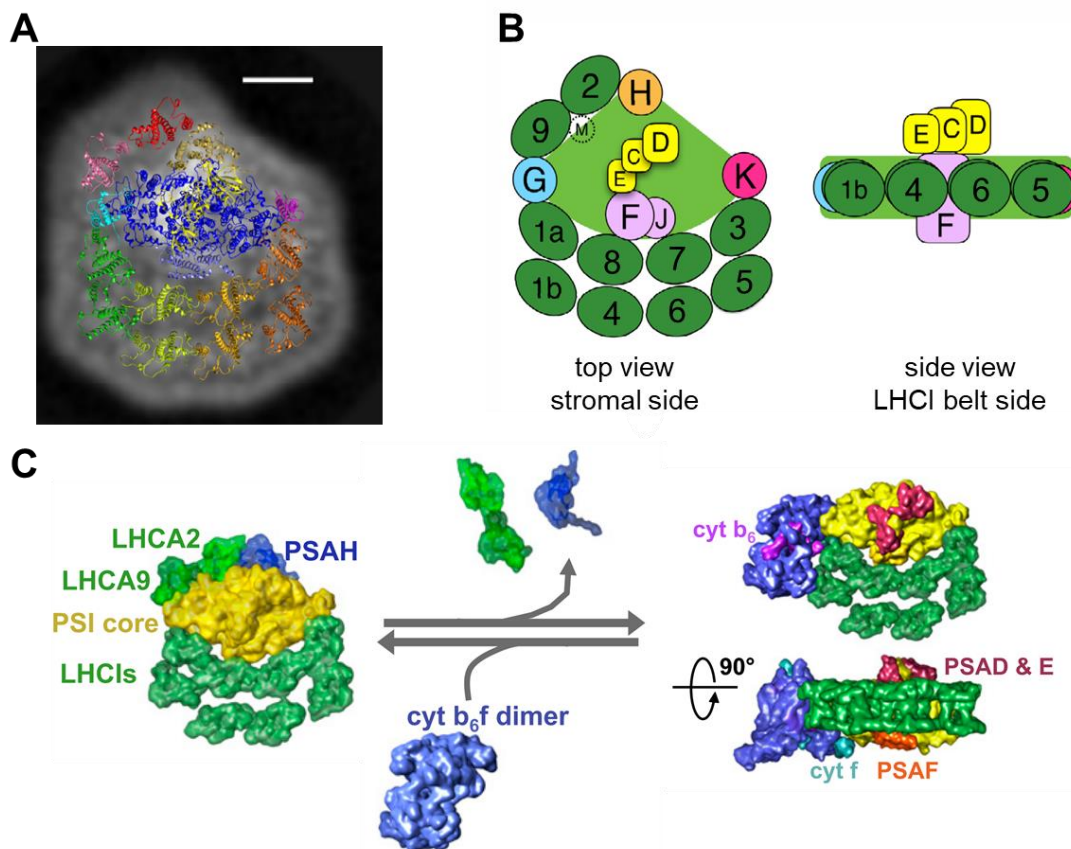

Figure 4: Model for the antenna organization in the PSI-LHCI supercomplex in *C. reinhardtii*. 2D projection map of single-particle cryo-EM of the PSI-LHCI supercomplex. (**A**) The crystal structure of the plant PSI-LHCI (PDB: 5L8R) and the model structures of LHCA2 and LHCA9 were overlaid on the projection maps of the PSI-LHCI from the 137c WT. (**B**) Schematic model of the PSI-LHCI supercomplex. The LHCI belt surrounds PSI in two layers. LHCI subunits (dark green) are numbered from 1-9 referring to Lhca1-9. PsaF and PsaJ (F and J, lilac), PsaG (G, cyan), PsaH (H, orange) and PsaK (K, pink) represent subunits of the PSI core complex, which is shown in light green. The figure is adapted from (Kubota-Kawai et al., 2019) and modified after (Ozawa et al., 2018; Steinbeck et al., 2018). (**C**) Model of the formation of the CEF supercomplex upon dissociation of LHCA2/9, and PSAH from PSI–LHCI. The PSI core is indicated in yellow, LHCI proteins in bright green, Cyt b_6f in purple. Plastocyanin- binding sites (cyt f, cyan and PSAF, orange) and ferredoxin- binding sites (PSAD/E, red and cyt b_6, pink) are indicated.

1.4 Acclimation to changing light intensities

Natural environments show a strong variation of light quantity and quality throughout the day and season. In particular, light intensities may vary in short periods (seconds to minutes) in order of magnitude, ranging from extremely high intensities of 2000µmol photons $m^{-2}s^{-1}$ at full sunlight to very low light intensities (< 20µmol photons $m^{-2}s^{-1}$) upon shading. Photosynthetic organisms must thus be able to adapt quickly to such variations to ensure optimal light utilization under all light conditions. Since light energy is the primary energy source for photosynthesis, most photosynthetic organisms are able to use efficiently very low light intensities, so that even moderate light intensities given under typical natural light conditions, already lead to the absorption of photons in excess of what can be utilized in photosynthesis (Erickson et al., 2015). Such excessively absorbed light energy, which cannot be used in photosynthetic electron transfer, accumulates in the light-harvesting antenna of PSII and PSI and is the major source for the undesired production of reactive oxygen species (ROS), which have a high potential of damaging proteins (including the photosystems), lipids and nucleic acids (Niyogi, 1999; Møller et al., 2007). ROS formation can be initiated by excess light either due to energy transfer from excited Chl molecules (leading to the formation of singlet oxygen, $^1O_2^*$) or due to electron transfer (leading to the formation of superoxide radicals ($O_2^{\cdot-}$) and in subsequent reactions to hydrogen peroxide (H_2O_2) and/or hydroxyl radicals ($OH^{\cdot}$)) (Møller et al., 2007). The formation of $^1O_2^*$ is predominantly initiated by absorption of excess light in the antenna of PSII, which increases the lifetime of excited chlorophylls ($^1Chl^*$) and favors the formation of long-living triplet Chl ($^3Chl^*$). $^3Chl^*$ transfers energy to O_2, resulting in the formation of highly reactive $^1O_2^*$ (Vass and Styring, 1993; Møller et al., 2007). Electron transfer to O_2 (and thus formation of $O_2^{\cdot-}$) occurs predominantly at PSI (Asada, 2006) in the so-called Mehler reaction (Mehler, 1951), but also in PSII (Pospíšil et al., 2004). $O_2^{\cdot-}$ can be effectively detoxified by conversion to H_2O_2, whereas highly reactive $^1O_2^*$ cannot. Consequently, $^1O_2^*$ represents the ROS molecule, which is predominantly responsible for photo-oxidative damage under *in vivo* conditions (Havaux et al., 2005; Triantaphylides et al., 2008). Plants and algae have evolved numerous short- and long-term acclimation strategies to either avoid or tolerate photo-oxidative damage mainly by reducing the formation of ROS (Li et al., 2009). Both, short- and long-term acclimation strategies are largely different in *C. reinhardtii* from those of vascular plants. An important short-term mechanism active at PSII, is the dissipation of excessive light energy as heat, termed non- photochemical quenching (NPQ) and will be described in detail in 1.4.1. The long-term high light (HL) acclimation of vascular plants generally takes days to weeks and involves the reduction of the photosynthetic antenna which results in less light absorption (Bailey et al., 2001) as well as the modification of carbon fixation (Schöttler and Toth, 2014) and of leaf architecture (Weston et al., 2000). Unlike sessile plants, which need to provide protection within seconds, motile green algae avoid light stress in the first place by

simply moving away. Not only their mobility, but also their short life cycle and hence the highly flexible metabolism give enough reason for differently organized short-term acclimation to HL (Cardol et al., 2011; Polukhina et al., 2016). Although dissipation of excess light energy is mainly regulated by the short-term HL acclimation in both vascular plants and green algae, there are major mechanistic differences such as different proteins required for efficient energy quenching, which will further be discussed below (section 1.4.2). Apart from NPQ, also the induction of CEF belongs to the short-term HL acclimation responses (Kukuczka et al., 2014), which additionally serves photoprotection by removing a surplus of electrons at the PSI acceptor side (Johnson et al., 2014).

1.4.1 Non - photochemical quenching (NPQ)

In *C. reinhardtii*, NPQ can only be efficiently activated after an initial HL acclimation period of several hours. NPQ consists of different mechanisms termed qE, qZ, qT, qI and qH that are active at different time periods in dependence of the light stress (Nilkens et al., 2010; Malnoë, 2018) in order to optimize acclimation to changing environmental conditions. The most prominent component in vascular plants and green algae is qE, which is the most rapidly activated mechanism (see below chapter 1.4.2, Fig. 5). While the contribution of qT to the overall NPQ is rather low in vascular plants (Nilkens et al., 2010), its importance in green algae can be considered as high as qE (Allorent et al., 2013). qZ, qT, qI and qH will be shortly introduced in the following, while qE will be presented in more detail thereafter.

qZ is defined as the zeaxanthin (Zx) dependent quenching component of NPQ and is activated within 10 to 30 min, along with the conversion of violaxanthin (Vx) to Zx, a carotenoid that controls and increases energy quenching in PSII (Demmig-Adams, 1990). The relaxation of qZ occurs within 10 to 60 min concomitant with the reconversion of Zx to Vx (Nilkens et al., 2010).

State transition (qT) is defined as a reversible process where LHCII trimers relocate between PSII and PSI in order to balance the energy distribution between both photosystems (Rochaix, 2014; Nawrocki et al., 2016; Allen, 2017). The LHCII relocation from PSII to PSI occurs within minutes and is dependent on the phosphorylation state of LHCII, which is regulated in *C. reinhardtii* by the membrane bound kinase STT7 (Takahashi et al., 2013) and a corresponding phosphatase, which has been identified so far only for Arabidopsis (Shapiguzov et al., 2010). When LHCII trimers are not phosphorylated and associated with PSII, PSI is being preferentially excited (state 1, PQ pool is oxidized). Phosphorylation through STT7, which is activated by a reduced PQ pool, induces relocation of LHCII from PSII to PSI located in the stroma lamellae (state 2).

qI describes photoinhibtition of PSII during prolonged HL exposure (hours) by inactivating the PSII core through damaged D1 and the formation of Zx (Krause, 1988; Jahns et al., 2009).

The inactive D1 thereby avoids formation of $^1O_2^*$ and $O_2^{·-}$ and hence reduces further harm to the cell (Adams III et al., 2006). The relaxation of qI involves a repair system with proteases and *de novo* synthesis of D1 (Gururani et al., 2015).

The recently discovered qH quenching is supposedly active in the peripheral LHCII (Malnoë et al., 2018). qH is defined as a sustained quenching which becomes activated under cold and HL stress, reduces lipid peroxidation levels, and hence provides photoprotection. Plastid lipocalin (LCNP) is predicted to be required for qH either directly by forming NPQ sites or indirectly by modifying the membrane structure for LHCII which results in sustained NPQ in LHCII (Malnoë et al., 2018).

1.4.2 pH dependent energy quenching (qE)

qE is defined as the ΔpH dependent component, which becomes activated upon light-induced lumen acidification (Fig. 5, Briantais et al., 1979).
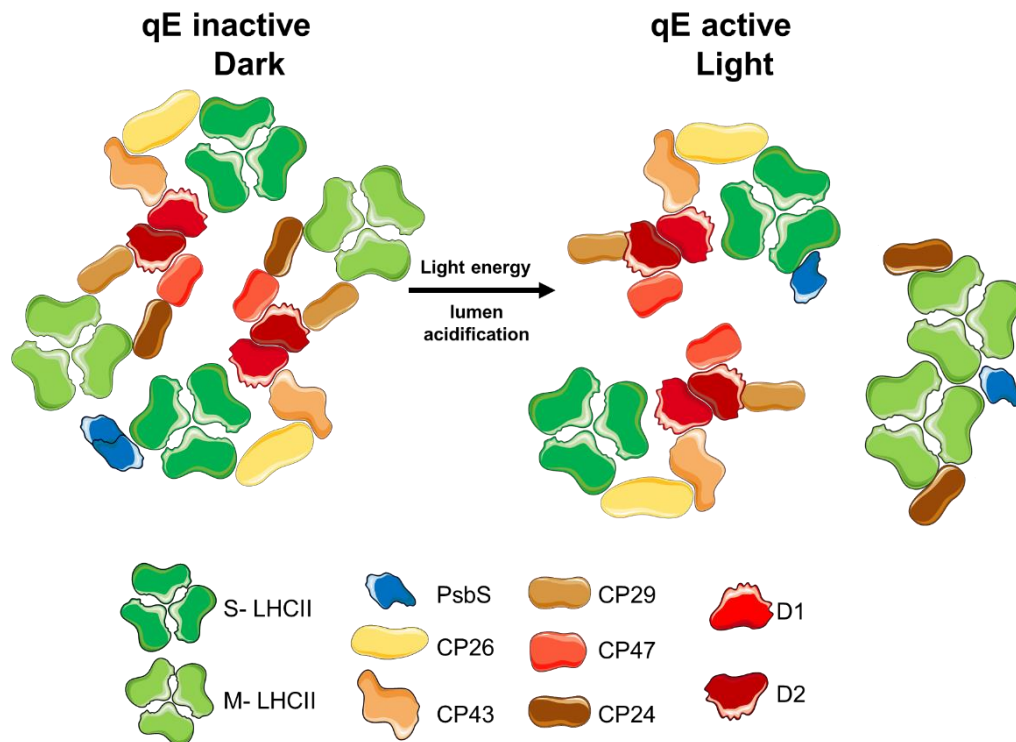

Figure 5: Light induced NPQ activation and reorganization of antenna complexes. Dimeric PsbS mainly interacts in the qE inactive (dark) state with S-LHCII and the PSII RC (CP47, CP43, D2) of PSII-LHCII. Light induced lumen acidification leads to monomerization of PsbS, enforcing a detachment of trimeric M-LHCII and thus activates qE. PsbS induced conformational changes occur along with the activation of the quenching sites Q1 (detached M-LHCII) and Q2 (PSII bound LHCII) (Holzwarth et al., 2009). S- and M-LHCII bind violaxanthin in the dark, and zeaxanthin in light. The model exemplarily shows that detached M-LHCII binds to CP24, but it is also possible that aggregated M-LHCII are present without further association. Simplified model adapted from (Correa-Galvis et al., 2016).

It is quickly activated in HL (within seconds) and represents the most prominent component of NPQ under most light conditions throughout the day (Krause and Jahns, 2004). This pH dependent energy quenching is strictly regulated by the lumen pH, which ensures that quenching is only active, when photosynthetic electron transport is not light-limited. In vascular plants, qE is controlled by the PsbS protein (Li et al., 2000), which acts as sensor of the lumen pH (Li et al., 2004), while qE in *C. reinhardtii* relies on the control of HL and UV-B induced LHCSR proteins for full activation of qE (Peers et al., 2009). However, in the moss *Physcomitrella patens*, both proteins PsbS and LHCSR contribute to qE capacity during excessive light conditions (Alboresi et al., 2010). The work of Alboresi and colleagues gave evidence that the PsbS dependent qE capacity of plants evolved before the LHCSR dependent qE mechanism was lost in land plant evolution.

1.4.2.1 PsbS in vascular plants

The 22kDa PsbS protein in vascular plants is encoded by the *NPQ4* gene (Li et al., 2000) and is constitutively expressed, although both *PSBS* transcription and PsbS protein synthesis are further upregulated upon a shift from LL to HL (Zones et al., 2015). PsbS belongs to the extended LHC protein super family (Engelken et al., 2010), but in contrast to the LHC proteins, which typically consist of three transmembrane helices and bind pigments, the PsbS protein consists of four transmembrane helices and does not bind pigments due to its compact structure (Fig. 6, Fan et al., 2015). PsbS in vascular plants is essential for qE regulation (Li et al., 2000). PsbS acts as sensor of the lumen pH and protonation of two lumen-exposed glutamate residues (E122, E226 in *A. thaliana*) facilitate the activation of qE (Li et al., 2004), likely through interaction with LHCII proteins (Correa-Galvis et al., 2016; Sacharz et al., 2017).
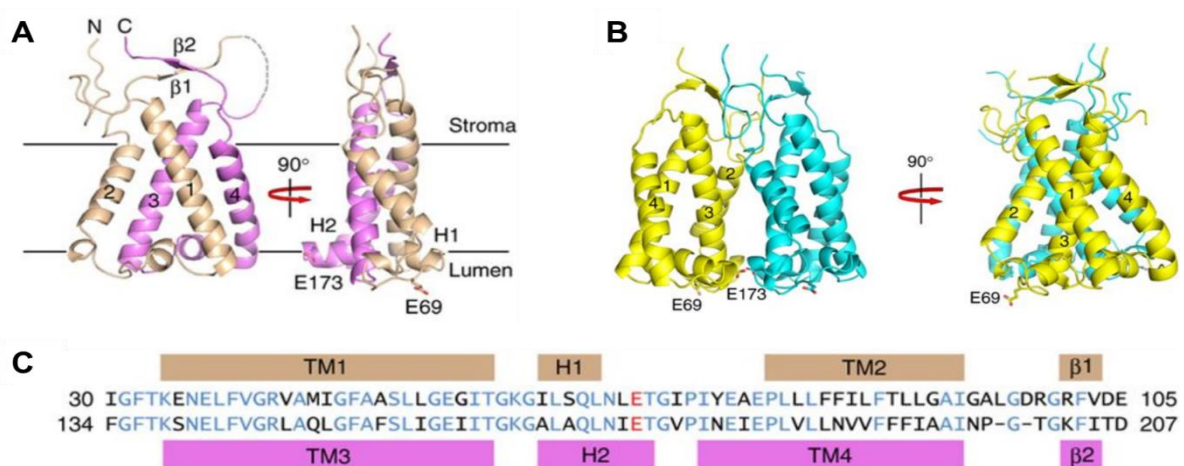

Figure 6: Structural model of the PsbS protein in vascular plants. (A) View from the membrane plane with indicated thylakoid membrane layer; (**B**) PsbS dimer with both monomers indicated in yellow and cyan; (**C**) Sequence alignment of the two halves of PsbS with both pH-sensing glutamate residues highlighted in red. Adapted after (Fan et al., 2015).

PsbS exists as a dimer in the dark (qE-inactive state) and is supposed to monomerize upon light-induced acidification of the thylakoid lumen (qE-active state) (Bergantino et al., 2003; Correa-Galvis et al., 2016). The homo-dimeric PsbS is stabilized by intermolecular interactions of the transmembrane helices 2 and 3 and the luminal loops containing the pH sensitive glutamate residues (Fig. 6, Fan et al., 2015). The PsbS-regulated conformational reorganization of the PSII antenna and a detachment of trimeric LHCII are supposed to provide the basis for the activation of the energy dissipative state (Fig. 5, Horton et al., 2008). It is thought that PsbS not only interacts with proteins in the same membrane, but also with proteins located in the neighboring grana stacks. PsbS is further supposed to interact specifically with LHCII trimers (Correa-Galvis et al., 2016) and monomers (Sacharz et al., 2017).

1.4.2.2   PsbS in *C. reinhardtii*

The PsbS in *C. reinhardtii* is encoded by two genes (*PSBS1, PSBS2)* on the first chromosome (Anwaruzzaman et al., 2004) and is supposed to consist of four transmembrane helices like in vascular plants with two pH sensing glutamate residues conserved at the luminal side of the thylakoid membrane. Unlike in vascular plants, which constitutively express the PsbS protein, the PsbS in *C. reinhardtii* only accumulates transiently after transfer into HL (or UV-B) with maximal expression after 4-10 hours of HL exposure and becomes degraded at longer HL acclimation time (Allorent et al., 2016; Correa-Galvis, Redekop et al., 2016; Tibiletti et al., 2016). Moreover, data show that down-regulation of PsbS leads to the reduction of NPQ capacity, indicating that PsbS in green algae might contribute to the establishment of NPQ, without being required for quenching mechanism (Correa-Galvis, Redekop et al., 2016).

1.4.2.3   LHCSR3 and LHCSR1

The 26.1kDa LHCSR3 (*LHCSR3.1* and *LHCSR3.2*) and LHCSR1 proteins are transmembrane proteins consisting of three transmembrane helices (Fig. 7) that are nuclear encoded by genes located on linkage group VIII (Peers et al., 2009). Like the PsbS in vascular plants, the LHCSR3 protein is essential for qE in *C. reinhardtii*, and accumulates only after initial HL exposure (Fig. 8). In contrast to the PsbS protein in *C. reinhardtii*, however, LHCSR3 amounts remain high in the fully HL acclimated state. The LHCSR3 protein controls the major portion of the maximal qE capacity, as evident from the strongly reduced qE capacity in the LHCSR3-deficient *npq4* mutant (Peers et al., 2009). The residual LHCSR3-independent qE capacity is completely abolished in the *npq4lhcsr1* double mutant (Ballottari et al., 2016) and can thus be assigned to the function of LHCSR1. LHCSR1 and LHCSR3 proteins show 82% amino acid identity (Fig. 7 C, Peers et al., 2009), and both proteins are exclusively present in mosses and algae, while they are missing in vascular plant (Teramoto et al., 2002). Though both proteins belong to the LHC protein superfamily, LHCSR expression patterns do not correlate with that

of most other LHC proteins, which function primarily as light-harvesting proteins. *LHCSR* mRNA increases not only in HL but also in response to low carbon availability (Chaux et al., 2017), indicating an important photoprotective role of NPQ under stress conditions. LHCSR3 has been shown to accomplish the function as pH sensor in qE regulation in *C. reinhardtii* due to three lumen-exposed amino acids, 1 Asp and 2 Glu residues (Fig. 7, Ballottari et al., 2016). Mutation of these three amino acids resulted in complete inhibition of LHCSR3 dependent qE (Ballottari et al., 2016).
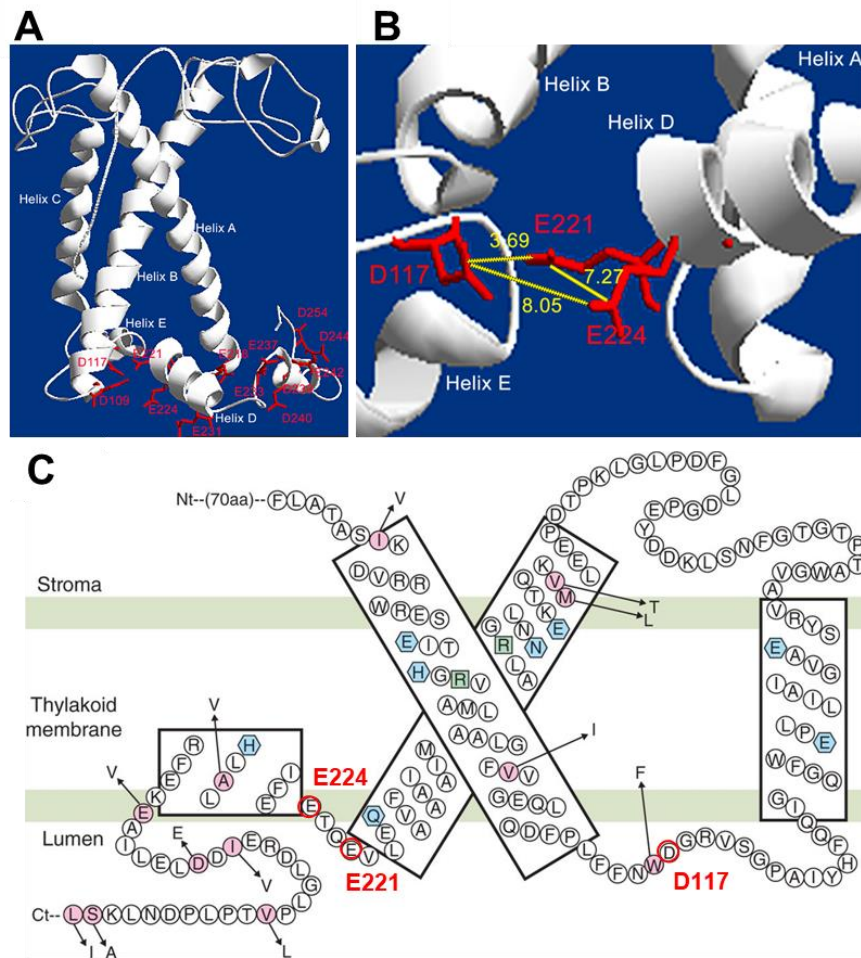

Figure 7: Model of the LHCSR3 structure. (**A, B**) Three-dimensional structure based on LHCII and CP29 crystallography. Presumed protonable sites are indicated in red (**A**). Magnified view on Asp117, Glu221, and Glu224 residues with distance between the residues indicated in yellow (**B**). Adapted from (Ballottari et al., 2016). (**C**) Schematic model of the LHCSR3 and LHCSR1. Pink circles represent amino acid residues of LHCSR3 that are different to LHCSR1 (equivalents of LHCSR1 are designated with black arrows). Chl-binding sides (blue hexagons) and charge-compensating arginine residues (green squares) were predicted based on related LHCII crystal structure (Kühlbrandt et al., 1994; Maruyama et al., 2014). Protonable amino acids in response to acidification of the lumen pH are marked in red and by corresponding numbers.

In contrast to PsbS, LHCSR also binds pigments and further acts as quencher (Bonente et al., 2011). Similar to PsbS in vascular plants, however, LHCSR3 binds the qE-inhibitor dicyclohexylcarbodiimide (DCCD) (Ballottari et al., 2016) and undergoes pH-inducible functional changes (Bonente et al., 2011; Liguori et al., 2013; Tokutsu and Minagawa, 2013). Similar to LHCSR3, also LHCSR1 expression is induced under HL, but LHCSR1 is thought to be specifically induced by UV-B light which is sensed by the UVR8 photoreceptor (Allorent et al., 2016). Recent studies suggested that LHCSR1 may contribute to energy dissipation by at least two different mechanisms, one based on energy transfer to LHCII (Dinc et al., 2016) and the other on energy transfer to PSI (Kosuge et al., 2018). Hence, LHCSR1 and LHCSR3 likely contribute both to the HL-induced quenching capacity of *C. reinhardtii*, but expression of both proteins is regulated differently, suggesting a differential regulation of photoprotection in response to light stress.
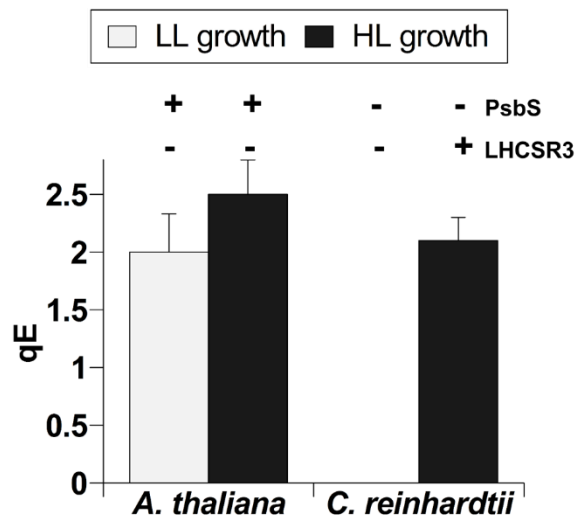

Figure 8: qE capacity of low-light (LL) and high-light (HL) acclimated *A. thaliana* plants and *C. reinhardtii* cells. High qE can be established in LL and HL acclimated *A. thaliana* plants, due to the constitutively accumulated PsbS protein. In *C. reinhardtii*, qE becomes only activated after HL acclimation, due to the HL-induced accumulation of LHCSR3.

2 Aims of the Work

The PsbS protein in vascular plants is well described and known to be essential for the pH regulated thermal energy dissipation of excess energy (qE). In green algae, this central regulatory role is facilitated by another protein, LHCSR3, which is absent in vascular plants. At the beginning of this work, the function of the PsbS protein in *C. reinhardtii* was completely unknown, since the PsbS protein was not found to accumulate in this organism. Preliminary research in the AG Jahns indicated, however, that PsbS accumulates transiently in *C. reinhardtii* after a shift from LL to HL. Therefore, this work aimed at the characterization of the role of PsbS in *C. reinhardtii* during HL acclimation, addressing the following topics:

A) Characterization of the dynamics of PsbS expression during HL acclimation in comparison with NPQ dynamics and LHCSR protein expression in *C. reinhardtii* wild-type and PsbS knock-down lines.

B) Localization of the PsbS protein in the cell and analysis of possible interaction partners in the thylakoid membrane.

C) Investigation of general characteristics (cell viability, thylakoid membrane dynamics, electron transport and NPQ characteristics) of HL acclimation and analysis of the impact of different PsbS levels (wild type, PsbS knock-down and over-expressing lines) on these parameters.

3 Hypothesis

A) Manuscript 1 characterizes the dynamics of PsbS expression in comparison with NPQ dynamics during HL acclimation in *C. reinhardtii.* The experimental data imply that the PsbS protein is a HL-induced protein, which accumulates only transiently during HL acclimation. The initial PsbS accumulation correlates with LHCSR1/3 accumulation and the NPQ induction, but prolonged HL acclimation leads to PsbS degradation without affecting the NPQ properties. Knock-down of PsbS expression reduces the accumulation of LHCSR1/3 and the NPQ capacity, indicating that PsbS might be required for the reorganization of the PSII antenna during establishment of a high NPQ capacity. Indeed, a fraction PsbS co-migrates with PSII complexes in detergent solubilized thylakoid membranes.

B) Manuscript 2 characterizes the impact of different PsbS levels on HL acclimation. Over-expression of PsbS does not increase the NPQ capacity but leads to improved resistance against HL stress. Also, over-expressed PsbS is strongly degraded during HL acclimation, indicating that degradation of PsbS is obligatory during HL acclimation. In contrast, reduced PsbS and LHCSR amounts lead to increased HL sensitivity, which underlines the importance of both proteins for photoprotection in *C. reinhardtii*. PsbS is localized predominantly in the grana region of the thylakoid membrane, supporting an association of PsbS with PSII.

4 Manuscript 1

Photosystem II Subunit PsbS is Involved in the Induction of LHCSR-dependent Energy Dissipation in *Chlamydomonas reinhardtii*

Photosystem II Subunit PsbS is Involved in the Induction of LHCSR-dependent Energy Dissipation in *Chlamydomonas reinhardtii*

Viviana Correa-Galvis[‡,a,1], Petra Redekop[‡,1], Katharine Guan[§], Annika Grieß[‡], Thuy B. Truong[§,b] Setsuko Wakao[§], Krishna K. Niyogi[§,¶], and Peter Jahns[‡,2]

[‡]Plant Biochemistry, Heinrich-Heine-University Düsseldorf, 40225 Düsseldorf, Germany; [§]Howard Hughes Medical Institute, Department of Plant and Microbial Biology, University of California, Berkeley, CA 94720-3102, USA; [¶]Molecular Biophysics and Integrated Bioimaging Division, Lawrence Berkeley National Laboratory, Berkeley, CA 94720, USA

[a]Current address: Max-Planck-Institute for Molecular Plant Physiology, Am Mühlenberg 1, 14476 Potsdam, Germany

[b]Current address: Donald Danforth Plant Science Center, St. Louis, MO 63132, USA

[1]These authors contributed equally to this work

Running title: *PsbS function in Chlamydomonas reinhardtii*

[2]To whom correspondence should be addressed: Peter Jahns, Plant Biochemistry, Heinrich-Heine-University Düsseldorf, D-40225 Düsseldorf, Germany, Telephone: +49 (211) 8113862; FAX: +49 (211) 8112706; E-mail: pjahns@hhu.de

Keywords: Chlamydomonas, Light acclimation, NPQ, Photoprotection, PsbS

ABSTRACT

Non-photochemical quenching of excess excitation energy is an important photoprotective mechanism in photosynthetic organisms. In *Arabidopsis thaliana*, a high quenching capacity is constitutively present and depends on the PsbS protein. In the green alga *Chlamydomonas reinhardtii*, non-photochemical quenching becomes activated upon high light acclimation and requires the accumulation of LHCSR proteins. Expression of the PsbS protein in *C. reinhardtii* has not been reported yet. Here, we show that PsbS is a light-induced protein in *C. reinhardtii*, whose accumulation under high light is further controlled by CO_2 availability. PsbS accumulated after several hours of high light illumination at low CO_2. At high CO_2, however, PsbS was only transiently expressed under high light and was degraded after 1 h of high light exposure. PsbS accumulation correlated with an enhanced non-photochemical quenching capacity in high-light-acclimated cells grown at low CO_2. However, PsbS could not compensate for the function of LHCSR in an LHCSR-deficient mutant. Knock-down of PsbS accumulation led to reduction of both non-photochemical quenching capacity and LHCSR3 accumulation. Our data suggest that PsbS is essential for the activation of non-photochemical quenching in *C. reinhardtii*, possibly by promoting conformational changes required for activation of LHCSR3-dependent quenching in the antenna of photosystem II.

Sunlight is the ultimate energy source for photosynthesis. Although efficient light absorption is essential for efficient photosynthesis, the absorption of light energy in excess of its utilization in photosynthesis may lead to the production of reactive oxygen species which cause cell damage (1,2). Oxygenic photosynthesis evolved in cyanobacteria and was transferred laterally to eukaryotes through endosymbiosis (3), and both cyanobacteria and photosynthetic eukaryotes have evolved photoprotective mechanisms allowing the dissipation of excess light energy as heat (4). One of the most important and pervasive mechanisms of minimizing photo-oxidative damage by excess light energy is the harmless de-activation of singlet excited chlorophylls in the light harvesting antenna as heat, known as non-photochemical quenching (NPQ)[3]. In land plants, NPQ is composed of different components, with the so-called qE-component being the dominant mechanism un-

[3]The abbreviations used are: HL, high light; HS, high salt; LHC, light-harvesting complex; LL, low light; NPQ, non-photochemical quenching; PSI, photosystem I; PSII, photosystem II; qE, energy-dependent quenching; TAP, tris-acetate-phosphate; WT, wild type

der most natural conditions (5). The qE mechanism is strictly regulated by changes in the pH of the thylakoid lumen (6) and thus operates on a very short time scale allowing a rapid response of the photosynthetic machinery to rapid changes in light intensities.

Although the function of qE is the same in green algae and plants, the underlying mechanisms differ among green algae and plants (7). In the green alga *Chlamydomonas reinhardtii*, qE depends on light-induced accumulation of the LHCSR proteins, specifically LHCSR3 (8). LHCSR3 is a pigment-binding member of the LHC family that is activated via protonation of acidic amino acid residues upon acidification of the lumen, allowing for the reversible switch from a light harvesting to a dissipative state (9-11). In land plants, the qE mechanism differs between vascular and non-vascular plants. In the moss *Physcomitrella patens*, qE is independently and additively activated by two types of proteins: LHCSRs (as in green algae) and PsbS, a non-pigment binding protein from the LHC family (12,13). Both proteins are activated in parallel by changes in the thylakoid luminal pH, but contrary to *C. reinhardtii* (14,15), pH-regulated synthesis of zeaxanthin from violaxanthin also significantly contributes to qE. In particular zeaxanthin binding to LHCSR enhances the LHCSR-dependent qE capacity (16). PsbS, on the other hand, is supposed to enhance the quenching of excess energy by direct interaction with LHCII trimer proteins (17). In vascular plants, qE requires pH-regulated activation of PsbS by protonation of two glutamate residues at its two luminal loops (18-20) and is further modulated by zeaxanthin synthesis (21). The qE mechanism has been extensively studied in *Arabidopsis thaliana*, being a model organism for the study of energy dissipation mechanisms since the essential role of PsbS in qE activation was described (18). In the current model for qE activation, acidification of the lumen activates PsbS and thus facilitates conformational changes in the LHCII-PSII supercomplexes, thereby promoting a rearrangement of LHCII (22-25). Activation of qE in *A. thaliana* is accompanied by an increased interaction of PsbS with trimeric LHCII and PSII reaction center proteins (23). It should be noted, however, that under *in vitro* conditions, qE can be induced even in absence of PsbS, when the lumen pH is artificially lowered below pH 5.5, indicating that PsbS controls the pH sensitivity of conformational changes required for qE (26).

PsbS homologs have been found in several lineages of green algae (15,27,28). In *C. reinhardtii*, two PsbS-encoding genes (*PSBS1* and *PSBS2*) have been identified (29). The encoded proteins differ only in one amino acid of the chloroplast transit peptide, and they show 48% similarity with *A. thaliana* PsbS, including the two pH-sensing glutamate residues at the luminal side (15). Transcriptomic analyses have revealed that mRNA levels of the two PsbS-encoding genes in *C. reinhardtii* (*PSBS1* and *PSBS2*) are upregulated upon nitrogen starvation (30) and after a shift from dark or low light to higher light intensities (31-33). However, expression and accumulation of the PsbS protein has not been reported so far, and earlier work showed that over-expressed PsbS does not localize to the thylakoid membrane in *C. reinhardtii* (27). In this work, we show that PsbS transiently accumulates in *C. reinhardtii* during activation of qE upon high light acclimation and that the accumulation and degradation of PsbS is regulated by CO_2 availability. Knock-down of PsbS expression leads to a pronounced reduction of LHCSR accumulation and qE activation. Our data suggest that PsbS is required for the activation of the qE capacity elicited by the LHCSR protein upon high light acclimation in *C. reinhardtii*.

Results

Inducible Expression of the PsbS Protein – Based on the predicted PsbS protein sequence (15), we designed an antibody that specifically recognizes PsbS of *C. reinhardtii*. The antibody binds to the C-terminal sequence of the protein, which is identical for the proteins encoded by the two genes *PSBS1* and *PSBS2*. Its reactivity was confirmed by immunodetection of partially purified recombinant *Cr*PsbS expressed in *E. coli* (Fig. 1*A*), and total protein extracts from *Cr*PsbS-expressing *E. coli* cells (Fig. 1*B*). The antibody showed no cross reaction with the *A. thaliana* PsbS (Fig. 1*B*).

At the transcript level, PsbS mRNA was shown to increase upon nitrogen starvation under mixotrophic growth (30) and after transferring photoautotrophically grown cells from dark or low light to high light (31-33). In order to identify specific conditions that trigger expression of the PsbS protein, we designed an experiment combining different light conditions, carbon and nitrogen availabilities. Cells were grown under low light (LL) or high light (HL), under either mixotrophic (TAP medium with acetate as a carbon source) or photoautotrophic (high salt minimal medium – HS) conditions, and in the presence or absence of a nitrogen source. In wild-type (WT) cells, PsbS was expressed in HL-acclimated cells grown under photoautotrophic conditions, and PsbS accumulation

was reduced upon nitrogen starvation (Fig. 2*A*). No PsbS protein was detected in LL-grown cells or in mixotrophically grown cells (Fig. 2*A*). It should be noted that PsbS protein could only be detected by immunoblot analysis when the amount of total protein loaded on the gel was increased to 40 µg instead of 5 µg for other proteins (Fig. 2), which might indicate a substoichiometric accumulation of PsbS compared to the photosystem II (PSII) reaction center core subunit D1 and LHCSR.

In the *npq4lhcsr1* double mutant, which lacks functional LHCSR3 and LHCSR1 (11), PsbS was more strongly expressed compared to the WT and was not degraded upon nitrogen starvation (Fig. 2*B*). Consequently, the light-induced expression and accumulation of PsbS does not depend on the accumulation of LHCSR proteins, but is enhanced in their absence. LHCSR amounts were higher under photoautotrophic conditions (HS medium) in both LL- and HL-grown cells compared to cells grown under mixotrophic conditions (TAP medium) in HL.

PsbS Expression During High Light Acclimation at Different CO_2 Availabilities – The responses of *C. reinhardtii* to HL are commonly studied by transferring LL-grown cells to HL, thus simulating long-term acclimation to HL upon increases in light intensities. Monitoring the expression of PsbS (and other proteins) under constant HL growth may thus not be an appropriate system to study the function of this protein, because *PSBS* mRNA is only transiently upregulated upon transition from low to high light intensities (31,32). Additionally, the energy quenching capacity in *C. reinhardtii* also depends on CO_2 availability (34-36). Thus, if the function of PsbS is related to the activation of qE under HL, CO_2-dependent changes in its expression are expected. To address these questions, WT and *npq4lhcsr1* cells were grown in photoautotrophic media under LL under different carbon regimes. For the purpose of this study, these regimes are defined as low CO_2 (no additional CO_2 input into the media), ambient CO_2 (supplied by air bubbling in the media) and high CO_2 (bubbling with air containing 5% CO_2). After reaching an exponential phase, cultures were transferred to HL, and the accumulation of PsbS and other proteins was analyzed by immunoblotting at different time points after HL illumination (Fig. 3).

Expression of PsbS was induced in WT and *npq4lhcsr1* mutant cells within 1 h after transfer of cells to HL, independent of the CO_2 concentration in the medium (Fig. 3). However, the PsbS content did not remain at a constant level, but decreased at longer HL exposure time, and the dynamics of PsbS accumulation showed a pronounced dependence on the CO_2 concentrations (Fig. 3). In WT and *npq4lhcsr1* cells grown under low CO_2, PsbS expression reached maximum levels after about 10 h and decreased to lower levels after 48 h of HL exposure (Fig. 3, *A* and *B*). At ambient CO_2 concentrations, maximum PsbS levels accumulated between 1 and 6 h after HL illumination. In WT cells, PsbS disappeared completely after 24 h, while low levels of PsbS were retained up to 48 h in *npq4lhcsr1* mutant cells (Fig. 3, *C* and *D*). Growth at high CO_2 concentrations, however, led to a pronounced accumulation of PsbS after 1 h of HL exposure and complete degradation at longer illumination times in both WT and mutant cells (Fig. 3, *E* and *F*). Similarly, the expression of LHCSR proteins in WT cells was regulated by light and carbon availability. In low-CO_2-grown cells, LHCSR proteins were already expressed under LL growth, and their expression levels increased only slightly upon HL exposure (Fig. *3A*). With increasing CO_2, the expression of the protein was activated upon transfer to HL (Fig. 3, *C* and *E*). LHCSR proteins accumulated gradually in WT cells grown at ambient CO_2 (Fig. 3*C*) but were degraded after 10 h of HL in high CO_2 grown cells (Fig. 3*E*). Remarkably, the expression of the CAH3 protein, a carbonic anhydrase located in the thylakoid lumen known to be essential for the carbon-concentrating mechanism under low CO_2 (37,38), was also expressed in cells under high CO_2 growth but degraded after 24 h of HL exposure (Fig. 3, *E* and *F*). In contrast, the protein level of PSII core subunit D1 appeared relatively constant (Fig. 3).

NPQ Activation During High Light Acclimation at Different CO_2 Availabilities – Since both PsbS and LHCSR had similar expression patterns in response to HL exposure at different CO_2 concentrations, we further investigated whether these changes correlated with the quenching capacity during HL acclimation. The activation of NPQ was strongly dependent on CO_2 availability (Fig. 4) and required the accumulation of LHCSR proteins (Fig. 4, *B,D* and *F*), emphasizing the essential role of these proteins for qE in *C. reinhardtii* (8). In WT, NPQ induction was inversely proportional to CO_2 availability: NPQ induction under HL conditions was fully suppressed in the presence of 5% CO_2 (Fig. 4*E*). At low CO_2 (Fig. 3A) and ambient CO_2 (Fig. 4*C*), however, activation of NPQ capacity was induced after 6 h of HL exposure. The rapid dark reversibility of this NPQ indicates that predominantly the pH-dependent qE

quenching was activated under these conditions (39). The small fraction of slowly inducible/relaxing NPQ, however, was rather reduced upon HL acclimation. These changes occurred independent of the CO_2 availability and the presence of LHCSR or PsbS, and thus likely reflect a general acclimation process. Interestingly, the gradual increase in qE capacity in low- and ambient CO_2-grown cells correlated with the time frame for PsbS accumulation (Fig. 3, *A* and *C*). However, the full induction of NPQ was delayed compared to peak expression of PsbS, and maximum PsbS levels were reached earlier at ambient CO_2 compared to low CO_2 conditions (Fig. 3, *A* and *C*). This suggests that the PsbS protein might be either directly involved in the activation of qE, or in other responses required for HL acclimation of cells, especially under limited CO_2 availability, and thus limited photosynthetic capacity. Nonetheless, PsbS could not compensate and/or complement the function of LHCSR, because no NPQ induction was observed in the *npq4lhcsr1* mutant under conditions leading to PsbS expression (Figs. 3 and 4). Therefore, PsbS was not sufficient for qE induction in absence of LHCSR proteins.

NPQ Activation and LHCSR Accumulation in PsbS Knock-down Lines – To further investigate the possible role of PsbS, we studied the activation of NPQ in cells with reduced PsbS expression. Using artificial micro RNA (amiRNA), several independent lines with reduced PsbS expression were identified. NPQ activation in cells grown at ambient CO_2 was determined in two of these lines (1-2 and 1-6) after transfer of cells from LL to HL (Fig. 5). Strikingly, the reduction of PsbS accumulation (Fig. 5*A*) led to a pronounced reduction of the NPQ capacity with a slightly more pronounced reduction in line 1-2, which showed lower PsbS accumulation (Fig. 5*B*). This implies that the accumulation of PsbS to normal levels is essential to induce the full NPQ capacity upon HL acclimation. The knock-down of PsbS accumulation was accompanied by a strong reduction in the LHCSR content (Fig. 5*A*), indicating that the reduced NPQ capacity is related to a reduced amount of LHCSR3. The accumulation of high LHCSR levels appears to depend on the accumulation of PsbS, suggesting that PsbS is a prerequisite for the stable accumulation of LHCSR3.

Localization of PsbS – The reduction of both the NPQ capacity and LHCSR3 accumulation in PsbS knock-down lines indicates a function of PsbS in thylakoid membranes. However, earlier work showed that over-expressed PsbS did not localize to thylakoid membranes (27). We investigated whether native PsbS accumulates in thylakoid

membranes and whether LHCSR3 and PsbS show a similar distribution among the protein complexes. For that, we isolated thylakoid membranes from LL- and HL-acclimated cells, and determined the distribution of PsbS and LHCSR3 after separating protein complexes under native conditions by sucrose gradient ultracentrifugation (Fig. 6). Indeed, the PsbS protein was detected in isolated thylakoids from WT cells exposed to HL, but PsbS and LHCSR showed a different distribution among the isolated fractions. Most of the PsbS comigrated with PSII core-enriched protein fraction B3, though weak bands were also detectable for PsbS in other bands, whereas LHCSR was found predominantly in fraction B1 (Fig. 6, *B* and *C*). This suggests that PsbS is associated with PSII core complexes, in contrast to LHCSR3, which migrates predominantly in band B1 that lacks PSII. It should be noted, however, that also very faint bands for LHCSR3 were visible in fractions B3 and B4, in accordance with the previously reported association of a small fraction of LHCSR3 with PSII-LHCII and PSI-LHCI supercomplexes (40). Conversely, in HL-acclimated qE-deficient cells (*npq4lhcsr1*), PsbS was mainly co-migrating with light-harvesting proteins (Fig. 6*C*). The differential PsbS distribution among complexes in cells with and without quenching capacity suggests that changes in the localization of PsbS might be related to the rearrangement of proteins during qE activation upon HL exposure. It is further worth noting that the HL-induced shift in the distribution of the PSII antenna protein Lhcbm5 towards the PSII core-enriched fraction B3 was only detectable in WT cells but not in HL-acclimated *npq4lhcsr1* cells (Fig. 6*C*). This suggests that a structural change involving the organization of the PSII-LHCII supercomplexes occurred in the HL-acclimated state in WT, and that this change was absent in the mutant lacking LHCSR proteins.

Discussion

The pH-regulated qE mechanism of energy dissipation in C. *reinhardtii* is controlled by the LHCSR3 protein (8) contrary to land plants; in mosses this function is performed by both PsbS and LHCSR (12,13) and in vascular plants only by PsbS (18). In this work, we presented evidence that the PsbS protein in C. *reinhardtii* is a HL-induced protein, which regulates the activation of the LHCSR-dependent qE capacity but is not sufficient for inducing qE in the absence of LHCSR proteins.

The qE response (induction and capacity) of C. *reinhardtii* is regulated at different levels. At the

transcript level, *LHCSR* and *PSBS* genes are up-regulated in response to changes from low to high light (8,31,34). The two *PSBS* genes (*PSBS1* and *PSBS2*) are upregulated similarly in response to high light stress (32). In the present work, this response was observed also at the protein level after a few hours of HL illumination (Figs. 2 and 3). Due to the identical amino acid sequence of PSBS1 and PSBS2, the antibody that we generated detects both proteins. In addition to a shift in light intensity, the availability of CO_2 (and hence the capacity of photosynthesis) plays an important role in the regulation of the qE machinery. In the absence of HL, LHCSR protein accumulated under low CO_2 conditions (Figs. 2*A* and 3*A*), which is likely due to an EEC motif (enhancer element of low CO_2-inducible genes) in its promoter region (34,41). Furthermore, the LL intensity of 30 µmol photons m^{-2} s^{-1} used here may already saturate photosynthesis at limiting CO_2 availability. PsbS protein level increased during HL under all CO_2 conditions tested (Figs. 2 and 3), but the sustained accumulation of PsbS protein during HL was observed only under low CO_2 conditions (Fig. 3). The promoter regions of both *PSBS* genes contain EECs (Fig. 7) and thus both genes are likely to be transcriptionally induced under our low CO_2 condition, although it does not exclude other possible modes of regulation. Additionally, the accumulation of LHCSR requires Ca^{2+} (42). However, whether or not HL-induced accumulation of PsbS is also Ca^{2+}-dependent, remains to be elucidated.

The analysis of NPQ induction curves along with the accumulation of PsbS and LHCSR under different growth conditions identified specific requirements for qE quenching in *C. reinhardtii.* The following important conclusions regarding the induction of qE in *C. reinhardtii* can be drawn: (i) The presence of LHCSR in LL-grown cells before the onset of HL illumination (Figs. 2*A* and 3*A*) is not sufficient for qE induction (Fig. 4). Consequently, further acclimation processes are required for establishing a high qE capacity. (ii) The presence of both PsbS and LHCSR3 after 1 h of HL exposure in high-CO_2-grown cells (Fig. 3*E*) is also not sufficient for qE induction (Fig. 4*E*). This result together with the rapid degradation of both PsbS and LHCSR during longer illumination periods, suggests that qE is generally not activated at high CO_2 concentrations. (iii) The presence of PsbS is not sufficient to induce any qE in the absence of LHCSR3, even after longer periods of HL acclimation (Fig. 3, *B* and *D*, Fig. 4, *B* and *D*). This underscores that LHCSR is essential for qE. (iv) PsbS accumulates only transiently to maximal lev-els during HL acclimation and undergoes degradation before induction of full qE capacity (Fig. 3, *A* and *C*, Fig. 4, *A* and *C*). Hence, the accumulation of both proteins, LHCSR and PsbS, is not sufficient to induce the full NPQ capacity, indicating a critical role of PsbS during the establishment of high qE capacity. (v) Knock-down of PsbS expression leads to a strong reduction of both LHCSR accumulation and NPQ capacity (Fig. 5), suggesting that PsbS controls processes that are essential to establish a specific interaction of LHCSR with PSII required for qE (and not mere stabilization of LHSCR because LHCSR was detected in multiple conditions in which PsbS was absent, Fig. 3, *A*–*C*). (vi) Complete degradation of PsbS is not required for maintaining a high qE capacity, since high qE can be induced in the presence of low PsbS levels after 48 h of HL acclimation under low CO_2 (Figs. 3*A* and 4*A*). This implies that PsbS does not interfere with the quenching site.

Similar to LHCSR, the expression of PsbS at the transcript and protein levels is regulated by light and CO_2 availability. However, PsbS accumulated only transiently during the establishment of qE capacity (Fig. 3). Together with the strongly reduced LHCSR accumulation and NPQ capacity in cells with reduced PsbS expression (Fig. 5), these characteristics are consistent with the hypothesis that PsbS is essential for conformational changes in the antenna of PSII that are required for the binding of LHCSR3 at a specific qE-quenching site. In general, such a function of PsbS resembles that in vascular plants, despite the fact that PsbS is constitutively expressed in vascular plants. Our recent finding that PsbS from *C. reinhardtii* can increase NPQ capacity when transiently expressed in the plant *Nicotiana benthamiana* (Leonelli L, Erickson E, Lyska D and Niyogi KK, unpublished data) supports the concept of a similar function for PsbS from green algae and plants. In contrast to over-expressed PsbS (27), native PsbS localized to the thylakoid membrane (Fig. 6). The mismatched localization of over-expressed PsbS is likely the result of the specific growth or expression conditions used in the former study (27).

In *C. reinhardtii,* two qE quenching sites have been proposed to be involved in qE: one in the minor light-harvesting complexes and another in aggregated LHCII trimers, detached from PSII (43), similar to the situation in *A. thaliana* (44). Within the thylakoid membrane, PsbS was found to co-migrate with PSII core proteins and not with LHCSR in HL-acclimated cells (Fig. 6*C*), suggesting an interaction of PsbS with the PSII reaction center upon HL acclimation. However, in the ab-

sence of LHCSR proteins (*npq4lhcsr1*), this affinity for PSII was reduced (Fig. 6*C*). Although PsbS did not co-localize with LHCSR proteins in the light (Fig. 6*C*), its affinity towards PSII in a quenched state could indicate that PsbS is involved in the detachment of LHCII proteins from PSII, which might be essential for subsequent LHCSR3 binding to the LHCs and hence qE induction. Such an interaction of PsbS resembles that in vascular plants, where an interaction of PsbS with LHCII and PSII reactions center proteins has been proven (23).

The strongly decreased levels of LHCSR proteins in *PSBS* knock-down lines (Fig. 5) indicates that the stable accumulation of LHCSR3 depends on the presence or action of PsbS. Whether a PsbS-controlled reorganization of the PSII antenna, such as the detachment of LHCII proteins, promotes binding of LHCSR3 to PSII or whether a direct interaction of PsbS with LHCSR3 is required for LHCSR3 binding to PSII remains to be clarified. However the following observations, (i) the presumably substoichiometric amount of PsbS accumulating upon HL acclimation, (ii) the delayed accumulation of LHCSR3 protein levels compared to that of PsbS (Fig. 3), and (iii) the different localization of PsbS and LHCSR proteins, argue against a direct interaction of PsbS and LHCSR3 upon activation of a high NPQ capacity. It is therefore conceivable that PsbS interacts with LHCII and PSII reaction center proteins, and thereby reorganizes the PSII antenna to promote binding of LHCSR3. It is tempting to speculate that PsbS induces the detachment/reorganization of specific PSII antenna proteins, which prevent binding of LHCSR3 to qE-specific sites. Such an action of PsbS would be only required transiently because the PsbS is no longer necessary once a high NPQ capacity is established (Figs. 3 and 4). This implies that the PsbS-induced reorganization of the PSII antenna is stable in the HL-acclimated state. Recently, the PSII subunit PsbR has been shown to be required for the binding of LHCSR3 to PSII upon HL acclimation (40). However, reduction of PsbR accumulation did not lead to reduced LHCSR3 accumulation (40). Presumably, functional binding of LHCSR3 to PSII is controlled by several factors, but PsbS is essential for accumulation of LHCSR3.

Our data have further important implications on the evolution of qE quenching in oxygenic photosynthetic organisms. In green algae, PsbS has already (as in vascular plants) an essential function in promoting conformational changes for qE activation, but the function of pH-regulation of qE is restricted to LHCSR3. At early stages of land colonization, as represented by the moss *P. patens*, PsbS gained an additional function as an independent pH-regulator of qE, while the function of LHCSR3 became independent of PsbS, so that both proteins can act independently in qE regulation. At late stages of land colonization, as in vascular plants, the function of LHCSR3 was completely lost and PsbS gained the full capacity as pH-regulator of qE quenching. Future work is required to understand the functional switch of both PsbS and LHCSR3 upon land colonization.

Experimental Procedures

Cells and growth conditions – *Chlamydomonas reinhardtii* wild-type strain 4A+ (137c genetic background) and the double mutant *npq4lhcsr1* (11) lacking the LHCSR3 and LHCSR1 proteins (encoded by *LHCSR3.1, LHCSR3.2, LHCSR1*) were grown in batch cultures at 23 °C and constantly stirred on a shaker at 112 rpm. Light regimes were defined as low light (LL: 30 µmol photons $m^{-2} s^{-1}$) and high light (HL: 480 µmol photons $m^{-2} s^{-1}$).

The artificial microRNA (amiRNA) target sequence, TCCAAGCTTGAGGGGGCACTA, was designed to silence both *PSBS1* and *PSBS2* using Web MicroRNA Designer (WMD3, http://wmd3.weigelworld.org/cgi-bin/webapp.cgi). The synthesized oligo was inserted into pChlamiRNA3int (45) and transformed into 4A+ (46). The resulting paromomycin-resistant strains were screened by immunoblotting of PsbS in LL- and HL-grown cells.

Nitrogen starvation experiments – WT 4A+ and *npq4lhcsr1* cells were grown in a 50 ml pre-culture in TAP (47) or HS (48) media containing 7.2 mM and 9.4 mM NH_4^+, respectively (+N media). Cells were grown under constant LL (30 µmol photons $m^{-2} s^{-1}$) for 3-5 days until the culture reached a density of 3-5 x 10^6 cells/ml. 25 ml of the pre-culture were used to inoculate 100 ml of the same media, and cultures were grown under LL or HL. Once the cultures reached 5 x 10^6 cells /ml, nitrogen starvation was induced by transferring the cells to media without any NH_4^+ (TAP or HS, -N) and cells were grown for the next 48 h under the respective light regime. Subsequently, cells were harvested by centrifugation at 3,850 x *g*, frozen in liquid nitrogen and stored at -20 °C for further analysis.

Growth at different carbon availabilities – For each strain, cells were grown in three 50 ml HS media pre-cultures under LL for 5 days. Each pre-culture was used to inoculate 700 ml of HS media

with either no additional air input (no CO_2) or bubbling with air (ambient $CO_2 \approx 0.035$-0.04 %) or air enriched with 5 % CO_2 (high CO_2). Cells were grown under LL until reaching a density of 5×10^6 cells / ml, and were subsequently transferred to HL. For protein analysis, 100 ml of sample were taken after 0, 1, 6, 10, 24, and 48 h of HL exposure. After harvesting the samples, 100 ml of fresh HS media was added to each culture. The same procedure was used when sampling cells after 0, 30, 60, 120, 180 and 360 minutes transfer to HL. In this case, cells were grown in HS without additional CO_2. All samples were harvested and stored for further analysis as described for the nitrogen starvation experiments.

Expression and purification of recombinant PsbS protein – Recombinant PsbS (gene bank ID 5715134) was cloned into the pET28a (+) vector (Novagen), kindly provided by Katrin Gärtner (Michigan State University), as described previously (27). Recombinant PsbS (*r*-PsbS) was over-expressed in BL21 gold *Escherichia coli* cells, extracted by French press treatment and purified by affinity chromatography (nickel–nitrilotriacetic acid column, Bio-Rad). Protein concentrations were quantified using the DC^{TM} Protein Assay (Bio-Rad), and *r*-PsbS was identified by immunoblotting (49) using an anti-His-tag antibody (Miltenyi Biotec*)* and an antibody specifically designed for *C. reinhardtii* PsbS (contracted work Pineda antibody service).

200 µl of frozen pellet ($\approx 1 \times 10^9$ cells/ml) was resuspended in 500 µl TMK buffer (10 mM Tris/HCl pH 6.8, 10 mM MgCl$_2$, 20 mM KCl) and 0.6 g of glass beads (200 µm), vortexed three times for 1 min with 2 min of ice cooling intervals. The supernatant was removed, the beads washed with 100 µl TMK buffer and the collected supernatants centrifuged for 5 min at 17,000 x g at 4 °C. The pellet was resuspended in 200 µl extraction buffer (1.6 % SDS, 1 M urea, 50 mM Tris/HCl pH 7.6, EDTA-*free* protease inhibitor cocktail, Roche), heated for 30 min at 95 °C under stirring and centrifuged for 20 min at 17,000 x g at room temperature. Protein content of the supernatants was quantified with the DC^{TM} Protein Assay (Bio-Rad). Proteins were separated on a NuPAGE® Novex® 10 % Bis-Tris gel (Life Sciences) according to the manufacturer's instructions. Specific proteins were detected by immunoblotting as described previously (49). PsbS was detected with the *C. reinhardtii* antibody (contracted work Pineda antibody service). The LHCSR antibody was provided by Michael Hippler (University of Münster, Germany). For all other proteins, Agrisera® antibodies were used. Coomassie

stained gels and Ponceau S stained membranes served as controls for protein loading and blotting efficiency.

Isolation of thylakoid membranes – WT (4A$^+$) and *npq4lhcsr1* mutant cells were grown in 1 L cultures (HS medium) under LL with air bubbling (ambient CO_2). After reaching the exponential phase (5×10^6 cells/ml), cells were illuminated at HL for 4 h. Cells were harvested by centrifugation at 12,000 x g for 10 minutes and resuspended in 20-25 ml buffer (250 mM sorbitol, 1 mM MnCl$_2$, 5 mM MgCl$_2$, 35 mM Hepes/NaOH pH 7.8, protease inhibitor cocktail, Roche). Cells were disrupted by pressure in a French press (1000 psi, 4 °C) for three times, and centrifuged for 10 min at 12,000 x g, 4 °C. The pellet was resuspended with a paint brush in 15 ml of 5 mM MgCl$_2$, centrifuged again, resuspended in 200-250 µl aliquots with 5 mM MgCl$_2$, frozen in liquid N$_2$ and stored at -20 °C.

Sucrose gradient ultracentrifugation – Protein complexes of the thylakoid membrane were separated by sucrose density gradient centrifugation as described by (51) with some modifications. Stacked membranes were unstacked by adding 1 volume of 5 mM EDTA and centrifuged for 1 min at 17,000 x g at 4 °C. Unstacked membranes were solubilized in a medium containing 25 mM MES pH 6.5 and 1% α-DM at a final concentration of 0.4 mg chlorophyll/ml. Insolubilized material was removed by centrifugation at 17000 x g for 10 min. Solubilized thylakoids corresponding to 200 µg Chl were loaded onto a discontinuous sucrose gradient (0.1/0.4/0.7/1.0/1.3 M sucrose, 25 mM MES, pH 6.5, 1 M Betaine, 0.02 % α-DM) and fractionated by ultracentrifugation for 16 h at 130,000 x g at 4 °C. After separation, each band was collected and half of the volume was used to quantify the pigment content by reverse HPLC (52) whereas the other half was used for protein analysis. Proteins corresponding to 2 µg chlorophyll (and 25 µg chlorophyll for PsbS detection) were separated on a NuPAGE® Novex® 10 % Bis-Tris gel (Life Sciences) and visualized with a Sypro® Ruby protein gel staining, according to the manufacturer's protocol. Immunological detection was performed as described*Chlorophyll fluorescence measurements* – Chlorophyll fluorescence was measured using a JTS-10 spectrometer (Bio Logic SAS, France). A volume corresponding to 2×10^7 cells was dark adapted under stirring at ambient CO_2 for 15 min and then filtered onto a glass fiber filter (PALL Corporation). The filter was fixed in a leaf cuvette and samples were exposed for 5 min to far red light (400 µmol photons m^{-2} s^{-1}) followed by 15 min illumination at 940

μmol photons m^{-2} s^{-1} of red actinic light and 6 min incubation in far red light. Saturation pulses (red light, 7900 μmol photons m^{-2} s^{-1}) were applied every 60 seconds. NPQ was calculated as (Fm/Fm') – 1 (53).

Cell counting – Cells in a 1 ml culture were fixed with 20 μl 0.25 % iodine (w/v in ethanol) and the number of cells/ml was calculated using a Thoma cell counting chamber (Marienfeld, Germany).

Conflict of Interest – The authors declare that they have no conflicts of interest with the contents of this article.

Author Contributions – V.C., S.W., K.K.N. and P.J. designed the research; V.C., P.R., K.G., A.G. and T.B.T. performed the experiments; V.C., P.R., S.W., K.K.N. and P.J. analyzed data; V.C. and P.J. wrote the manuscript.

REFERENCES

1. Moller, I. M., Jensen, P. E., and Hansson, A. (2007) Oxidative modifications to cellular components in plants. *Annu Rev Plant Biol* **58**, 459-481.
2. Li, Z. R., Wakao, S., Fischer, B. B., and Niyogi, K. K. (2009) Sensing and responding to excess light. *Annu Rev Plant Biol* **60,** 239-260.
3. Hohmann-Marriott, M. F., and Blankenship, R. E. (2011) Evolution of Photosynthesis. *Annu Rev Plant Biol* **62,** 515-548.
4. Niyogi, K. K., and Truong, T. B. (2013) Evolution of flexible non-photochemical quenching mechanisms that regulate light harvesting in oxygenic photosynthesis. *Curr Opin Plant Biol* **16,** 307-314.
5. Nilkens, M., Kress, E., Lambrev, P., Miloslavina, Y., Müller, M., Holzwarth, A. R., and Jahns, P. (2010) Identification of a slowly inducible zeaxanthin-dependent component of non-photochemical quenching of chlorophyll fluorescence generated under steady-state conditions in Arabidopsis. *Biochim Biophys Acta* **1797,** 466-475.
6. Briantais, J.-M., Vernotte, C., Picaud, M., and Krause, G. H. (1979) A quantative study of the slow decline of chlorophyll a fluorescence in isolated chloroplasts. *Biochim Biophys Acta* **548,** 128-138.
7. Goss, R., and Lepetit, B. (2015) Biodiversity of NPQ. *J Plant Physiol* **172,** 13-32.
8. Peers, G., Truong, T. B., Ostendorf, E., Busch, A., Elrad, D., Grossman, A. R., Hippler, M., and Niyogi, K. K. (2009) An ancient light-harvesting protein is critical for the regulation of algal photosynthesis. *Nature* **462**, 518-521.
9. Bonente, G., Ballottari, M., Truong, T. B., Morosinotto, T., Ahn, T. K., Fleming, G. R., Niyogi, K. K., and Bassi, R. (2011) Analysis of LhcSR3, a protein essential for feedback de-excitation in the green alga Chlamydomonas reinhardtii. *PLoS Biol* **9**:e1000577.
10. Liguori, N., Roy, L. M., Opacic, M., Durand, G., and Croce, R. (2013) Regulation of light harvesting in the green alga Chlamydomonas reinhardtii: the C-terminus of LHCSR is the knob of a dimmer switch. *J Am Chem Soc* **135,** 18339-18342.
11. Ballottari, M., Truong, T. B., De Re, E., Erickson, E., Stella, G. R., Fleming, G. R., Bassi, R., and Niyogi, K. K. (2016) Identification of pH-sensing sites in the light harvesting complex stress-related 3 protein essential for triggering non-photochemical quenching in *Chlamydomonas reinhardtii*. *J Biol Chem* **291,** 7334-7346.
12. Alboresi, A., Gerotto, C., Giacometti, G. M., Bassi, R., and Morosinotto, T. (2010) *Physcomitrella patens* mutants affected on heat dissipation clarify the evolution of photoprotection mechanisms upon land colonization. *Proc Natl Acad Sci USA* **107,** 11128-11133.
13. Gerotto, C., Alboresi, A., Giacometti, G. M., Bassi, R., and Morosinotto, T. (2012) Coexistence of plant and algal energy dissipation mechanisms in the moss *Physcomitrella patens*. *New Phytol* **196,** 763-773.
14. Niyogi, K. K., Björkman, O., and Grossman, A. R. (1997) Chlamydomonas xanthophyll cycle mutants identified by video imaging of chlorophyll fluorescence quenching. *Plant Cell* **9,** 1369-1380.
15. Anwaruzzaman, M., Chin, B., Li, X., Lohr, M., Martinez, D. A., and Niyogi, K. K. (2004) Genomic analysis of mutants affecting xanthophyll biosynthesis and regulation of photosynthetic light harvesting in *Chlamydomonas reinhardtii*. *Photosyn Res* **82,** 265–276.
16. Pinnola, A., Dall'Osto, L., Gerotto, C., Morosinotto, T., Bassi, R., and Alboresi, A. (2013) Zeaxanthin binds to light-harvesting complex stress-related protein to enhance nonphotochemical quenching in *Physcomitrella patens*. *Plant Cell* **25**, 3519-3534.
17. Gerotto, C., Franchin, C., Arrigoni, G., and Morosinotto, T. (2015) In vivo identification of photosystem II light harvesting complexes interacting with Photosystem II subunit S. *Plant Physiol* **168**, 1747-1761.
18. Li, X., Björkman, O., Shih, C., Grossman, A. R., Rosenquist, M., Jansson, S., and Niyogi, K. K. (2000) A pigment-binding protein essential for regulation of photosynthetic light harvesting. *Nature* **403,** 391-395.
19. Li, X. P., Gilmore, A. M., Caffarri, S., Bassi, R., Golan, T., Kramer, D., and Niyogi, K. K. (2004) Regulation of photosynthetic light harvesting involves intrathylakoid lumen pH sensing by the PsbS protein. *J Biol Chem* **279,** 22866-22874.

20. Fan, M., Li, M., Liu, Z., Cao, P., Pan, X., Zhang, H., Zhao, X., Zhang, J., and Chang, W. (2015) Crystal structures of the PsbS protein essential for photoprotection in plants. *Nature Struct Mol Biol* **22**, 729-735.

21. Niyogi, K. K., Grossman, A. R., and Björkman, O. (1998) Arabidopsis mutants define a central role for the xanthophyll cycle in the regulation of photosynthetic energy conversion. *Plant Cell* **10**, 1121-1134.

22. Bergantino, E., Segalla, A., Brunetta, A., Teardo, E., Rigoni, F., Giacometti, G. M., and Szabo, I. (2003) Light- and pH-dependent structural changes in the PsbS subunit of photosystem II. *Proc Natl Acad Sci USA* **100**, 15265-15270.

23. Correa-Galvis, V., Poschmann, G., Melzer, M., Stühler, K., and Jahns, P. (2016) PsbS interactions involved in the activation of energy dissipation in Arabidopsis. *Nature Plants* **2**, 15225

24. Johnson, M. P., Goral, T. K., Duffy, C. D. P., Brain, A. P. R., Mullineaux, C. W., and Ruban, A. V. (2011) Photoprotective energy dissipation involves the reorganization of photosystem II light-harvesting complexes in the grana membranes of spinach chloroplasts. *Plant Cell* **23**, 1468-1479.

25. Betterle, N., Ballottari, M., Zorzan, S., de Bianchi, S., Cazzaniga, S., Dall'Osto, L., Morosinotto, T., and Bassi, R. (2009) Light-induced dissociation of an antenna hetero-oligomer is needed for non-photochemical quenching induction. *J Biol Chem* **284**, 15255-15266.

26. Johnson, M. P., and Ruban, A. V. (2011) Restoration of rapidly reversible photoprotective energy dissipation in the absence of PsbS protein by enhanced delta pH. *J Biol Chem* **286**, 19973-19981

27. Bonente, G., Passarini, F., Cazzaniga, S., Mancone, C., Buia, M. C., Tripodi, M., Bassi, R., and Caffarri, S. (2008) The occurrence of the psbS gene product in Chlamydomonas reinhardtii and in other photosynthetic organisms and its correlation with energy quenching. *Photochem Photobiol* **84**, 1359-1370.

28. Teramoto, H., Nakamori, A., Minagawa, J., and Ono, T. A. (2002) Light-intensity-dependent expression of Lhc gene family encoding light-harvesting chlorophyll-a/b proteins of photosystem II in Chlamydomonas reinhardtii. *Plant Physiol* **130**, 325-333.

29. Merchant, S. S., Prochnik, S. E., Vallon, O., Harris, E. H., Karpowicz, S. J., Witman, G. B., Terry, A., Salamov, A., Fritz-Laylin, L. K., Marechal-Drouard, L., Marshall, W. F., Qu, L.-H., Nelson, D. R., Sanderfoot, A. A., Spalding, M. H., Kapitonov, V. V., Ren, Q., Ferris, P., Lindquist, E., Shapiro, H., Lucas, S. M., Grimwood, J., Schmutz, J., Cardol, P., Cerutti, H., Chanfreau, G., Chen, C.-L., Cognat, V., Croft, M. T., Dent, R., Dutcher, S., Fernandez, E., Fukuzawa, H., Gonzalez-Ballester, D., Gonzalez-Halphen, D., Hallmann, A., Hanikenne, M., Hippler, M., Inwood, W., Jabbari, K., Kalanon, M., Kuras, R., Lefebvre, P. A., Lemaire, S. D., Lobanov, A. V., Lohr, M., Manuell, A., Meier, I., Mets, L., Mittag, M., Mittelmeier, T., Moroney, J. V., Moseley, J., Napoli, C., Nedelcu, A. M., Niyogi, K., Novoselov, S. V., Paulsen, I. T., Pazour, G., Purton, S., Ral, J.-P., Riano-Pachon, D. M., Riekhof, W., Rymarquis, L., Schroda, M., Stern, D., Umen, J., Willows, R., Wilson, N., Zimmer, S. L., Allmer, J., Balk, J., Bisova, K., Chen, C.-J., Elias, M., Gendler, K., Hauser, C., Lamb, M. R., Ledford, H., Long, J. C., Minagawa, J., Page, M. D., Pan, J., Pootakham, W., Roje, S., Rose, A., Stahlberg, E., Terauchi, A. M., Yang, P., Ball, S., Bowler, C., Dieckmann, C. L., Gladyshev, V. N., Green, P., Jorgensen, R., Mayfield, S., Mueller-Roeber, B., Rajamani, S., Sayre, R. T., Brokstein, P., Dubchak, I., Goodstein, D., Hornick, L., Huang, Y. W., Jhaveri, J., Luo, Y., Martinez, D., Ngau, W. C. A., Otillar, B., Poliakov, A., Porter, A., Szajkowski, L., Werner, G., Zhou, K., Grigoriev, I. V., Rokhsar, D. S., Grossman, A. R. (2007) The Chlamydomonas genome reveals the evolution of key animal and plant functions. *Science* **318**, 245-251

30. Miller, R., Wu, G., Deshpande, R. R., Vieler, A., Gartner, K., Li, X., Moellering, E. R., Zauner, S., Cornish, A. J., Liu, B., Bullard, B., Sears, B. B., Kuo, M. H., Hegg, E. L., Shachar-Hill, Y., Shiu, S. H., and Benning, C. (2010) Changes in transcript abundance in Chlamydomonas reinhardtii following nitrogen deprivation predict diversion of metabolism. *Plant Physiol* **154**, 1737-1752.

31. Mettler, T., Muhlhaus, T., Hemme, D., Schottler, M. A., Rupprecht, J., Idoine, A., Veyel, D., Pal, S. K., Yaneva-Roder, L., Winck, F. V., Sommer, F., Vosloh, D., Seiwert, B., Erban, A., Burgos, A., Arvidsson, S., Schonfelder, S., Arnold, A., Gunther, M., Krause, U., Lohse, M., Kopka, J., Nikoloski, Z., Mueller-Roeber, B., Willmitzer, L., Bock, R., Schroda, M., and Stitt, M. (2014) Systems analysis of the response of photosynthesis, metabolism, and growth to an increase in irradiance in the photosynthetic model organism *Chlamydomonas reinhardtii*. *Plant Cell* **26**, 2310-2350.

32. Zones, J. M., Blaby, I. K., Merchant, S. S., and Umen, J. G. (2015) High-resolution profiling of a synchronized diurnal transcriptome from *Chlamydomonas reinhardtii* reveals Continuous cell and metabolic differentiation. *Plant Cell* **27**, 2743-2769.

33. Duanmu, D., Casero, D., Dent, R. M., Gallaher, S., Yang, W., Rockwell, N. C., Martin, S. S., Pellegrini, M., Niyogi, K. K., Merchant, S. S., Grossman, A. R., and Lagarias, J. C. (2013) Retrograde bilin signaling enables Chlamydomonas greening and phototrophic survival. *Proc Natl Acad Sci USA* **110**, 3621-3626.

34. Maruyama, S., Tokutsu, R., and Minagawa, J. (2014) Transcriptional regulation of the stress-responsive light harvesting complex genes in Chlamydomonas reinhardtii. *Plant Cell Physiol* **55**, 1304-1310.

35. Minagawa, J., and Tokutsu, R. (2015) Dynamic regulation of photosynthesis in *Chlamydomonas reinhardtii*. *Plant J* **82**, 413-428.

36. Förster, B., Osmond, C. B., and Boynton, J. E. (2001) Very high light resistant mutants of *Chlamydomonas reinhardtii*: Responses of photosystem II, nonphotochemical quenching and xanthophyll pigments to light and CO2. *Photosynth Res* **67**, 5-15.

37. Karlsson, J., Clarke, A. K., Chen, Z. Y., Hugghins, S. Y., Park, Y. I., Husic, H. D., Moroney, J. V., and Samuelsson, G. (1998) A novel α-type carbonic anhydrase associated with the thylakoid membrane in Chlamydomonas reinhardtii is required for growth at ambient CO_2. *EMBO J* **17**, 1208-1216.

38. Park, Y.-I., Karlsson, J., Rojdestvenski, I., Pronina, N., Klimov, V., Öquist, G., and Samuelsson, G. (1999) Role of a novel photosystem II-associated carbonic anhydrase in photosynthetic carbon assimilation in *Chlamydomonas reinhardtii*. *FEBS Lett* **444**, 102-105.

39. Allorent, G., Tokutsu, R., Roach, T., Peers, G., Cardol, P., Girard-Bascou, J., Seigneurin-Berny, D., Petroutsos, D., Kuntz, M., Breyton, C., Franck, F., Wollman, F. A., Niyogi, K. K., Krieger-Liszkay, A., Minagawa, J., and Finazzi, G. (2013) A dual strategy to cope with high light in *Chlamydomonas reinhardtii*. *Plant Cell* **25**, 545-557.

40. Xue, H., Tokutsu, R., Bergner, S. V., Scholz, M., Minagawa, J., and Hippler, M. (2015) Photosystem II subunit R is required for efficient binding of light-harvesting complex stress-related protein 3 to photosystem II light-harvesting supercomplexes in *Chlamydomonas reinhardtii*. *Plant Physiol* **167**, 1566-1578.

41. Kucho, K., Yoshioka, S., Taniguchi, F., Ohyama, K., and Fukuzawa, H. (2003) Cis-acting elements and DNA-binding proteins involved in CO_2-responsive transcriptional activation of Cah1 encoding a periplasmic carbonic anhydrase in *Chlamydomonas reinhardtii*. *Plant Physiol* **133**, 783-793.

42. Petroutsos, D., Busch, A., Janssen, I., Trompelt, K., Bergner, S. V., Weinl, S., Holtkamp, M., Karst, U., Kudla, J., and Hippler, M. (2011) The chloroplast calcium sensor CAS is required for photoacclimation in *Chlamydomonas reinhardtii*. *Plant Cell* **23**, 2950-2963.

43. Amarnath, K., Zaks, J., Park, S. D., Niyogi, K. K., and Fleming, G. R. (2012) Fluorescence lifetime snapshots reveal two rapidly reversible mechanisms of photoprotection in live cells of *Chlamydomonas reinhardtii*. *Proc Natl Acad Sci USA* **109**, 8405-8410.

44. Holzwarth, A. R., Miloslavina, Y., Nilkens, M., and Jahns, P. (2009) Identification of two quenching sites active in the regulation of photosynthetic light-harvesting studied by time-resolved fluorescence. *Chem Phys Lett* **483**, 262-267.

45. Molnar, A., Bassett, A., Thuenemann, E., Schwach, F., Karkare, S., Ossowski, S., Weigel, D., and Baulcombe, D. (2009) Highly specific gene silencing by artificial microRNAs in the unicellular alga *Chlamydomonas reinhardtii*. *Plant J* **58**, 165-174.

46. Kindle, K. L., Schnell, R. A., Fernandez, E., and Lefebvre, P. A. (1989) Stable nuclear transformation of Chlamydomonas using the Chlamydomonas gene for nitrate reducatse. *J Cell Biol* **109,** 2589-2601.

47. Gorman, D. S., and Levine, R. P. (1965) Cytochrome f and plastocyanin: their sequence in the photosynthetic electron transport chain of Chlamydomonas reinhardi. *Proc Natl Acad Sci USA* **54**, 1665-1669.

48. Sueoka, N. (1960) Mitotic replication of deoxyribonucleic acid in *Chlamydomonas reinhardtii*. *Proc Natl Acad Sci USA* **46,** 83-91.

49. Schwarz, N., Armbruster, U., Iven, T., Brückle, L., Melzer, M., Feussner, I., and Jahns, P. (2015) Tissue-specific accumulation and regulation of zeaxanthin epoxidase in Arabidopsis reflect the multiple functions of the enzyme in plastids. *Plant Cell Physiol* **56**, 346-357.

50. Ossenbühl, F., Gohre, V., Meurer, J., Krieger-Liszkay, A., Rochaix, J. D., and Eichacker, L. (2004) Efficient assembly of photosystem II in *Chlamydomonas reinhardtii* requires Alb3.1p, a homolog of Arabidopsis ALBINO3. *Plant Cell* **16**, 1790-1800.

51. Tokutsu, R., Kato, N., Bui, K. H., Ishikawa, T., and Minagawa, J. (2012) Revisiting the supramolecular organization of photosystem II in *Chlamydomonas reinhardtii*. *J Biol Chem* **287**, 31574-31581

52. Färber, A., Young, A. Y., Ruban, A., Horton, P., and Jahns, P. (1997) Dynamics of xanthophyll-cycle activity in different antenna subcomplexes in the photosynthetic membranes of higher plants. *Plant Physiol* **115,** 1609-1618

53. Krause, G. H., and Jahns, P. (2004) Non-photochemical energy dissipation determined by chlorophyll fluorescence quenching: Characterization and function. Chlorophyll a fluorescence, Advances in Photosynthesis and Respiration, eds Papageorgiou G & Govindjee (Springer Netherlands), Vol **19**, pp 463-495.

54. Tokutsu, R., Kato, N., Bui, K. H., Ishikawa, T., and Minagawa, J. (2012) Revisiting the supramolecular organization of photosystem II in *Chlamydomonas reinhardtii*. *J Biol Chem* **287**, 31574-31581.

55. Tokutsu, R., and Minagawa, J. (2013) Energy-dissipative supercomplex of photosystem II associated with LHCSR3 in *Chlamydomonas reinhardtii*. *Proc Natl Acad Sci USA* **110**, 10016–10021.

56. Drop, B., Webber-Birungi, M., Yadav, S. K., Filipowicz-Szymanska, A., Fusetti, F., Boekema, E. J., and Croce, R. (2014) Light-harvesting complex II (LHCII) and its supramolecular organization in *Chlamydomonas reinhardtii*. *Biochim Biophys Acta* **1837**, 63-72.
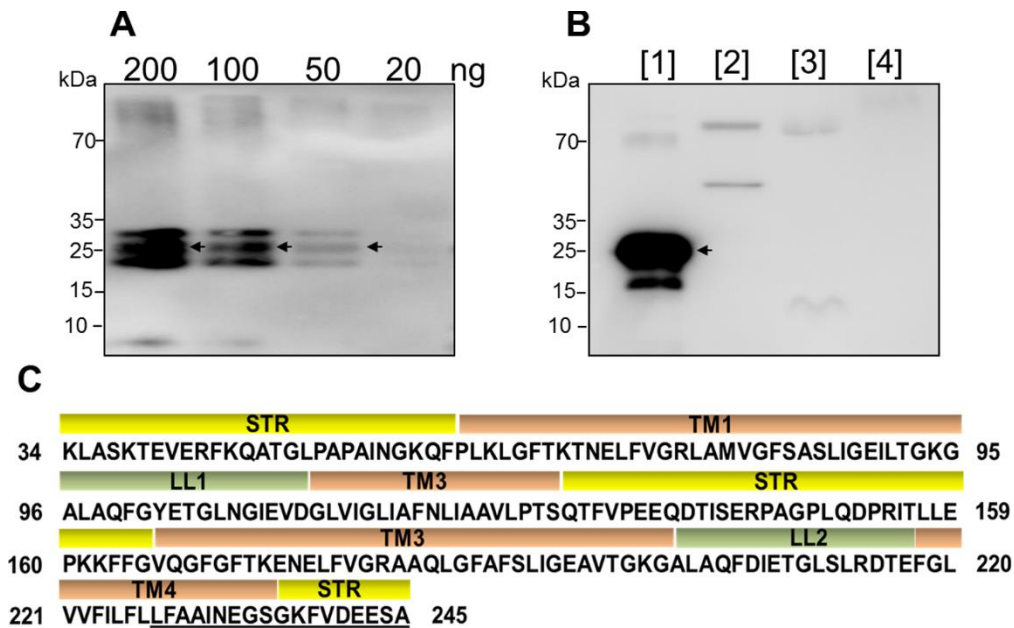
A

kDa 200 100 50 20 ng

70-
35-
25-
15-
10-

B

kDa [1] [2] [3] [4]

70-
35-
25-
15-
10-

C

```
                    STR                              TM1
 34 KLASKTEVERFKQATGLPAPAINGKQFPLKLGFTKTNELFVGRLAMVGFSASLIGEILTGKG  95
              LL1          TM3                     STR
 96 ALAQFGYETGLNGIEVDGLVIGLIAFNLIAAVLPTSQTFVPEEQDTISERPAGPLQDPRITLLE 159
                         TM3                        LL2
160 PKKFFGVQGFGFTKENELFVGRAAQLGFAFSLIGEAVTGKGALAQFDIETGLSLRDTEFGL 220
           TM4              STR
221 VVFILFLLFAAINEGSGKFVDEESA 245
```

FIGURE 1. **Immunoblot detection of the PsbS protein.** (A) Immunodetection of partially purified recombinant PsbS (r-CrPsbS) by the anti-PsbS antibody raised against the C-terminal peptide of *C. reinhardtii* PsbS. (B) Reactivity of the PsbS antibody to [1] r-CrPsbS from total protein extracts of *E.coli* cells, [2] *C. reinhardtii* WT cells (2.9 x 10^5 cells grown under low light in TAP media), [3] thylakoids isolated from *C. reinhardtii* cells (10 µg Chl, cells grown as in [2]), and [4] thylakoids isolated from *A. thaliana* (10 µg Chl). The apparent molecular mass is indicated for each blot. (C) CrPsbS sequence according to (15), indicating the binding site of the antibody (underlined). (STR) Stroma exposed regions; (TM) transmembrane helices; (LL) luminal loops.
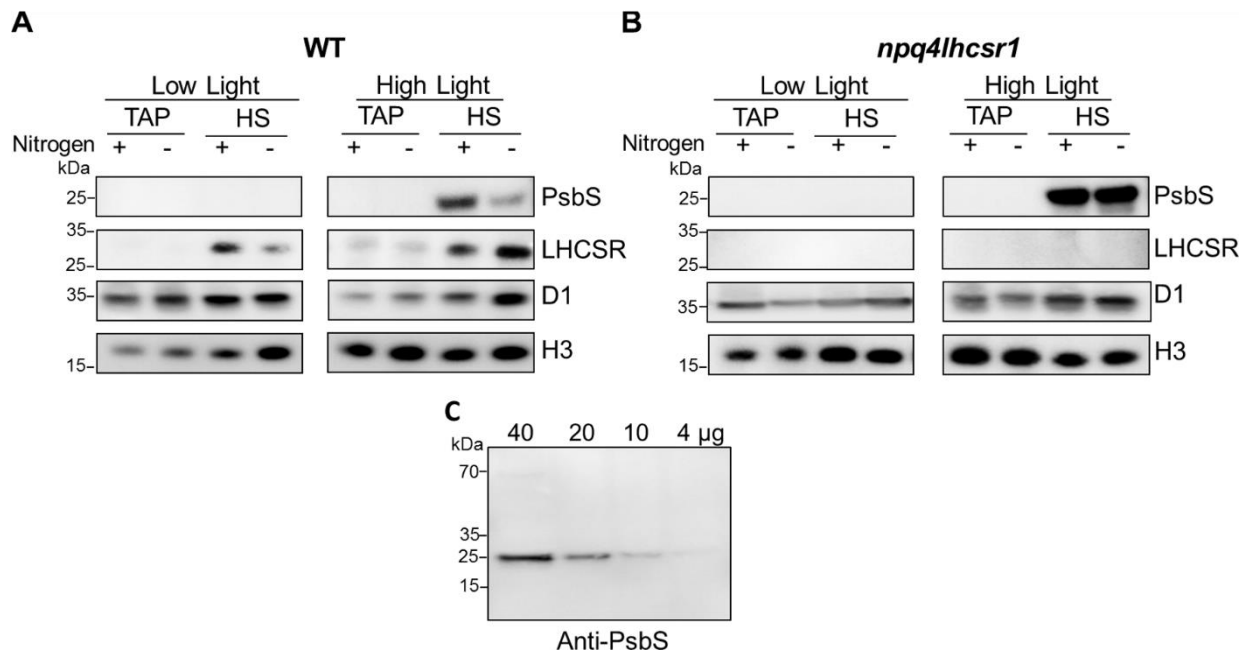
FIGURE 2. **PsbS expression under different light, carbon, and nitrogen conditions**. Cells were grown under LL (30 μmol photons m^{-2} s^{-1}) or HL (480 μmol photons m^{-2} s^{-1}) in either TAP (containing acetate as a carbon source) or HS medium (no additional carbon source in the media). Each growth condition was tested in presence (+N) or absence (-N) of nitrogen by depriving the cells for 48 h in a medium without NH$_4^+$. **(A)** WT (4A$^+$). **(B)** *npq4lhcsr1* mutant. 40 μg of total protein was loaded in each lane for PsbS detection, and 5 μg for LHCSR, D1 and Histone H3 detection. D1 and H3 were used as protein loading control. **(C)** Dilutions series of total protein extracts from HL-acclimated WT (4A$^+$) cells grown in HS medium. Representative blots from 2-4 independent biological replicates are shown. The apparent molecular mass is indicated for each blot.
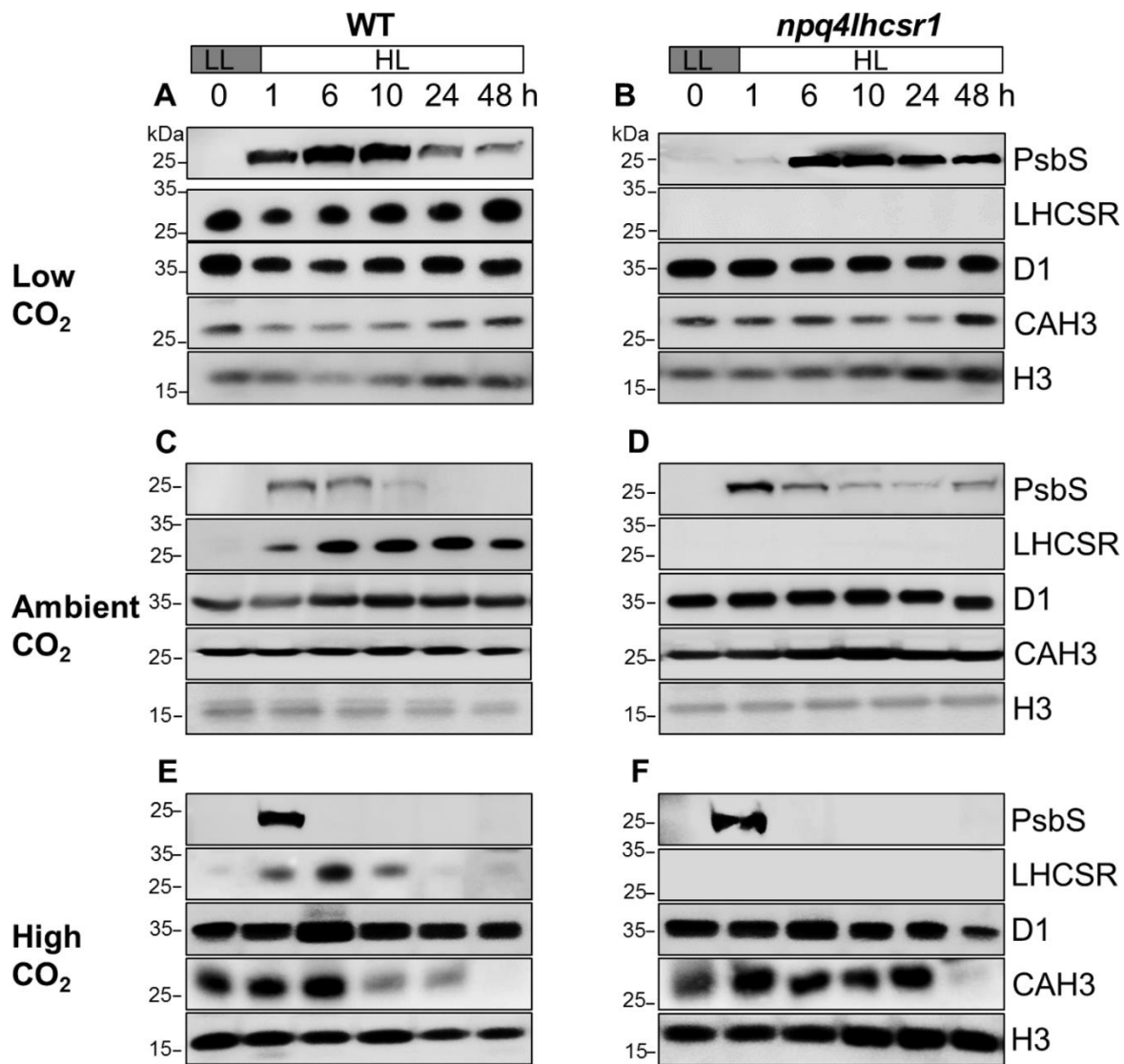
FIGURE 3. **Protein expression after transfer to high light in cells grown at different CO_2 concentrations.** WT (4A[+]) **(A, C, E)** and *npq4lhcsr1* **(B, D, F)** cells were grown in HS medium under LL (30 µmol photons m^{-2} s^{-1}) at either **(A, B)** low CO_2 (no additional air input), **(C, D)** ambient CO_2 (bubbling with air) or **(E, F)** high CO_2 (bubbling with air containing 5 % CO_2). After reaching a cell density of 5 x 10^6 cells/ml, cultures were transferred to HL (480 µmol photons m^{-2} s^{-1} and equal culture volumes were taken for protein extraction at 0, 1, 6, 10, 24, and 48 h after transfer to HL. For immunoblot analysis of PsbS, 40 µg total protein was loaded onto the gels, while 5 µg were used for the other proteins. D1 and H3 were used as protein loading control. CAH3 = carbonic anhydrase. Representative blots from 2-4 independent biological replicates are shown. The apparent molecular mass is indicated for each blot.
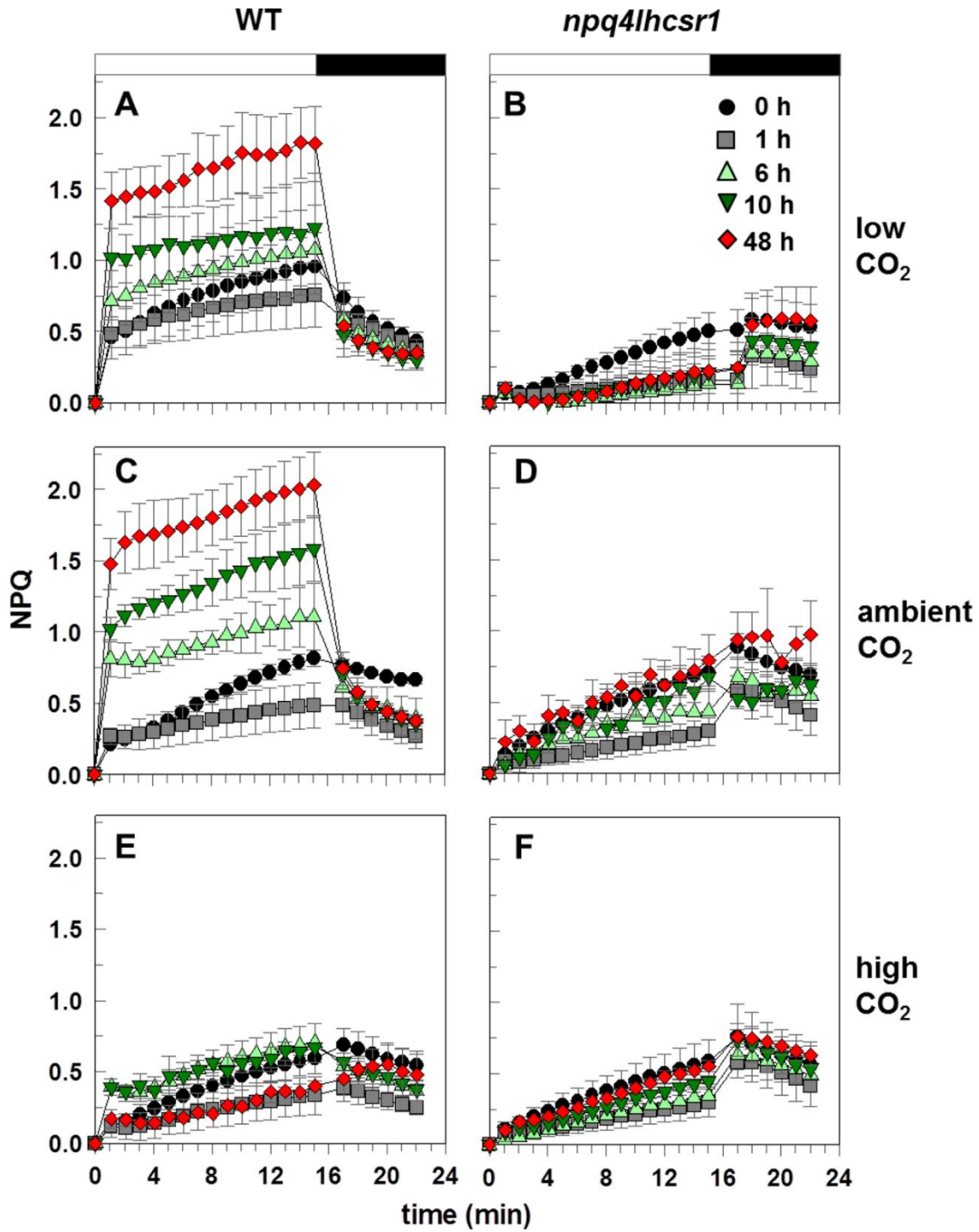
FIGURE 4. **NPQ induction in *C. reinhardtii* cells grown at different CO_2 concentrations**. Cells were grown in HS medium either at low CO_2 **(A, B)**, ambient CO_2 **(C, D)** or high CO_2 **(E, F)**. After growth under LL, cells were transferred to HL. NPQ was determined during 15 min of illumination at 825 μmol photons m^{-2} s^{-1} and a subsequent dark period of 5 min after 0, 1, 6, 10, and 48 h transfer to high light. Values represent mean ± SD (n = 4 biological replicates).
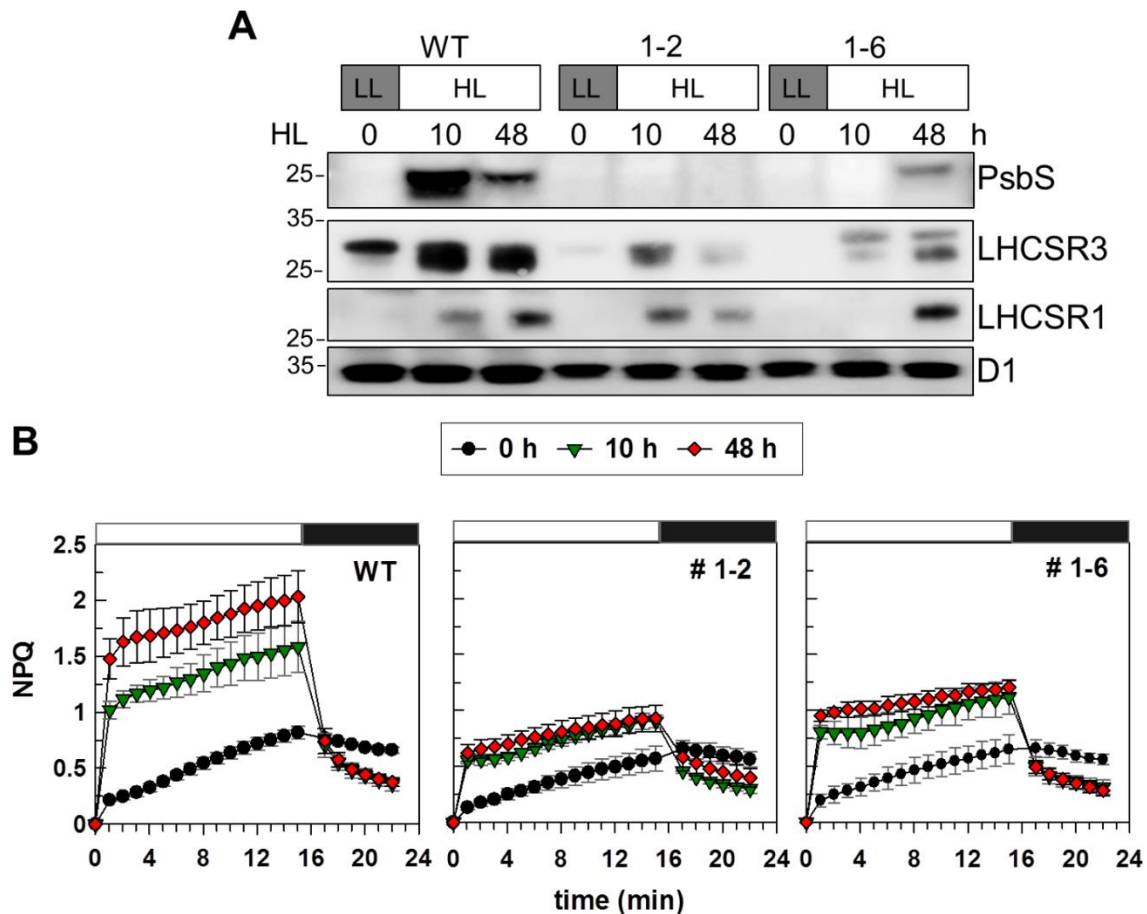
FIGURE 5. **Protein expression and NPQ induction in *PSBS* amiRNA *C. reinhardtii* cells.** Cells were grown in HS medium at ambient CO_2. After growth under LL, cells were transferred to HL. **(A)** Immunoblot analysis of PsbS, LHCSR and D1 protein content. For analysis of PsbS, 40 µg total protein was loaded onto the gels, while 5 µg was used for the other proteins. D1 was used as protein loading control. Representative blots from 2-4 independent biological replicates are shown. The apparent molecular mass is indicated for each blot. **(B)** NPQ was determined in WT and *PSBS* amiRNA lines after 0, 10, and 48 h transfer to HL. Values represent mean ± SD (n = 3-4 biological replicates).
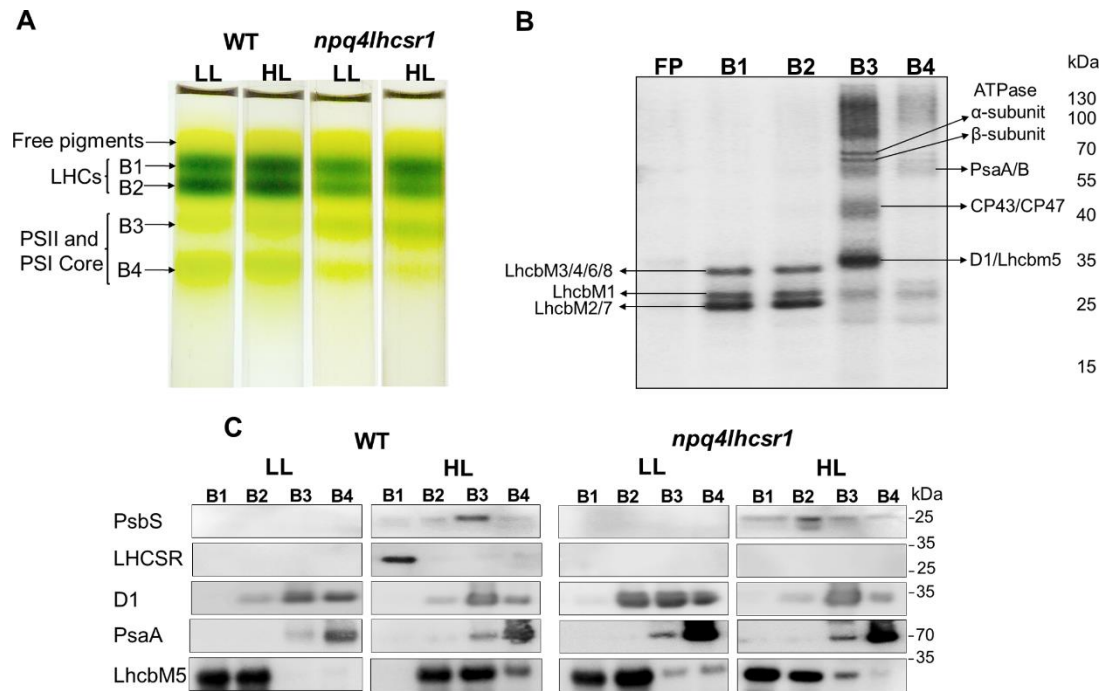
FIGURE 6. **Localization of PsbS in *C. reinhardtii*.** Thylakoids from WT (4A$^+$) and *npq4lhcsr1* cells grown under LL and ambient CO_2 were extracted before and after a 4 h exposure of cells to HL. Thylakoid membranes were solubilized with 1 % α-DM and protein complexes (corresponding to 200 µg chlorophyll) were separated by sucrose gradient centrifugation. **(A)** Separated bands were identified according to (54,55) as: free pigments (FP), dissociated LHCs (B1 and B2: monomers and trimers, respectively), and PSII and PSI enriched fractions (B3 and B4, respectively). **(B)** Proteins in each band were analyzed by NuPAGE® and visualized using a Sypro® Ruby protein staining. The distribution of the proteins is representative for all light treatments and both genotypes. Individual proteins were identified based on their molecular mass as previously reported (56). The apparent molecular mass is indicated on the right side of the gel. **(C)** Immunoblot analysis of representative proteins in each fraction. Representative blots from 2-3 independent biological replicates are shown. The apparent molecular mass is indicated for each blot.
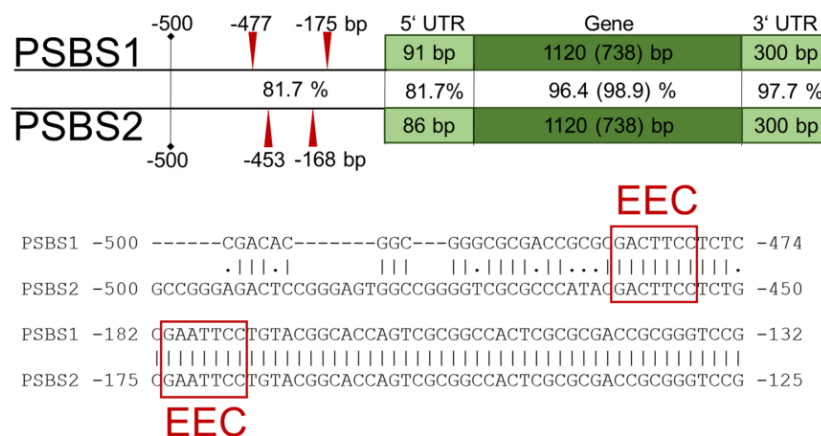

FIGURE 7. **Conserved motifs in the promoter region of PSBS genes that respond to low CO_2.** Two EEC conserved motifs corresponding to enhancer elements of low CO_2 inducible promoters were identified for PSBS1 (at -477 and -175 bp) and PSBS2 (-453 and -168 bp) genes (29). The EEC motif sequence is shown for both genes by a nucleotide sequence alignment upstream of the 5' UTR region. The diagram was modified for the PsbS encoding genes after (32).

5 Manuscript 2

Short title: The Role of PsbS in *Chlamydomonas reinhardtii*

Author for contact details: Peter Jahns

Plant Biochemistry

Heinrich-Heine-University Düsseldorf

Universitätsstr. 1

40225 Düsseldorf, Germany

Tel: +49-211-8113862

E-mail: pjahns@hhu.de

Research Area: Membranes, Transport, and Bioenergetics

One-sentence summary: The PsbS protein in Chlamydomonas increases vitality and reduces light stress sensitivity during high light acclimation independent of energy dissipation

PsbS Contributes to Photoprotection in *Chlamydomonas reinhardtii* Independent of Energy Dissipation

Petra Redekop[a], Natalie Rothhausen[a], Natascha Rothhausen[a], Michael Melzer[b], Laura Mosebach[c], Stefano Caffarri[d], Michael Hippler[c] and Peter Jahns[a,1]

[a]Plant Biochemistry, Heinrich-Heine-Universität Düsseldorf, 40225 Düsseldorf, Germany

[b]Physiology and Cell Biology, IPK Gatersleben, 06466 Gatersleben, Germany

[c]Institute of Plant Biology and Biotechnology, Westfälische Wilhelms Universität, 48143 Münster, Germany

[d]Aix Marseille Univ, CEA, CNRS, BIAM, Plant Genetics and Biophysics, 13009 Marseille, France

[1]**Author for contact:** pjahns@hhu.de

Author contributions: P.R., M.H. and P.J designed and supervised the experiments, and analyzed the data; P.R. performed most of the experiments; N.R. and N.R. contributed to protein and NPQ analysis and performed photoinhibition experiments; L.M. contributed to spectroscopic measurements and data analysis; M.M. contributed to electron microscopy and performed immunogold labelling; S.C. provided the *oePsbS(CC-124)* and *oePsbS(npq4)* strains; P.R. and P.J. conceived the project and wrote the article with contributions of all the authors.

Abstract

Photosynthetic organisms are frequently exposed to excess light conditions and hence to photo-oxidative stress. To counteract photo-oxidative damage, land plants and most algae make use of non- photochemical quenching (NPQ) of excess light energy, in particular the rapidly inducible and relaxing qE-mechanism. In vascular plants, the constitutively active PsbS protein is the key regulator of qE. In the green algae *C. reinhardtii*, however, qE activation is only possible after initial high-light (HL) acclimation for several hours and requires the synthesis of LHCSR proteins which act as qE regulators. The precise function of PsbS, which is transiently expressed during HL acclimation in *C. reinhardtii*, is still unclear. Here, we investigated the impact of different PsbS amounts on HL acclimation characteristics of *C. reinhardtii* cells. We demonstrate that lower PsbS amounts negatively affect HL acclimation at different levels, including NPQ capacity, electron transport characteristics, antenna organization and morphological changes, resulting in an overall increased HL sensitivity and lower vitality of cells. Contrarily, higher PsbS amounts do not result in a higher NPQ capacity, but nevertheless provide higher fitness and tolerance towards HL stress. Strikingly, constitutively expressed PsbS protein was found to be degraded during HL acclimation. We propose that PsbS is transiently required during HL acclimation for the reorganization of thylakoid membranes and/or antenna proteins along with the activation of NPQ and adjustment of electron transfer characteristics, and that degradation of PsbS is essential in the fully HL acclimated state.

INTRODUCTION

Efficient light utilization is essential for the competitiveness and survival of photosynthetic organisms. To ensure sufficient light capture even at low light (LL) intensities, as given on cloudy days or in dense stands, the photosystems (PS) are provided with efficient light-harvesting systems. However, light intensities often vary rapidly in orders of magnitude, so that light energy is frequently absorbed in excess to the light utilization capacity of the photosynthetic apparatus. Absorption of excess light energy is known to induce the generation of reactive oxygen species (ROS) which have a high damaging potential for all cell components (Moller et al., 2007). Plants and algae have developed a number of different short- and long-term acclimation strategies to cope with this risk of photo-oxidative damage, aiming particularly at the reduction of ROS formation (Li et al., 2009).

One important short-term strategy is the dissipation of excess light energy as heat, known as non-photochemical quenching (NPQ), which contributes to photoprotection at different time scales. In the short-term (scale of minutes), the pH-regulated qE component of NPQ provides the most rapid and flexible response to high-light (HL) due to the strict regulation by the thylakoid lumen pH (Briantais et al., 1979). In vascular plants, qE is controlled by the constitutively expressed non-pigment binding protein PsbS (Li et al., 2000), which acts as a sensor of the lumen pH. PsbS becomes activated by protonation of two lumen-exposed glutamate residues (Li et al., 2002; Li et al., 2004) which leads to the activation of qE in the PSII antenna through interaction with light-harvesting antenna complexes (LHC) of PSII (Gerotto et al., 2015; Correa-Galvis et al., 2016a; Sacharz et al., 2017). qE is further modulated by the xanthophyll zeaxanthin which allows fine-tuning of the qE capacity and dynamics (Horton et al., 2008; Jahns and Holzwarth, 2012). Modification of the dynamics of zeaxanthin conversion was recently shown to provide a promising tool to improve the photosynthetic efficiency of plants due to a more rapid short-term acclimation response (Kromdijk et al., 2016). Long-term acclimation of land plants to HL typically requires several days or weeks and occurs at different levels, such as the reduction of light absorption (e.g. through reduction of the antenna size (Bailey et al., 2001) or the increase of leaf thickness (Weston et al., 2000), the adjustment of electron transport and carbon assimilation (Boardman, 1977; Schoettler and Toth, 2014) and the increase of the anti-oxidative capacity (Foyer and Shigeoka, 2011).

The HL acclimation response of the green alga *Chlamydomonas reinhardtii* is largely different and more complex than in land plants. Some reasons for the different regulation are the high mobility of the unicellular alga and the shorter life cycle, which results in a flexible metabolism and allows growth under both phototrophic and heterotrophic conditions (Cardol et al., 2011; Erickson et al., 2015; Polukhina et al., 2016). Like in vascular plants, the dissipation of excess light energy essentially contributes to the short-term HL acclimation response of *C. reinhardtii*. However, the qE-mechanism differs from that in vascular plants in several aspects. In *C. reinhardtii*, the full activation of qE is only possible after several hours of HL acclimation of the cells and requires the synthesis of LHCSR proteins (Peers et al., 2009; Allorent et al., 2013). The pH sensing function and thus pH-regulation of qE is carried out mainly

by the HL-induced LHCSR3 protein (Ballottari et al., 2016), and to minor extent by the UV-induced LHCSR1 protein (Ballottari et al., 2016; Dinc et al., 2016; Kosuge et al., 2018). Moreover, zeaxanthin plays only a minor role in the modulation of the qE capacity (Niyogi et al., 1997). The time of at least 4h required for LHCSR3 synthesis and full qE activation (Allorent et al., 2013; Correa-Galvis et al., 2016b) suggests the demand for a more rapid photoprotective mechanism in the initial phase after exposure to HL. One candidate for this task is the mechanism of state transitions which gives rise to the qT component of NPQ. State transitions regulate the energy distribution between PSII and PSI through redox-regulated, reversible phosphorylation of LHCII proteins (Allen, 2017). In the non-phosphorylated state 1, LHCII transfers the excitation energy to PSII and in the phosphorylated state 2 to PSI. In *C. reinhardtii*, up to 80% of LHCII proteins may become phosphorylated in state 2 (Delosme et al., 1996), in contrast to land plants where only a minor fraction of LHCII is able to interact with PSI. In fact, rapid activation of qT after HL exposure has recently been shown to contribute to photoprotection in *C. reinhardtii* during the initial phase of HL acclimation when the qE capacity is low (Allorent et al., 2013). This feature is in contrast to Arabidopsis, where the contribution of qT to NPQ under HL is negligible (Nilkens et al., 2010).

Another photoprotective process that becomes activated early on during HL acclimation is cyclic electron flow (CEF) around PSI. CEF serves two essential functions: It contributes to the acidification of the thylakoid lumen for efficient ATP synthesis and NPQ activation (Joliot and Johnson, 2011) and furthermore provides photoprotection of PSI by removing excess electrons at the acceptor side of PSI (Suorsa et al., 2012; Johnson et al., 2014). It has been reported earlier, that transition from state 1 to state 2 induces the switch from linear to cyclic electron flow (Finazzi et al., 2002), although the causal relation of both processes has been challenged more recently (Terashima et al., 2012; Takahashi et al., 2013). Nevertheless, the early activation of state transitions and CEF might represent a concerted photoprotective strategy for *C. reinhardtii* during the initial phase of HL acclimation. Indeed, NPQ and CEF are complementary for HL acclimation (Kukuczka et al., 2014). Additionally, the CO_2 availability determines the HL acclimation response of *C. reinhardtii*. It has been shown that the HL-induced expression of LHCSR3 (but not that of LHCSR1) is suppressed at high CO_2 levels (Yamano et al., 2008; Maruyama et al., 2014), which explains why the full activation of qE during HL acclimation occurs only under CO_2 limiting conditions (Correa-Galvis et al., 2016b; Polukhina et al., 2016). High CO_2 availability also stimulates CEF (Lucker and Kramer, 2013; Chapman et al., 2015) and leads to increased stacking of thylakoid membranes (Polukhina et al., 2016). Interestingly, recent work with spinach showed that increased thylakoid membrane stacking favors an increase of CEF (Wood et al., 2018). Thus, enhanced CEF might generally compensate for reduced photoprotection capacity through energy dissipation.

The role of PsbS in *C. reinhardtii* is still under debate. PsbS in *C. reinhardtii* has been described as a HL-induced protein which accumulates only transiently during the first 4-8h of HL exposure and is degraded after about 24h of HL acclimation (Correa-Galvis et al., 2016b; Tibiletti et al., 2016). PsbS

accumulation is strongly dependent on carbon availability: Reduced CO_2 levels favor more pronounced and more stable PsbS accumulation, whereas increased CO_2 concentrations lead to more rapid degradation of PsbS (Correa-Galvis et al., 2016b). Although PsbS accumulates in parallel with the establishment of a high NPQ capacity, the subsequent degradation of PsbS does not result in a decrease of NPQ capacity. Furthermore, PsbS accumulation in the LHCSR deficient *npq4lhcsr1* mutant does not induce reasonable NPQ in HL-acclimated cells (Correa-Galvis et al., 2016b) and over-expression of PsbS is unable to induce pronounced NPQ in LL-acclimated cells (Tibiletti et al., 2016). These characteristics exclude a direct function of PsbS in NPQ. However, knock-down of PsbS results in reduced accumulation of LHCSR proteins and hence in lower NPQ capacity and PsbS is associated with PSII during HL acclimation (Correa-Galvis et al., 2016b). It has thus been proposed that PsbS in *C. reinhardtii* might be required for the activation of LHCSR3-dependent energy dissipation in PSII, possibly by endorsing conformational changes in the light harvesting antenna (Correa-Galvis et al., 2016b). On the other hand, the accumulation of PsbS and LHCSR1, but not of LHCSR3, was found to be inducible in LL-acclimated cells by UV-B light (Allorent et al., 2016). Interestingly, NPQ was inducible in wild-type (WT) strains by a 6h UV-B treatment to similar extent as by 6h HL treatment and to low extent in the LHCSR3-deficient *npq4* mutant, indicating that NPQ activation is possible in absence of LHCSR3 under UV-B (Allorent et al., 2016). Since PsbS alone is unable to promote NPQ induction, it is likely that LHCSR1-dependent NPQ is induced in response to UV-B, supporting the proposed function of LHCSR1 in NPQ due to energy transfer to either LHCII (Dinc et al., 2016) or to PSI (Kosuge et al., 2018).

In the present work, we analyzed the HL acclimation response of *C. reinhardtii* at different levels ranging from morphological changes to thylakoid membrane organization and light utilization characteristics, comparing the response of WT cells with that of PsbS over-expressing, PsbS knock-down and LHCSR3 knock-out lines. Our data suggest that increased PsbS amounts lead to improved resistance against HL stress, independent of a function in NPQ, while the reduction of PsbS and/or LHCSR3 amount results in increased HL sensitivity. This implies that both PsbS and LHCSR3 serve important photoprotective functions in *C. reinhardtii*.

RESULTS

To investigate the impact of different PsbS amounts on HL acclimation, two PsbS over-expressing mutants and one PsbS knock-down mutant were compared with their respective WT. In the two transplastomic over-expressing mutants, *C. reinhardtii* PsbS is constitutively over-expressed either in the WT CC-124 (*oePsbS(CC-124)*) or in the LHCSR3 lacking *npq4* mutant (genetic background WT 4A+) (*oePsbS(npq4)*), in both cases under control of the *PSAA* promoter (Tibiletti et al., 2016). The knock-down mutant *kdPsbS(4A+)* was designed by using artificial microRNA(amiRNA) to silence the *PSBS* genes and showed reduced PsbS accumulation in comparison to the corresponding WT 4A+ (Correa-Galvis et al., 2016b).

PsbS protein degradation is obligatory during HL acclimation

Immunoblot analyses were performed to evaluate the dynamics of the accumulation of PsbS and LHCSR proteins during 48h of HL acclimation (Fig. 1). It has to be noted that for immunoblot analysis of PsbS 8fold higher amounts of total protein (40µg instead of 5µg) were loaded for the samples of all strains, except for both PsbS over-expressing lines, where 5µg of total protein were sufficient to visualize PsbS. For all other proteins, 5µg of total protein was analyzed.

Both WT strains (Fig. 1A, E) and *npq4* cells (Fig. 1C) showed rapid PsbS expression after 1h and maximal PsbS accumulation after 4 to 10h HL exposure. At longer illumination time, PsbS was degraded and no longer detectable after 48h of HL acclimation. PsbS expression in *kdPsbS(4A+)* (Fig. 1F) was strongly down-regulated. Maximal PsbS accumulation to levels of about 25% of maximal WT amounts was found after 4h HL, followed by a degradation below detection levels after 24h HL. As expected, PsbS accumulated to high amounts already under LL conditions in both over-expression lines (Fig. 1B, D). Surprisingly, even the constitutively over-expressed PsbS was degraded at longer HL exposure time, indicating that active degradation of PsbS might be required for HL acclimation (Fig. 1).

LHCSR1 accumulated continuously after transfer from LL into HL in all investigated genotypes. In both PsbS over-expressing lines, *oePsbS(CC-124)* (Fig. 1B) and *oePsbS(npq4)* (Fig. 1D), LHCSR1 accumulation was delayed in comparison with the corresponding genetic background CC-124 (Fig. 1A) and *npq4* (Fig. 1C), respectively. Slightly reduced LHCSR1 at longer HL accumulation time was visible in *kdPsbS(4A+)* (Fig. 1F) compared to the corresponding WT 4A+ (Fig. 1E). LHCSR3 accumulated rapidly and continuously upon HL exposure in the two WT strains, CC-124 (Fig. 1A) and 4A+ (Fig. 1E). In *oePsbS(CC-124)*, LHCSR3 expression was delayed (Fig. 1B) in comparison to CC-124, and in *kdPsbS(4A+)* cells (Fig. 1F), LHCSR3 accumulation was again slightly reduced compared to the corresponding WT 4A+ (Fig. 1E). As expected, no LHCSR3 protein was detectable in the two LHCSR3-deficient strains *npq4* and *oePsbS(npq4)* (Fig. 1C,D). Expression of D1, the core subunit of PSII, was nearly constant during HL acclimation in *oePsbS(CC-124)* and its respective WT (Fig. 2A,B). In contrast, the D1 content decreased during HL acclimation in all other strains (Fig. 1C-F), suggesting an increased sensitivity upon HL in these genotypes.

We conclude, that constitutively expressed PsbS (i) leads to slightly delayed accumulation of LHCSR proteins and (ii) becomes actively degraded after longer HL acclimation time.
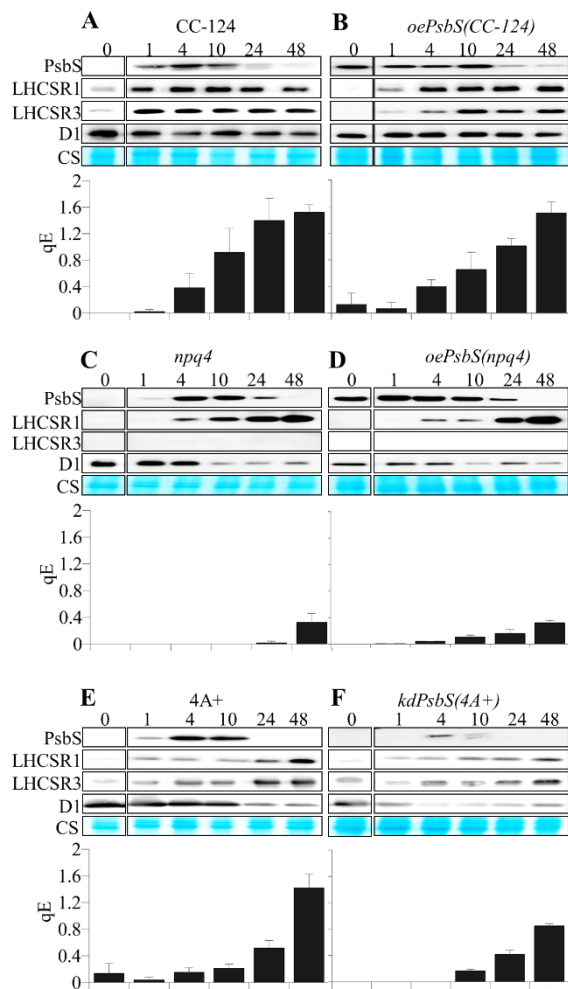

Figure 1. Protein expression and NPQ dynamics**.** A, WT CC-124. B, *oePsbS(CC-124)*. C, *npq4*. D, *oePsbS(npq4)*. E, WT 4A+. F, *kdPsbS(4A+)*. Cells were grown in LL and then exposed to 1, 4, 10, 24 and 48h of HL. For immunoblot analysis, 5µg of total protein was loaded for all samples, except for the analysis of PsbS in both WT strains and the mutant lines *npq4* and *kdPsbS(4A+)*, where 40µg of total protein was loaded. NPQ was determined at the end of 20min illumination with red light (940µmol photons $m^{-2} s^{-1}$) and qE was estimated from the fraction of total NPQ that was dark-reversible within 5min. Data represent mean values ± SD (n = 3-4 biological replicates with 4 technical replicates each).

Increased amounts of PsbS do not increase the NPQ capacity

To investigate the impact of different PsbS amounts on NPQ in LL- and HL-acclimated cells, we determined the qE capacity during 48h of HL acclimation. In comparison with the WT CC-124, the higher amounts of PsbS in *oePsbS(CC-124)* induced a very low qE in LL-acclimated cells, in agreement with (Tibiletti et al., 2016), whereas no positive effect on NPQ was observable during 48h of HL acclimation (Fig. 1A, B). In contrast, higher PsbS amounts rather led to a delayed establishment of maximal qE, indicating that increased PsbS amounts may alter the dynamics of NPQ establishment but not the maximum NPQ capacity. As expected, only very low qE levels were inducible during HL acclimation

in the two LHCSR3-deficient lines *npq4* and *oePsbS(npq4)* (Fig. 1C, D), demonstrating that LHCSR3 is essential for qE and cannot be functionally replaced by PsbS. The low NPQ inducible in *npq4* is likely related to LHCSR1 accumulation. Reduction of the PsbS content in *kdPsbS(4A+)* cells led to reduced qE capacity in comparison with the corresponding WT 4A+ (Fig. 1E, F). It can thus be concluded, that WT amounts of PsbS are required for the establishment of NPQ, but over-accumulation of PsbS does not increase the maximum NPQ capacity.

PsbS localizes predominantly to thylakoid grana regions

Immunogold labelling with a PsbS-specific antibody was applied to localize the PsbS protein in *C. reinhardtii* cells (Fig. 2). In WT cells, only very few PsbS associated gold particles (GP) were found in LL-acclimated (1-2 GP/μm^2) and 24h HL-acclimated (1-2 GP/μm^2) cells (Fig. 2A), supporting the low expression level of PsbS (Tibiletti et al., 2016). As expected, much higher amounts of labels were detectable in *oePsbS(CC-124)* cells grown either constantly in LL (10 GP/μm^2) or after 24h exposure to HL (8 GP/μm^2), in agreement with the estimated about 5fold higher PsbS accumulation in the over-expressing line (Tibiletti et al., 2016). Detailed analysis of the distribution of the GPs revealed that about 80% of the labels localized to the stacked grana regions of the thylakoid membrane and about 20% to the stroma exposed regions. This distribution pattern resembles that of PSII (Allen and Forsberg, 2001), and supports an interaction of PsbS with PSII complexes. Additionally, an average of 30 GP, associated with PsbS, have been detected per pyrenoid, an effect that can be explained by thylakoid membranes spanning through the pyrenoid that are likely reflecting PsbS accumulation in the pyrenoid.
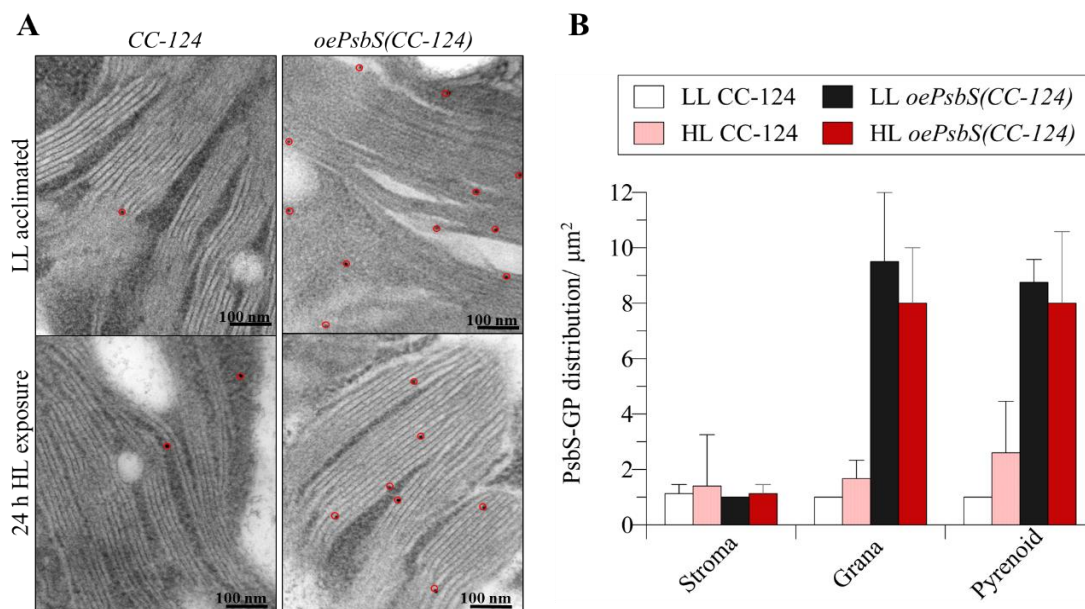

Figure 2. Immunolocalization of PsbS. A, Electron micrographs of thylakoid membranes visualizing immunogold labeled PsbS protein in *oePsbS(CC-124)* and CC-124 cells in LL and 24h HL. Representative images from a total of 30 are shown. For better visualization, immunogold particles are marked by red circles. B, Quantification of the distribution of PsbS between grana and stroma exposed regions of the membrane, as well as inside the pyrenoid. Mean values + SD derived from analysis of 15 images are shown.

PsbS amounts affect HL-induced stress symptoms and thylakoid membrane dynamics

Electron micrographs were analyzed to evaluate the impact of different PsbS amounts on HL-induced changes in cell morphology and thylakoid membrane dynamics. LL-acclimated cells were compared with those from different stages of HL acclimation (1, 10 and 96h) (Supplemental Table S1, Fig. 3). All analyzed strains showed a slight transient increase of the cell size during HL acclimation with maximal diameters occurring after 1h and 10h of HL exposure. Largest cells were found in *npq4* cultures, while WT showed smallest cells. No clear trend of changes during HL acclimation was visible for this parameter, except for *npq4* cells, showing a reduction of the cell size at later stages (> 10h) of HL acclimation (Supplemental Table S1). In most genotypes, the pyrenoid size increased transiently during HL acclimation with maximal size after about 10h of HL acclimation (Supplemental Table S1). The number of starch bodies/cell was significantly ($p \leq 0.01$) higher in the two LHCSR deficient strains *oePsbS(npq4)* and *npq4* compared to all other strains at most stages of HL acclimation, and reached transient maximal values of about 20 after 4-10h of HL exposure in these two lines (Supplemental Table S1). A transient increase of the number of starch bodies peaking at 10h HL exposure was also detectable in WT and *kdPsbs(4A+)* cells, though at lower absolute levels of about 10, but not in *oePsbS(CC-124)* (Supplemental Table S1).

Furthermore, HL acclimation of WT cells was accompanied by the enhanced formation of palmelloids. After 10h of HL, about 20% of the cells were embedded in palmelloids consisting of 3 cells, whereas 24 and 48h of HL exposure led to inclusion of 73% of the cells in palmelloids consisting of 5 cells (Supplemental Table S1). Moreover, the highest number of non-functional WT cells (about 10%) was detectable after 24 and 48h of HL exposure, indicating that the HL-induced stress was highest at these stages of HL acclimation. Strikingly, *oePsbS(CC-124)* cultures did not produce palmelloids and further did not contain any non-functional cells, indicating a higher stress resistance of *oePsbS(CC-124)* and thus a NPQ-independent photoprotective function of PsbS. Compared to WT cells, palmelloid formation was also reduced in *oePsbS(npq4)* cells, but the number of non-functional cells was much higher in this LHCSR3-deficient strain (about 50% of the cells after longest HL exposure time), supporting the photoprotective function of LHCSR3-dependent NPQ. This function was even more obvious in *npq4* cells, which appeared to be the most HL sensitive mutant, with a constant high percentage of cells embedded in palmelloids and at the same time a tremendous high percentage of non-functional cells, with up to 72% at longest HL exposure. Upon reduction of the PsbS amount in *kdPsbS(4A+)*, HL exposure did not induce palmelloid formation, but strongly increased the fraction of non-functional cells to about 60% at longer HL exposure time. The increased photosensitivity of this strain is likely a combined result of reduced PsbS and LHCSR3 amounts, supporting the photoprotective function of both proteins.

The thickness of grana stacks was used as a measure for possible HL-induced changes in the thylakoid membrane structure. WT cells showed a transient increase of grana thickness during HL acclimation by about 50% compared to LL-acclimated cells, with a maximum of about 120nm after 10h

HL exposure (Fig. 3, Supplemental Table S1), which positively correlates with the transient PsbS accumulation. Similar changes were observed for *npq4*, which also showed unaltered PsbS expression. Also the *oePsbS(CC-124)* and *kdPsbS(4A+)* mutants showed transient patterns, although the transient modification was less pronounced, indicating that different PsbS amounts do not affect the general HL response of thylakoid membrane organization. Only the *oePsbS(npq4)* mutant did not exhibit a transient increase, but rather a slight transient decrease of grana thickness during HL acclimation. The different genotypes further differed in absolute values of thylakoid membrane thickness, although most differences were not statistically significant. Thickest grana were found in *kdPsbS(4A+)* and lowest in *oePsbS(npq4)* (Fig. 3, Supplemental Table S1), pointing at a possible impact of PsbS and/or LHCSR3 amounts on thylakoid membrane stacking.
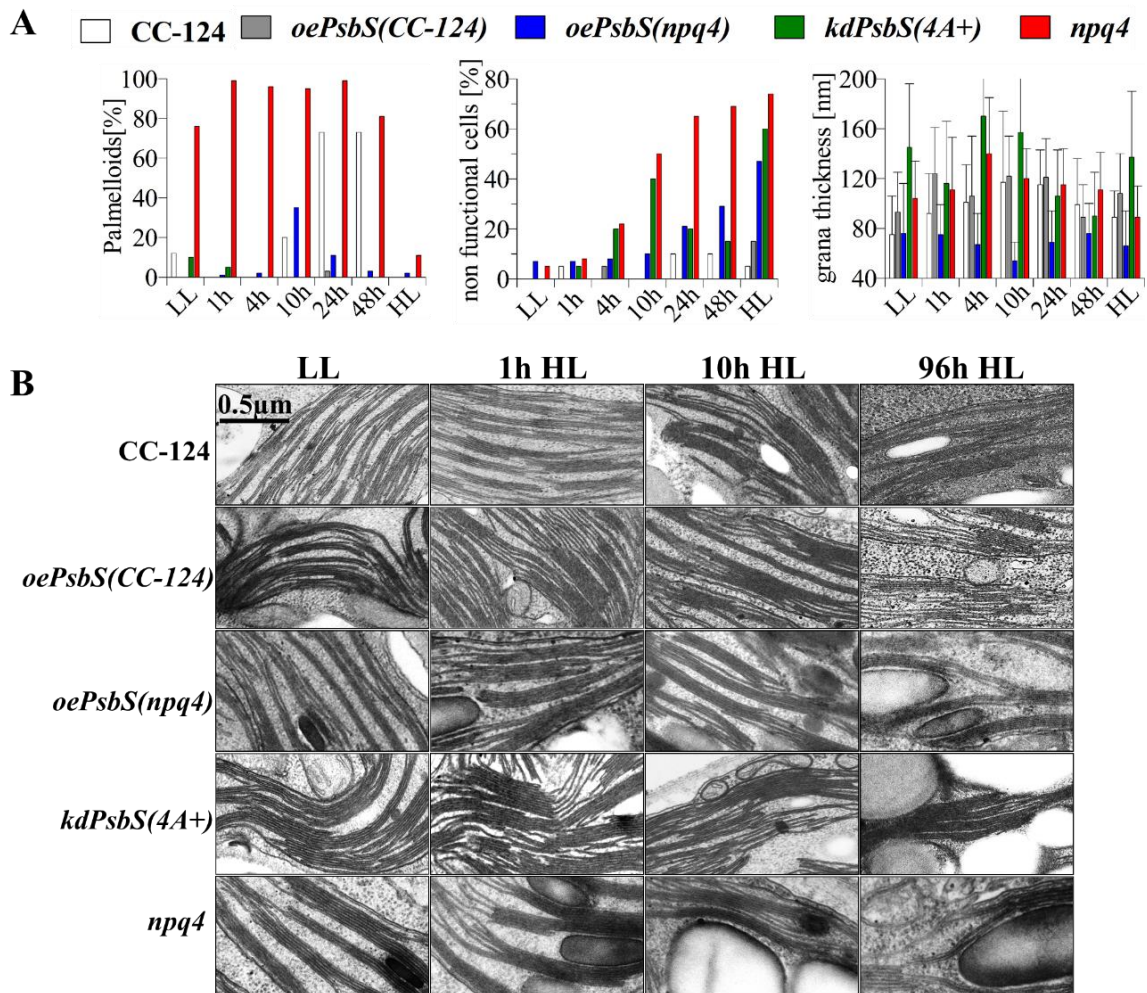

Figure 3. Cell and thylakoid membrane morphology. LL-acclimated cells were exposed for up to 96h to HL and morphology of cells and thylakoid membranes were derived from light and electron microscopic images. A, fraction of cells organized in palmelloids (left panel), fraction of non-functional cells (middle panel) and thickness of grana thylakoids (right panel). B, Electron micrographs of the thylakoid membrane structure in CC-124, *oePsbS(CC-124)*, *oePsbS(npq4)*, *kdPsbS(4A+)* and *npq4* cells, as indicated. Representative images (from a total of 30) are depicted for cells acclimated to LL or after 1h, 10h or 96h of HL acclimation. Scale bar = 500 nm.

PsbS and LHCSR amounts affect HL acclimation of electron transfer and functional PSII antenna size

Chlorophyll fluorescence induction transients (= OJIP transients) were measured at LL and HL (72h) acclimated states to evaluate differences in electron transfer processes and in the PSII antenna size. Figure 4A shows the fluorescence increase from O (F_0) up to the P level (F_M). The light-induced fluorescence increase was reduced in HL-acclimated cells compared to LL-acclimated ones in all genotypes, reflecting that the F_v/F_m decreases during HL acclimation. O-J kinetics provide information about the antenna size of PSII (Malkin et al., 1981). Upon HL acclimation, the O-J rise became significantly slower in CC-124 ($p \leq 0.05$), remained nearly unchanged in the two PsbS over-expressing lines and in WT 4A+, but became significantly ($p \leq 0.001$) faster in *kdPsbS(4A+)* and *npq4* cells (Fig. 4 C,D). This indicates a slight reduction of the functional PSII antenna size in CC-124, but an increase of the PSII antenna size in *kdPsbS(4A+)* and *npq4,* implying that LHCSR3 and/or PsbS are required for the adjustment of the functional PSII antenna size during HL acclimation. Analysis of the J-P phases revealed that LL-acclimated cells of all genotypes showed a faster J-I rise and a slower I-P rise than HL-acclimated cells (Fig. 4B). This indicates a faster reduction of the PQ pool and a slower electron transfer to PSI in LL-acclimated cells, in agreement with the HL acclimation responses known from Arabidopsis (Schumann et al., 2017). In HL-acclimated *kdPsbS(4A+)* cells, however, electron transfer from PSII to PSI was generally slowed down. It can thus be concluded that all strains, except *kdPsbS(4A+),* show the typical HL acclimation response of electron transfer from PSII to PSI and that PsbS and/or LHCSR3 are needed for reorganization of the functional PSII antenna size upon HL acclimation.
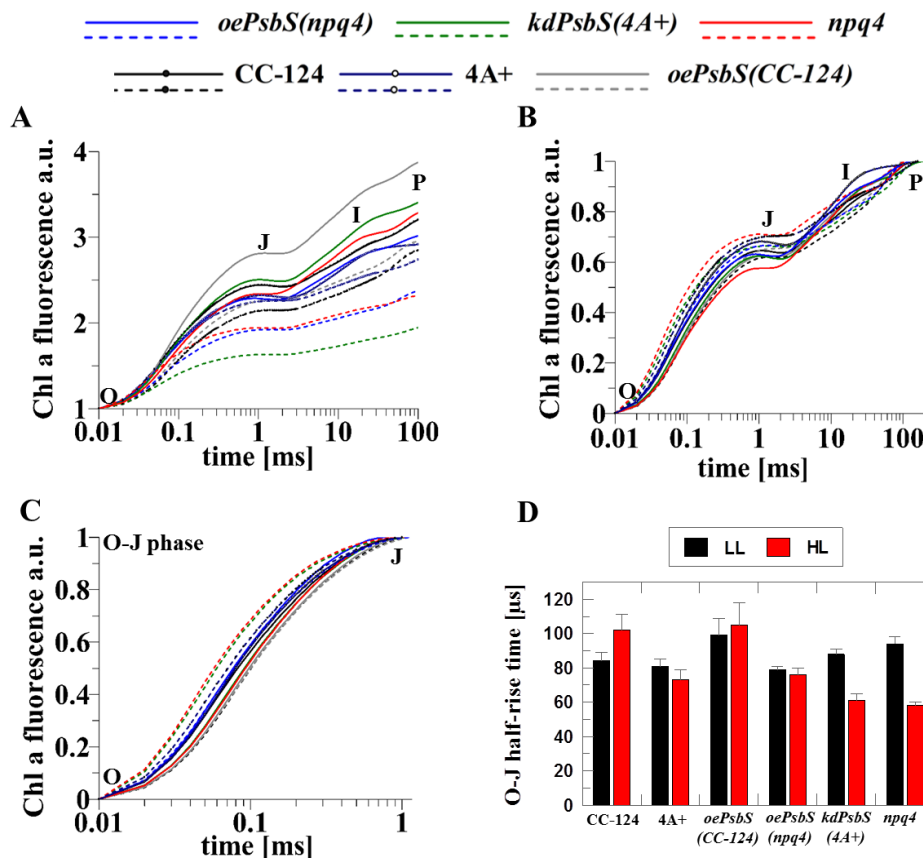
Figure 4. Chl a fluorescence induction transients. A, Entire kinetic showing all phases from O-P. B, normalized O-P transient. C, normalized O-J transient. D, half-rise time for O-J rise in µs. Solid lines represent LL-acclimated cells, dashed lines represent HL-acclimated cells. Normalization of the different transitions allows a direct evaluation of the fluorescence kinetics. O = original fluorescence, F_0; J and I = intermediate states; P = F_M, fluorescence peak. Mean values of 10 measurements are shown. SD < 0.035, corresponding to about twice the size of the line width.

Reduced PsbS amounts affect energy transfer to PSI during HL acclimation

PSI/PSII ratios were derived from ECS measurements in presence and absence of PSII inhibitors (Fig. 5A). No significant changes of the PSI/PSII ratio were detectable among the different genotypes and during HL acclimation. Only the LHCSR deficient *npq4* mutant showed a lower ratio in the LL-acclimated state and an increase upon longer time of HL exposure (Fig. 5A), indicating a HL-induced degradation of PSII, in accordance with the HL stress sensitivity of this strain (Table 1).

Low temperature Chl fluorescence emission spectra were recorded for whole cells from selected acclimation states (LL, 10h HL, 48h HL) to assess possible changes in PSII and PSI fluorescence emission at about 685 and 710nm, respectively, during HL acclimation. In general, the relative contribution of PSI related fluorescence emission around 710nm was increased after 48h HL acclimation in all genotypes (Fig. 5B), although the emission spectra of all LL-acclimated cells showed strong variations, particular when comparing the strains derived from WT CC-124 (CC-124 and *oePsbS(CC-124)*) with those derived from WT 4A+ (4A+, *oePsbS(npq4)*, *kdPsbS(4A+)* and *npq4*). For most genotypes, cells exposed for 48h to HL exhibited a slight increase of the PSI related fluorescence emission. However, a significant

(p≤0.05) increase was detected for *npq4* and particularly *kdPsbS(4A+)* mutants (Fig. 5B). The increase in fluorescence emission at 710nm in HL-acclimated *npq4* cells is in agreement with the determined increase of the PSI/PSII ratio during HL acclimation in this mutant (Fig. 5A). The strong increase in the *kdPsbS(4A+)* mutant, however, is likely related to uncoupling of LHCI proteins from the PSI reaction center. The latter conclusion can be derived from the difference of the emission maximum of PSI between *kdPsbS(4A+)* and all other strains. While both WT strains, both PsbS over-expressing lines and the *npq4* mutant showed a red-shift of the emission maximum of the PSI related peak during HL acclimation by about 3nm, the *kdPsbS(4A+)* did not show this shift during HL acclimation (708.5-709nm) (Fig. 5C). The lower wavelength of the emission maximum is a typical feature of a high portion of uncoupled LHCI (Schmitz et al., 2012). Taken together, the low temperature fluorescence emission spectra underline the above described HL sensitivity of *npq4* and *kdPsbS(4A+)*, and thus support an important role of PsbS and LHCSR3 in photoprotection.
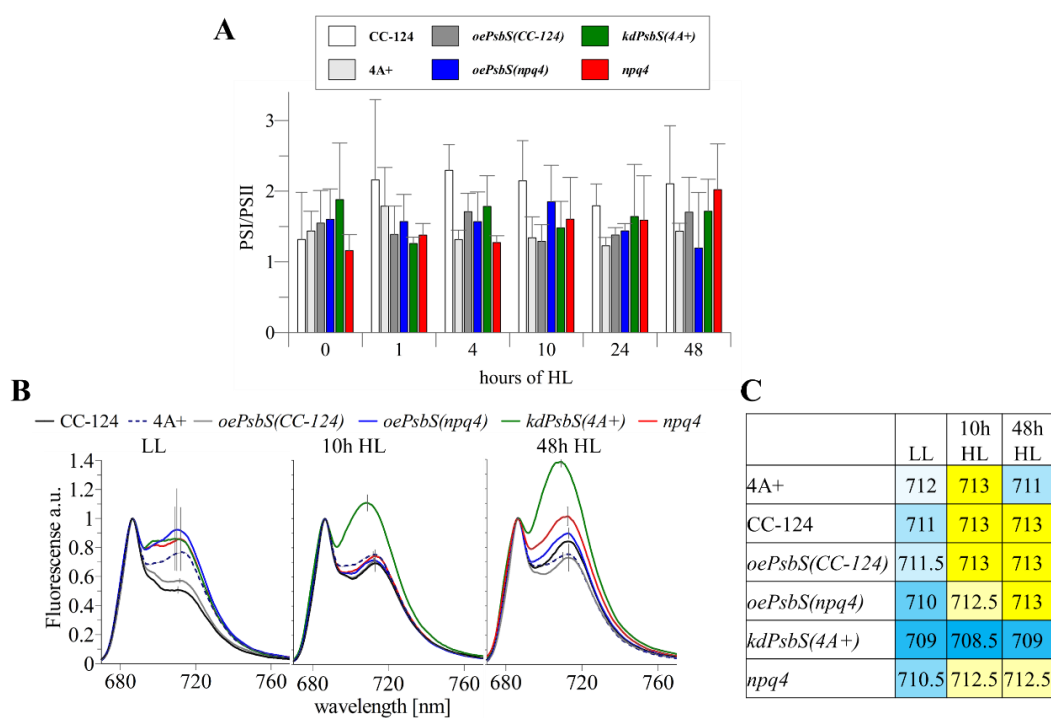

		10h HL	48h HL
	LL		
4A+	712	713	711
CC-124	711	713	713
oePsbS(CC-124)	711.5	713	713
oePsbS(npq4)	710	712.5	713
kdPsbS(4A+)	709	708.5	709
npq4	710.5	712.5	712.5

Figure 5. PSI/PSII ratios and 77K fluorescence emission spectra. A, PSI/PSII ratios. The PSI/PSII ratio at different stages of HL acclimation was calculated from the charge separation capacity of PSI and PSII derived from electrochromic shift measurements at 520nm. B, 77K emission spectra. Cells (equivalent to 2µg of total Chl) acclimated to LL or after HL exposure for 10h and 48h were excited at 435nm and the fluorescence emission spectra were recorded in the range from 670 – 770nm. Traces were normalized at 686nm. The shown spectra represent averages of 3 biological replicates with 5 technical replicates each. C, Wavelength of emission maximum of PSI fluorescence. The values were derived from the traces shown in panel B, as indicated by the respective bars at the maximum of the fluorescence emission peak deriving from PSI (708.5-713nm).

Different amounts of PsbS modify electron transfer at the PSI acceptor side

We further investigated the transient P700 oxidation and re-reduction kinetics from dark-to-light and re-reduction kinetics during light-to-dark transition in vivo in the presence of DCMU and HA, so that only CEF can be analyzed. The P700 oxidation kinetics upon dark-to-light transition at non-saturating light intensities was slightly faster or remained unaltered (within the statistical error) in most genotypes when comparing LL-acclimated and HL-acclimated cells. Only *kdPsbS(4A+)* cells showed significantly faster oxidation in HL than in LL. Moreover, the two PsbS over-expressing lines revealed slower P700 oxidation kinetics than their respective WT strains, although less pronounced for *oePsbS(npq4)* when compared to the corresponding background strain *npq4* (Fig. 6A). These character-istics indicate that different amounts of PsbS lead to modifications of electron transfer at the PSI acceptor side. Re-reduction of P700 during subsequent light-to-dark transition was found to be faster in all HL-acclimated lines as compared to LL-acclimated cultures, indicating enhanced electron transfer on the donor side in HL-acclimated cells. However, this HL acclimation response was independent of PsbS, since similar changes and rates were determined for the different PsbS affected mutants in comparison with the corresponding WT (Fig. 6B).
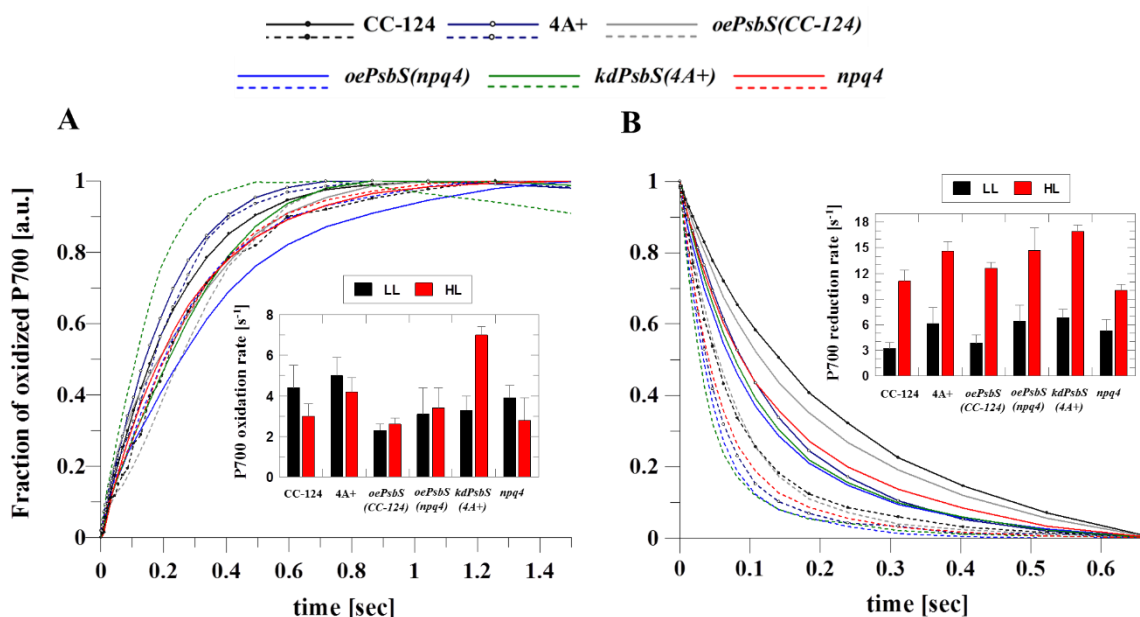

Figure 6. P700 oxidation and reduction kinetics. A, Light-induced P700 oxidation. B, P700 re-reduction upon light-dark transition. Measurements were performed in the presence of DCMU and HA, applying a light intensity of 150μmol photons m^{-2} s^{-1}. Averages of 3-4 biological replicates are shown. Solid lines indicate LL-acclimated cells, dashed lines indicate 48h HL-acclimated cells. Table inserts show mean values (+SD) of the first order rate constants determined from mono-exponential fits.

The rate of CEF increases upon HL acclimation independent of the PsbS amount

We further analyzed the apparent rate of CEF through P700 according to (Takahashi et al., 2013) and determined a 2 to 3.5fold increase of CEF after HL acclimation (Fig. 7). Both PsbS over-expressing lines and *npq4* showed similar CEF rates as their respective WT in LL-acclimated cells, whereas CEF

rates in LL-acclimated *kdPsbS(4A+)* were slightly (but not significantly) higher than those of its respective WT. When comparing the absolute rates of the different genotypes in the HL-acclimated state, again only *kdPsbS(4A+)* showed slightly (but not significantly) higher CEF rates than its WT, whereas both PsbS over-expressing strains showed nearly identical CEF rates as their corresponding control strains. These data thus support the photoprotective role of increased CEF rates during HL acclimation, and this HL response seems to be independent of the PsbS amount.
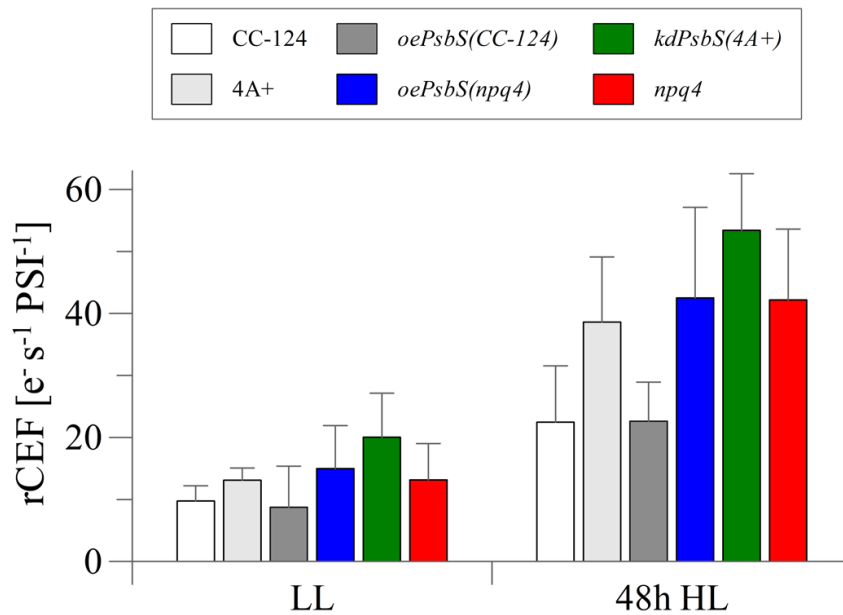

Figure 7. Rate of cyclic electron flow (CEF). The rate of CEF was determined for LL-acclimated and HL-acclimated cells from the initial maximal rate of P700 oxidation and the fraction of reduced P700 in the steady state as described in (Takahashi et al., 2013).

Xanthophyll conversion and PSII efficiency under photoinhibitory conditions

To evaluate the susceptibility of the different genotypes to photoinhibition, xanthophyll conversion and PSII quantum yield (F_v/F_m) were measured in LL-acclimated cells and in cells from different HL acclimation states exposed to 1.5h photoinhibitory light (1000µmol photons m^{-2} s^{-1}) followed by a 0.5h recovery phase in LL (15µmol photons m^{-2} s^{-1}). The VAZ pool size did not change during the photoinhibitory treatment, but generally increased during HL acclimation (Fig. 8A). In LL-acclimated cells, similar values were determined for all genotypes ranging between about 45-50 VAZ per 1000 Chl (a+b). The VAZ pool size increased in all genotypes to values ranging from about 65 VAZ per 1000 Chl (a+b) in *kdPsbs(4A+)* cells to about 85 VAZ per 1000 Chl (a+b) in *npq4* cells (Fig. 8A). This increase in VAZ pool size in all genotypes is a typical long-term response to HL and reflects the photoprotective role of the xanthophyll cycle in *C. reinhardtii*. Hence, the strongest increase of the VAZ pool in *npq4* supports the highest sensitivity to long-term HL exposure in this mutant.

The de-epoxidation state (DEPS) of the VAZ pool defines the fraction of de-epoxidized epoxy groups of the xanthophyll cycle pigments and finally reflects the trans-thylakoid pH gradient, which regulates the violaxanthin (Vx) de-epoxidase (VDE) activity and thus zeaxanthin (Zx) synthesis (Jahns

et al., 2009). Compared to cells acclimated to 10h and 48h of HL, LL-acclimated cells displayed the lowest initial DEPS values (10-20%) and the strongest DEPS increase (up to 50-60%) in response to 1.5h of photoinhibitory treatment (Fig. 8B). Cells exposed to HL for 10h and 48h already showed high DEPS values before exposure to photoinhibitory conditions, reflecting that those cells already contain high levels of zeaxanthin (Zx) (Fig. 8B). However, no further significant increase of the DEPS was visible during the photoinhibitory treatment of HL-acclimated cells, indicating that the VDE already reached maximal activity in the HL-acclimated state. It is further worth to note, that highest DEPS values were found in all genotypes after 1.5h photoinhibitory treatment of LL-acclimated cells, indicating that the convertibility of Vx to Zx becomes reduced during HL acclimation. After transfer of cells from photoinhibitory light to LL (Fig. 8B, recovery phase) DEPS values decreased in all cases irrespective of the light acclimation state. However, the decrease of the DEPS was highest in LL-acclimated cells and lowest in 48h HL-acclimated cells (Fig. 8B), indicating that prolonged HL acclimation leads to down-regulation of the zeaxanthin epoxidase (ZEP) activity. Comparing the different genotypes, the most ob-vious trend was detectable for the reconversion of Zx to Vx in the recovery phase, where the two mutants *kdPsbs(4A+)* and *npq4* exhibited less efficient conversion among all genotypes. This suggests that ZEP activity is reduced more strongly in these two mutants, reflecting again the high HL sensitivity of these two strains.

The F_v/F_m (Fig. 8C) of all genotypes was similar before exposure to photoinhibitory treatment, ranging from values between 0.5 and 0.6. Only in 48h HL acclimated cells, the F_v/F_m of the two WT strains was slightly increased compared to the mutants (Fig. 8C, 48h HL, control). As expected, the photoinhibitory treatment resulted in significantly decreased F_v/F_m ratios in all strains. For most geno-types, the strongest decrease was observed in LL-acclimated cells, suggesting that HL acclimation im-proves the HL resistance of the cells. Only the two LHCSR3 deficient mutants, *oePsbS(npq4)* and *npq4*, showed the largest reduction of the PSII quantum yield in 48h HL-acclimated cells (Fig. 8C), supporting the photoprotective role of LHCSR3 during HL acclimation. Recovery of the F_v/F_m during subsequent LL exposure (Fig. 8C, recovery) was most efficient in the two WT strains and the PsbS over-expressing line *oePsbs(CC-124)*. In these three genotypes, the initial F_v/F_m was fully restored with 30min of LL recovery. In all other mutants, initial F_v/F_m was not recovered, supporting again the photoprotective role of PsbS and LHCSR3 during HL acclimation.
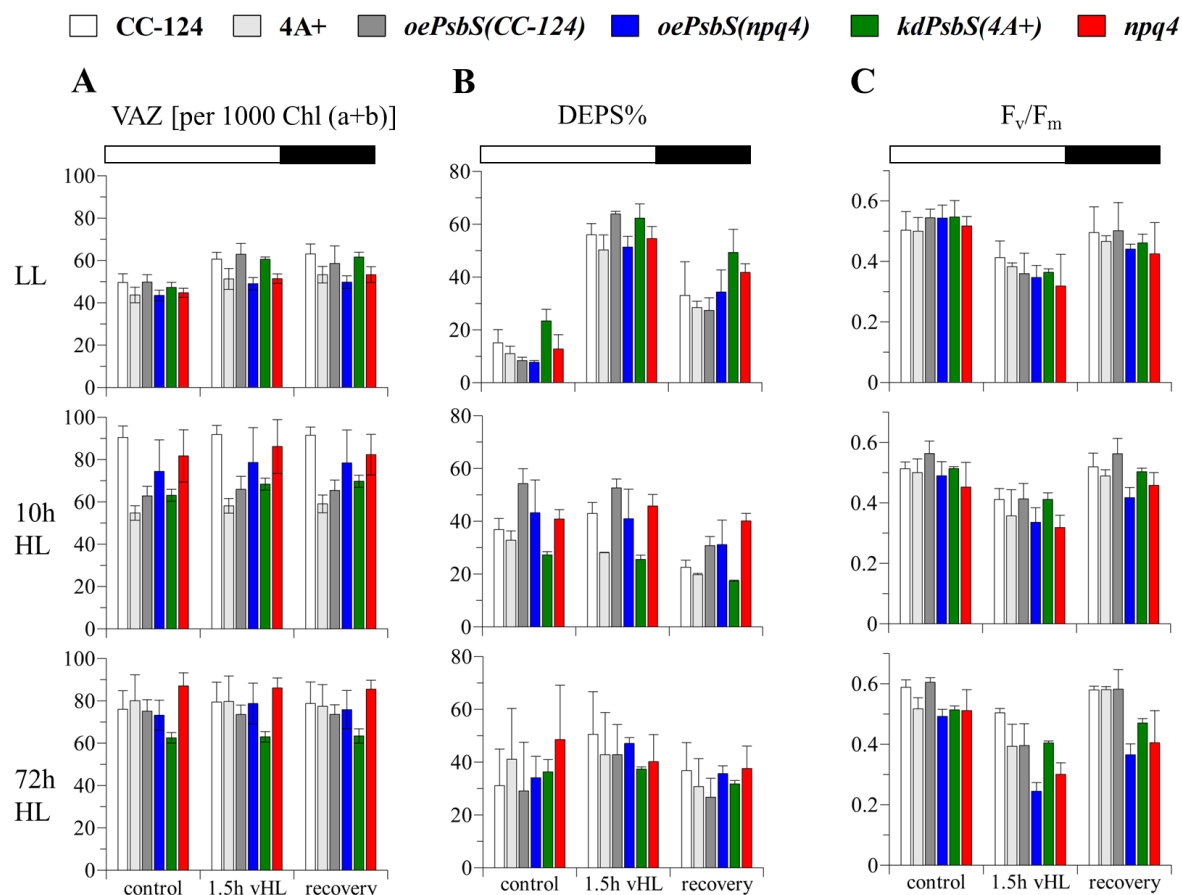
Figure 8. Xanthophyll conversion and photoinhibition. A, Pool size of the xanthophyll cycle pigments violaxanthin (V), antheraxanthin (A) and zeaxanthin (Z) (= VAZ pool). Values are normalized to the total chlorophyll content [mmol/mol Chl (a+b)]. B, De-epoxidation state (DEPS) of VAZ pigments, calculated as (Z+0.5A)/(V+A+Z)*100. C, F_v/F_m ratio. VAZ, DEPS and F_v/F_m valus were determined before (control) and after (very high light: vHL) 1.5h photoinhibitory treatment at 1000µmol photons m^{-2} s^{-1} and after a subsequent 30min recovery phase at 15µmol photons m^{-2} s^{-1} (recovery). All data represent mean values ± SD of 3 biological replicates (n = 3).

DISCUSSION

In this work we addressed the impact of altered PsbS and LHCSR3 amounts on photosynthetic performance and the HL acclimation response of *C. reinhardtii*. Our data support the view that increased amounts of PsbS improve the HL resistance, while lower amounts of PsbS and absence of LHCSR3 severely affect the HL acclimation response, suggesting an essential photoprotective role of both proteins in *C. reinhardtii*.

HL acclimation in WT cells is known to involve the generation of a high NPQ capacity concomitant with the sustained accumulation of LHCSR proteins (Peers et al., 2009) and the transient accumulation of PsbS (Correa-Galvis et al., 2016b; Tibiletti et al., 2016). Apart from these known features, HL acclimation of WT strains was found to be accompanied by the following alterations: (i) transient formation of palmelloids, (ii) transient changes of thylakoid membrane stacking, (iii) reduced functional PSII antenna size, (iv) accelerated P700 reduction and increased CEF, and (v) increase of the VAZ pool size. Most of these characteristics reflect typical HL acclimation responses also known from land plants (Schumann et al., 2017). In particular the formation of palmelloids, however, represents a unique feature of some unicellular algae, including *C. reinhardtii*. Palmelloids are clusters of cells embedded in secreted exopolysaccharides (Crayton, 1982) which are typically formed by *C. reinhardtii* cells in response to stress (Khona et al., 2016). The transient formation of palmelloids in WT cells in response to HL exposure is thus an indicator of transient stress of cells during HL acclimation. The time range of palmelloid formation largely coincided with the transient accumulation of PsbS, suggesting that PsbS contributes to photoprotection during HL acclimation either by supporting NPQ activation or other changes required for optimal HL acclimation. In agreement with this interpretation, over-expression of PsbS in the WT background (*oePsbS(CC-124)*) nearly completely suppressed palmelloid formation (Fig. 3). However, reduction of the PsbS content (*kdPsbS(4A+)*) did not result in increased palmelloid formation, but instead the fraction of non-functional cells increased (Fig. 3A), Interestingly, knock-out of LHCSR3 in *npq4* showed highest levels of both non-functional cells and palmelloid formation, supporting an essential photoprotective role of LHCSR3 during HL acclimation. Since over-expression of PsbS in the *npq4* background (*oePsbS(npq4)*) strongly reduced palmelloid formation and to a lower extent also the level of non-functional cells, the HL sensitivity of *npq4* is only partly related to NPQ-deficiency. This suggests that PsbS, and possibly also LHCSR3, contribute to photoprotection in an NPQ-independent way. Because LHCSR3 accumulation is reduced upon knock-down of PsbS (Fig. 1; (Correa-Galvis et al., 2016b)) it can be speculated that both proteins interact during HL acclimation. One possible NPQ-independent function could be related to the HL-induced reorganization of the PSII antenna and/or the thylakoid membrane, since both parameters were affected by reduced amounts of PsbS and/or LHCSR3 (Figs. 4 and 5).

At the level of electron transport, the typical HL responses were not severely affected by different PsbS amounts. Only cells with reduced PsbS content (*kdPsbS(4A+)*) showed some peculiarities such as a faster P700 oxidation (Fig. 6) in the HL-acclimated state and the highest rates of CEF (Fig. 7).

Moreover, *kdPsbS(4A+)* lines revealed the probable presence of uncoupled LHCI (Fig. 5). All these features point to alterations at the level of PSI, suggesting a role of PsbS in HL acclimation of PSI function or organization. Together with the largest functional PSII antenna size in the HL-acclimated state observed for this mutant (Fig. 4), this supports a role of PsbS in the reorganization of both photosystems during HL acclimation.

Immunogold labelling showed that PsbS is localized predominantly within grana stacks and not in stroma exposed regions of the thylakoid membrane, indicating a preferential co-localization with PSII. On the other hand, the transient accumulation of PsbS coincided with transient changes in thylakoid membrane stacking (Fig. 3). In vascular plants, thylakoid membrane stacking depends on the decrease of the negative surface charge of the thylakoid membrane in the appressed regions and requires the presence of trimeric LHCII proteins (Barber, 1982; Anderson, 1986). Since accumulation of LHCSR proteins is also induced upon HL acclimation, changes in membrane stacking might be related to PsbS controlled, transient interactions of LHCSR1 and/or LHCSR3 with PSII. It can be speculated that such an action of PsbS involves direct interaction with LHCSR1 and/or LHCSR3, which would resemble the situation in land plants, where PsbS has been shown to interact with LHCII proteins (Gerotto et al., 2015; Correa-Galvis et al., 2016a; Sacharz et al., 2017) upon reorganization of the PSII antenna during NPQ activation. In contrast to vascular plants, however, PsbS in *C. reinhardtii* is not directly involved in NPQ activation, since (i) increased amounts of PsbS in *oePsbS(CC-124)* did not increase the NPQ activity but rather led to a delayed activation of the full NPQ capacity compared to the WT CC-124 and (ii) PsbS is degraded at later stages of HL acclimation without reduction of NPQ capacity in both WT strains and *oePsbS(CC-124)*. The delayed increase of NPQ in response to higher PsbS amounts might either be related to better photoprotection in the initial phase of HL acclimation which could reduce the demand for NPQ activation. Alternatively, increased PsbS amounts might perturb the NPQ activation process, possibly by interfering with LHCSR binding sites involved in NPQ. The latter scenario might also explain why PsbS is degraded at later stages of HL acclimation. Recent work suggested that LHCSR1 contributes to NPQ through energy transfer to LHCII (Dinc et al., 2016) or PSI (Kosuge et al., 2018), which likely explains the low NPQ capacity of LHCSR3 deficient *npq4* mutants (Fig. 1C). Over-expression of PsbS in the *npq4* background did not result in increased NPQ levels, but in earlier formation of this low NPQ activity (Fig, 2D). This indicates that PsbS might also interfere with interactions of LHCSR1 with PSII and/or PSI. The possible impact of PsbS on PSI is further supported by the observed changes in electron and energy transfer in PSI upon reduction of PsbS amounts (Figs 7-9). Over-expression of PsbS in the WT CC-124 background, however, induced a low qE even in the LL-acclimated state (Tibiletti et al., 2016); Fig. 1B). This might result from either low LHCSR3 or LHCSR1 amounts, but supports again PsbS mediated activation of LHCSR dependent NPQ in cells not yet acclimated to HL.

In conclusion, our data suggest that PsbS contributes to photoprotection during HL acclimation of *C. reinhardtii* at different levels, including NPQ-independent and NPQ-dependent mechanisms.

MATERIAL AND METHODS

Cells and Growth Conditions

The following *C. reinhardtii* strains were used: WT CC-124, WT 4A+, the LHCSR3 deficient mutant *npq4* (Peers et al., 2009), the PsbS over-expressing mutants *oePsbS(CC-124)* and *oePsbS(npq4)* (Tibiletti et al., 2016), genetic background either CC-124 and *npq4*, respectively, and a PsbS knockdown mutant *kdPsbS(4A+)* (Correa-Galvis et al., 2016b). Cells were grown at 21 °C and constantly bubbled with ambient air (ambient CO_2) in HSM (photoautotrophic, low carbon). Light regimes were defined as low light (LL: 30 μmol photons m^{-2} s^{-1}) and high light (HL: 350μmol photons m^{-2} s^{-1}).

Cell Counting

Cells in a 1ml culture were fixed with 20μl 0.25% iodine (w/v in ethanol) and the number of cells/ml was calculated using a Thoma cell counting chamber (Marienfeld, Germany).

Protein and Immunoblot Analysis

For protein analysis, 50ml of sample were harvested and centrifuged. The pellet ($\approx 1 \times 10^9$ cells/ml) was frozen in liquid nitrogen until further analysis. The frozen pellet was resuspended in 900μl TMK buffer (10mM Tris/HCl pH 6.8, 10mM $MgCl_2$, 20mM KCl) and 0.6g glass beads (200μm) by vortexing (3 x 1min). Between each interval, the sample was cooled on ice. The supernatant was centrifuged for 5min at 17.000 x *g* at 4°C and the resulting pellet was resuspended in 200μl extraction buffer (1.6% SDS, 1M urea, 50mM Tris/HCl pH 7.6), incubated for 30min at 95°C under shaking and centrifuged 20min at 17.000 x g at room temperature. Protein concentration was quantified with the DC^{TM} Protein Assay (Bio-Rad, Düsseldorf, Germany). Protein separation was carried out by SDS-PAGE and immunoblot analysis was performed as described earlier (Schwarz et al., 2015). PsbS was detected with an antibody specifically designed for *C. reinhardtii* PsbS (contracted work Pineda antibody service, Berlin, Germany). The LHCSR3 antibody was raised against a specific peptide of *C. reinhardtii* LHCSR3 as described (Naumann et al., 2007). Antibodies from Agrisera® (Vännäs, Sweden) were used for LHCSR1 (AS142819) and D1 (AS05084). Coomassie stained gels and Ponceau S stained membranes served as controls for protein loading and blotting efficiency.

Chlorophyll Fluorescence Analysis

Chlorophyll fluorescence was measured using a JTS-10 spectrometer (Bio Logic SAS, Seyssinet-Pariset, France). 1×10^7 cells were dark adapted on a vertical shaker for 20min and then filtered on a glass fiber filter (PALL Corporation, Dreieich, Germany). The filter was fixed in a leaf cuvette and samples were pre-illuminated for 5min with far red light (400μmol photons m^{-2} s^{-1}). Fluorescence quenching analysis was performed during 15min illumination with red actinic light (940μmol photons m^{-2} s^{-1}) followed by 6min illumination with far red light. Saturation pulses (red light, 7900μmol photons m^{-2} s^{-1}) were applied every 60s. NPQ was calculated as (Fm/Fm'-1).

Absorption spectroscopy

Absorption spectroscopy was conducted in liquid cultures (20µg Chl ml^{-1} in 20mM HEPES-KOH pH 7.2, 10% ficoll) using the JTS-10 spectrometer (BioLogic, France). Saturating single turnover flashes were provided by a dye laser emitting at 640nm, pumped by the second harmonic of a Minilite II Nd:YAG laser (Continuum). Detection light for electrochromic shift (ECS) measurements was provided by a white LED light passing through interference filters (520nm and 546nm for background subtraction), the detecting photodiodes were covered with BG39 band-pass filters. Detection light for P700 measurements was provided by a LED light peaking at 700nm passing through interference filters (705nm and 740nm for background subtraction), the detecting photodiodes were covered with RG695 long-pass cut-off filters. Continuous actinic illumination was provided by an orange LED (150µmol photons m^{-2} s^{-1}). To assess photochemical charge separation events at the two photosystems, the amplitude of the initial ECS rise in response to a saturating single turnover flash was evaluated. The signal produced by PSI alone was discriminated via addition of PSII inhibitors (10µM DCMU, 1 M hydroxylamine), while contributions of PSII were calculated as the fraction being sensitive to these inhibitors. This procedure enables a determination of the stoichiometry of functional reaction centers (PSI/PSII). To assess residual steady state CEF rates in the presence of PSII inhibitors, the initial maximal P700 oxidation rate at 150µmol photons m^{-2} s^{-1} was derived from the ECS signal. The obtained rate was multiplied with the fraction of reduced P700 in the steady state, derived from the P700 signal after 10s of continuous illumination followed by a 20ms saturating pulse to fully oxidize P700. Finally, the obtained rate was normalized to the ECS signal corresponding to a single charge separation per PSI (see also Takahashi et al., 2013).

Low Temperature (77K) Fluorescence Measurements

Whole cells (0.2µg Chl) were frozen in liquid nitrogen. 77K fluorescence emission spectra were measured with the FP-6500 spectrofluorometer (Jasco, Groß-Umstadt, Germany). Data were normalized to the PSII emission peak at 685nm.

Chlorophyll Fluorescence Induction (OJIP) Transients

OJIP measurements (Stirbet and Govindjee, 2011) were applied to analyze the fluorescence state in PSII at a timescale of milliseconds. Cells were dark acclimated for 20min and then filtered on a glass fiber filter (PALL Corporation). Measurements were performed with a Handy PEA device (Hansatech Instruments, Norfolk, UK). To analyze the Chl fluorescence transient, cells were then illuminated for 2s at 3000µmol photons m^{-2} s^{-1} applying a gain multiplication of 10.

Immunogold Labeling

Immunogold labeling was used for semi-quantitative analysis of PsbS localization in *C. reinhardtii* WT and *oePsbS*(CC-*124)* cells grown in constant LL or after transfer into HL for 24h. High

pressure freezing of cells in nitrocellulose tubes was carried out as described (Daghma et al., 2011). Cryosubstitution in an automated freeze substitution unit (AFS, Leica Microsystems, Wetzlar, Germany) and embedding of cells in Lowicryl HM20 resin (Plano GmbH) were performed as described in Supplemental Table2.

Ultra-microtome sections (70-90nm) were mounted on copper grids and used for subcellular localisation of PsbS. Immunogold labeling using polyclonal PsbS antibody (primary antibody) at a dilution of 1:20 and transmission electron microscopy analysis was performed as previously reported (Schwarz et al., 2015).

Transmission Electron Microscopy (TEM)

15ml cell culture were pelleted by centrifugation (5000 x g for 2min) and resuspended in 2.5% glutaraldehyde. Subsequently, cells were washed in 100mM sodium cacodylate buffer for 1h, and then incubated for 2h in 2% OsO_4 containing 0.8% potassium ferrocyanide. Cells were then washed again for 1h in 100mM sodium cacodylate buffer, prior to a series of washing steps with EtOH: 10min/ 60% EtOH, 24h (4°C)/ 70% EtOH, 10min/80% EtOH, and four steps for 15min in 90%/96%/100%/100% EtOH. After incubation for 30min in propylene oxide, samples were then incubated at 20°C in epoxide:propylene oxide at a ratio of 1:2 for 1h, followed by 1h incubation at a 1:1 ratio and subsequently overnight incubation at a 2:1 ratio. Cells were incubated for 24h in 100% epoxide, then embedded in fresh 100% epoxide and incubated for 24h at 40°C and finally polymerized during 24h at 60°C. Ultrathin sections (70nm) were cut (either with ultramicrotome Ultracut E Reichert Jung or Ultracut EM UC7; Fa. Leica) with a diamond knife (Diatome type ultra 45°), mounted on single-slot copper grids (SP162, 200M copper grids with Pioloform, Plano, Wetzlar, Germany) and incubated for 10-25min in 1.5% uranyl acetate and 8min in lead citrate solution. Micrographs were taken using either a transmission electron microscope (Zeiss CEM 902, CCD Camera Controller Sharp:eye; Jena, Germany) or H600 TEM (Gatan Camera system; Hitachi, Tokyo, Japan). Images were subsequently processed by the Digital Micrograph Software (Gatan, Munich, Germany).

LITERATURE CITED

Allen JF (2017) Why we need to know the structure of phosphorylated chloroplast light-harvesting complex II. Physiol Plant **161:** 28-44

Allen JF, Forsberg J (2001) Molecular recognition in thylakoid structure and function. Trends Plant Sci **6:** 317-326

Allorent G, Lefebvre-Legendre L, Chappuis R, Kuntz M, Truong TB, Niyogi KK, Ulm R, Goldschmidt-Clermont M (2016) UV-B photoreceptor-mediated protection of the photosynthetic machinery in Chlamydomonas reinhardtii. Proc Natl Acad Sci USA **113:** 14864-14869

Allorent G, Tokutsu R, Roach T, Peers G, Cardol P, Girard-Bascou J, Seigneurin-Berny D, Petroutsos D, Kuntz M, Breyton C, Franck F, Wollman F-A, Niyogi KK, Krieger-Liszkay A, Minagawa J, Finazzi G (2013) A Dual Strategy to Cope with High Light in Chlamydomonas reinhardtii. Plant Cell **25:** 545-557

Anderson JM (1986) Photoregulation of the composition, function, and structure of thylakoid membranes. Annu Rev Plant Physiol Plant Mol Biol **37:** 93-136

Bailey S, Walters RG, Jansson S, Horton P (2001) Acclimation of Arabidopsis thaliana to the light environment: the existence of separate low light and high light responses. Planta **213:** 794-801

Ballottari M, Truong TB, De Re E, Erickson E, Stella GR, Fleming GR, Bassi R, Niyogi KK (2016) Identification of pH-sensing sites in the Light Harvesting Complex Stress-Related 3 protein essential for triggering non-photochemical quenching in Chlamydomonas reinhardtii. J Biol Chem **291**: 7334-7346

Barber J (1982) Influence of surface charges on thylakoid structures and function. Annu Rev Plant Physiol **33:** 261-295

Boardman NK (1977) Comparative photosynthesis of sun and shade plants. Annu Rev Plant Physiol Plant Mol Biol **28:** 355-377

Briantais J-M, Vernotte C, Picaud M, Krause GH (1979) A quantative study of the slow decline of chlorophyll *a* fluorescence in isolated chloroplasts. Biochim Biophys Acta **548:** 128-138

Cardol P, Forti G, Finazzi G (2011) Regulation of electron transport in microalgae. Biochim Biophys Acta **1807:** 912-918

Chapman SP, Paget CM, Johnson GN, Schwartz J-M (2015) Flux balance analysis reveals acetate metabolism modulates cyclic electron flow and alternative glycolytic pathways in Chlamydomonas reinhardtii. Front Plant Sci **6:** 474, doi: 10.3389/fpls.2015.00474

Correa-Galvis V, Poschmann G, Melzer M, Stühler K, Jahns P (2016a) PsbS interactions involved in the activation of energy dissipation in *Arabidopsis*. Nat Plants **2:** 15225

Correa-Galvis V, Redekop P, Guan K, Griess A, Truong TB, Wakao S, Niyogi KK, Jahns P (2016b) Photosystem II Subunit PsbS Is Involved in the Induction of LHCSR Protein-dependent Energy Dissipation in Chlamydomonas reinhardtii. J Biol Chem **291:** 17478-17487

Crayton MA (1982) A COMPARATIVE CYTOCHEMICAL STUDY OF VOLVOCACEAN MATRIX POLYSACCHARIDES. J Phycol **18:** 336-344

Daghma DS, Kumlehn J, Melzer M (2011) The use of cyanobacteria as filler in nitrocellulose capillaries improves ultrastructural preservation of immature barley pollen upon high pressure freezing. J Microsc **244:** 79-84

Delosme R, Olive J, Wollman F-A (1996) Changes in light energy distribution upon state transitions: an in vivo photoacustic study of the wild type and photosynthesis mutants from *Chlamydomonas reinhardtii*. Biochim Biophys Acta **1273:** 150-158

Dinc E, Tian L, Roy LM, Roth R, Goodenough U, Croce R (2016) LHCSR1 induces a fast and reversible pH-dependent fluorescence quenching in LHCII in Chlamydomonas reinhardtii cells. Proc Natl Acad Sci USA **113:** 7673-7678

Erickson E, Wakao S, Niyogi KK (2015) Light stress and photoprotection in Chlamydomonas reinhardtii. Plant J **82:** 449-465

Finazzi G, Rappaport F, Furia A, Fleischmann M, Rochaix JD, Zito F, Forti G (2002) Involvement of state transitions in the switch between linear and cyclic electron flow in Chlamydomonas reinhardtii. EMBO Rep **3:** 280-285

Foyer CH, Shigeoka S (2011) Understanding Oxidative Stress and Antioxidant Functions to Enhance Photosynthesis. Plant Physiol **155:** 93-100

Gerotto C, Franchin C, Arrigoni G, Morosinotto T (2015) In Vivo Identification of Photosystem II Light Harvesting Complexes Interacting with PHOTOSYSTEM II SUBUNIT S. Plant Physiol **168:** 1747-1761

Horton P, Johnson MP, Perez-Bueno ML, Kiss AZ, Ruban AV (2008) Photosynthetic acclimation: Does the dynamic structure and macro-organisation of photosystem II in higher plant grana membranes regulate light harvesting states? FEBS J **275:** 1069-1079

Jahns P, Holzwarth AR (2012) The role of the xanthophyll cycle and of lutein in photoprotection of photosystem II. Biochim Biophys Acta **1817:** 182-193

Jahns P, Latowski D, Strzalka K (2009) Mechanism and regulation of the violaxanthin cycle: The role of antenna proteins and membrane lipids. Biochim Biophys Acta **1787:** 3-14

Johnson X, Steinbeck J, Dent RM, Takahashi H, Richaud P, Ozawa S-I, Houille-Vernes L, Petroutsos D, Rappaport F, Grossman AR, Niyogi KK, Hippler M, Alric J (2014) Proton Gradient Regulation 5-Mediated Cyclic Electron Flow under ATP- or Redox-Limited Conditions: A Study of Delta ATPase pgr5 and Delta rbcL pgr5 Mutants in the Green Alga Chlamydomonas reinhardtii. Plant Physiol **165:** 438-452

Joliot P, Johnson GN (2011) Regulation of cyclic and linear electron flow in higher plants. Proc Natl Acad Sci USA **108:** 13317-13322

Khona DK, Shirolikar SM, Gawde KK, Hom E, Deodhar MA, D'Souza JS (2016) Characterization of salt stress-induced palmelloids in the green alga, Chlamydomonas reinhardtii. Algal Res **16:** 434-448

Kosuge K, Tokutsu R, Kim E, Akimoto S, Yokono M, Ueno Y, Minagawa J (2018) LHCSR1-dependent fluorescence quenching is mediated by excitation energy transfer from LHCII to photosystem I in Chlamydomonas reinhardtii. Proc Natl Acad Sci USA **115:** 3722-3727

Kromdijk J, Glowacka K, Leonelli L, Gabilly ST, Iwai M, Niyogi KK, Long SP (2016) Improving photosynthesis and crop productivity by accelerating recovery from photoprotection. Science **354:** 857-861

Kukuczka B, Magneschi L, Petroutsos D, Steinbeck J, Bald T, Powikrowska M, Fufezan C, Finazzi G, Hippler M (2014) Proton Gradient Regulation5-Like1-Mediated Cyclic Electron Flow Is Crucial for Acclimation to Anoxia and Complementary to Nonphotochemical Quenching in Stress Adaptation. Plant Physiol **165:** 1604-1617

Li X-P, Björkman O, Shih C, Grossman AR, Rosenquist M, Jansson S, Niyogi KK (2000) A pigment-binding protein essential for regulation of photosynthetic light harvesting. Nature **403:** 391-395

Li XP, Gilmore AM, Caffarri S, Bassi R, Golan T, Kramer D, Niyogi KK (2004) Regulation of photosynthetic light harvesting involves intrathylakoid lumen pH sensing by the PsbS protein. J Biol Chem **279:** 22866-22874

Li XP, Phippard A, Pasari J, Niyogi KK (2002) Structure-function analysis of photosystem II subunit S (PsbS) in vivo. Funct Plant Biol **29:** 1131-1139

Li ZR, Wakao S, Fischer BB, Niyogi KK (2009) Sensing and Responding to Excess Light. Annu Rev Plant Biol **60:** 239-260

Lucker B, Kramer DM (2013) Regulation of cyclic electron flow in Chlamydomonas reinhardtii under fluctuating carbon availability. Photosyn Res **117:** 449-459

Malkin S, Armond PA, Mooney HA, Fork DC (1981) PHOTOSYSTEM-II PHOTOSYNTHETIC UNIT SIZES FROM FLUORESCENCE INDUCTION IN LEAVES - CORRELATION TO PHOTOSYNTHETIC CAPACITY. Plant Physiol **67:** 570-579

Maruyama S, Tokutsu R, Minagawa J (2014) Transcriptional Regulation of the Stress-Responsive Light Harvesting Complex Genes in Chlamydomonas Reinhardtii. Plant Cell Physiol **55:** 1304-1310

Moller IM, Jensen PE, Hansson A (2007) Oxidative modifications to cellular components in plants. Annu Rev Plant Biol **58:** 459-481

Naumann B, Busch A, Allmer J, Ostendorf E, Zeller M, Kirchhoff H, Hippler M (2007) Comparative quantitative proteomics to investigate the remodeling of bioenergetic pathways under iron deficiency in Chlamydomonas reinhardtii. Proteomics **7:** 3964-3979

Nilkens M, Kress E, Lambrev PH, Miloslavina Y, Müller M, Holzwarth AR, Jahns P (2010) Identification of a slowly inducible zeaxanthin-dependent component of non-photochemical quenching of chlorophyll fluorescence generated under steady state conditions in *Arabidopsis*. Biochim Biophys Acta **1797:** 466-475

Niyogi KK, Björkman O, Grossman AR (1997) Chlamydomonas xanthophyll cycle mutants identified by video imaging of chlorophyll fluorescence quenching. Plant Cell **9:** 1369-1380

Peers G, Truong TB, Ostendorf E, Busch A, Elrad D, Grossman AR, Hippler M, Niyogi KK (2009) An ancient light-harvesting protein is critical for the regulation of algal photosynthesis. Nature **462:** 518-U215

Polukhina I, Fristedt R, Dinc E, Cardol P, Croce R (2016) Carbon Supply and Photoacclimation Cross Talk in the Green Alga Chlamydomonas reinhardtii. Plant Physiol **172:** 1494-1505

Sacharz J, Giovagnetti V, Ungerer P, Mastroianni G, Ruban AV (2017) The xanthophyll cycle affects reversible interactions between PsbS and light-harvesting complex II to control non-photochemical quenching. Nat Plants **3:** 16225-16225

Schmitz J, Schoettler MA, Krueger S, Geimer S, Schneider A, Kleine T, Leister D, Bell K, Fluegge U-I, Haeusler RE (2012) Defects in leaf carbohydrate metabolism compromise acclimation to high light and lead to a high chlorophyll fluorescence phenotype in Arabidopsis thaliana. BMC Plant Biol **12: 8**

Schoettler MA, Toth SZ (2014) Photosynthetic complex stoichiometry dynamics in higher plants: environmental acclimation and photosynthetic flux control. Frontiers in Plant Science **5**

Schumann T, Paul S, Melzer M, Doermann P, Jahns P (2017) Plant Growth under Natural Light Conditions Provides Highly Flexible Short-Term Acclimation Properties toward High Light Stress. Front Plant Sci **8:** 681

Schwarz N, Armbruster U, Iven T, Brueckle L, Melzer M, Feussner I, Jahns P (2015) Tissue-Specific Accumulation and Regulation of Zeaxanthin Epoxidase in Arabidopsis Reflect the Multiple Functions of the Enzyme in Plastids. Plant Cell Physiol **56:** 346-357

Stirbet A, Govindjee (2011) On the relation between the Kautsky effect (chlorophyll a fluorescence induction) and Photosystem II: Basics and applications of the OJIP fluorescence transient. J Photochem Photobiol B **104:** 236-257

Suorsa M, Jarvi S, Grieco M, Nurmi M, Pietrzykowska M, Rantala M, Kangasjarvi S, Paakkarinen V, Tikkanen M, Jansson S, Aro EM (2012) Proton Gradient Regulation5 Is Essential for Proper Acclimation of Arabidopsis Photosystem I to Naturally and Artificially Fluctuating Light Conditions. Plant Cell **24:** 2934-2948

Takahashi H, Clowez S, Wollman FA, Vallon O, Rappaport F (2013) Cyclic electron flow is redox-controlled but independent of state transition. Nature Comms **4**: 1954

Terashima M, Petroutsos D, Hudig M, Tolstygina I, Trompelt K, Gabelein P, Fufezan C, Kudla J, Weinl S, Finazzi G, Hippler M (2012) Calcium-dependent regulation of cyclic photosynthetic electron transfer by a CAS, ANR1, and PGRL1 complex. Proc Natl Acad Sci USA **109:** 17717-17722

Tibiletti T, Auroy P, Peltier G, Caffarri S (2016) Chlamydomonas reinhardtii PsbS Protein Is Functional and Accumulates Rapidly and Transiently under High Light. Plant Physiol **171:** 2717-2730

Weston E, Thorogood K, Vinti G, Lopez-Juez E (2000) Light quantity controls leaf-cell and chloroplast development in Arabidopsis thaliana wild type and blue-light-perception mutants. Planta **211:** 807-815

Wood WHJ, MacGregor-Chatwin C, Barnett SFH, Mayneord GE, Huang X, Hobbs JK, Hunter CN, Johnson MP (2018) Dynamic thylakoid stacking regulates the balance between linear and cyclic photosynthetic electron transfer. Nat Plants **4:** 116-127

Yamano T, Miura K, Fukuzawa H (2008) Expression analysis of genes associated with the induction of the carbon-concentrating mechanism in Chlamydomonas reinhardtii. Plant Physiology **147:** 340-354

Supplemental Table S1. Quantitative analysis of morphological parameters. Micrographs were analyzed for CC-124, *oePsbS(CC-124), oePsbS(npq4)* and *kdPsbS(4A+)* and *npq4* cells acclimated to LL or after 1, 4, 10, 24, 48h and constant HL illumination. Mean values ± SD obtained from analysis of at least 30 images are shown.

	Cell size (µm)	Pyrenoid size (µm)	Starch-body/Cell	Cells/ Palmelloid	Palmelloids (%)	nonfunctional (%)	Grana thickness (nm)
CC-124 LL	6.2±0.8	2.0±0.3	4±3	2	12	0	75±31
CC-124 1h	7.3±1.3	1.4±0.3	4±3	0	0	5	92±32
CC-124 4h	6.8±0.7	1.6±0.2	12±2	0	0	0	101±30
CC-124 10h	7.9±1.2	1.5±0.3	8±3	3	20	0	117±57
CC-124 24h	7.0±1.4	1.7±0.3	7±2	5	73	10	115±28
CC-124 48h	6.8±1.3	1.5±0.3	6±3	5	73	10	99±37
CC-124 HL	6.5±0.9	1.4±0.2	8±2	0	0	5	89±21
oePsbS(CC-124) LL	8.1±1.1	1.9±0.4	4±2	0	0	0	93±32
oePsbS(CC-124) 1h	8.1±1.5	2.0±0.5	9±5	0	0	0	124±37
oePsbS(CC-124) 4h	7.9±1.4	2.0±0.5	7±5	0	0	5	106±48
*oePsbS(CC-124)*10h	8.2±1.4	2.4±0.5	2±2	0	0	0	122±32
oePsbS(CC-124) 24h	7.8±1.0	2.0±0.4	4±3	4	3	0	121±31
oePsbS(CC-124) 48h	7.4±0.8	1.9±0.4	6±3	0	0	0	89±26
oePsbS(CC-124) HL	7.8±1.5	2.2±0.4	5±2	0	0	15	108±32
oePsbS(npq4) LL	8.0±1.0	1.4±0.3	7±4	0	0	7	76±40
oePsbS(npq4) 1h	8.4±0.8	1.6±0.3	16±3	3	1	7	75±24
oePsbS(npq4) 4h	8.6±1.1	2.0±0.3	17±5	5	2	8	67±25
oePsbS(npq4) 10h	9.8±1.2	1.8±0.1	22±8	3	35	10	54±15
oePsbS(npq4) 24h	7.6±1.0	1.8±0.3	6±2	3	11	21	69±25
oePsbS(npq4) 48h	7.3±0.6	1.7±0.2	8±1	3	3	29	76±24
oePsbS(npq4) HL	7.5±1.5	1.6±0.2	11±2	3	2	47	66±28
kdPsbS(4A+) LL	7.5±1.4	1.3±0.3	2±1	3	10	0	145±51
kdPsbS(4A+) 1h	7.2±1.3	1.7±0.4	6±4	2	5	5	116±50
kdPsbS(4A+) 4h	7.5±1.6	1.8±0.5	7±5	0	0	20	170±59
kdPsbS(4A+) 10h	8.7±1.3	2.0±0.4	10±4	0	0	40	157±68
kdPsbS(4A+) 24h	7.9±1.2	1.6±0.4	6±3	0	0	20	106±37
kdPsbS(4A+) 48h	7.0±1.2	1.5±0.3	9±3	0	0	15	90±35
kdPsbS(4A+) HL	7.9±1.3	1.4±0.3	13±4	0	0	60	137±53
npq4 LL	9.6±1.3	2.1±0.4	7±2	3	76	5	104±30
npq4 1h	9.4±1.0	2.2±0.5	19±5	3	99	8	111±42
npq4 4h	10.1±1.2	2.4±0.5	23±8	4	96	22	140±45
npq4 10h	9.2±1.2	2.3±0.6	19±4	4	95	50	121±24
npq4 24h	8.9±1.6	2.1±0.5	21±4	4	99	65	115±29
npq4 48h	7.2±1.6	1.5±0.4	10±3	3	81	69	111±30
npq4 HL	7.6±0.9	1.5±0.3	7±2	3	11	74	89±25

low

Supplemental Table S2. Cryosubstitution and embedding into Lowicryl HM20

Process	Chemical	Temperature [C°]	Time [h]
Cryosubstitution in an AFS	100 % Acetone with exchange each 24 hrs	-80 -80 to -70 -70 -70 to -50 -50 -50 to -35 -35 -35 to -10 -10 to 20	72 6 24 6 24 6 24 6 4
Resin infiltration on shaker	25% Lowicryl HM20/Acetone 50% Lowicryl HM20/Acetone 75% Lowicryl HM20/Acetone 100% Lowicryl HM20	RT RT RT RT	2 2 2 12
UV Polymerisation in gelatine capsules in an AFS	Lowicryl HM20	-10°C	72
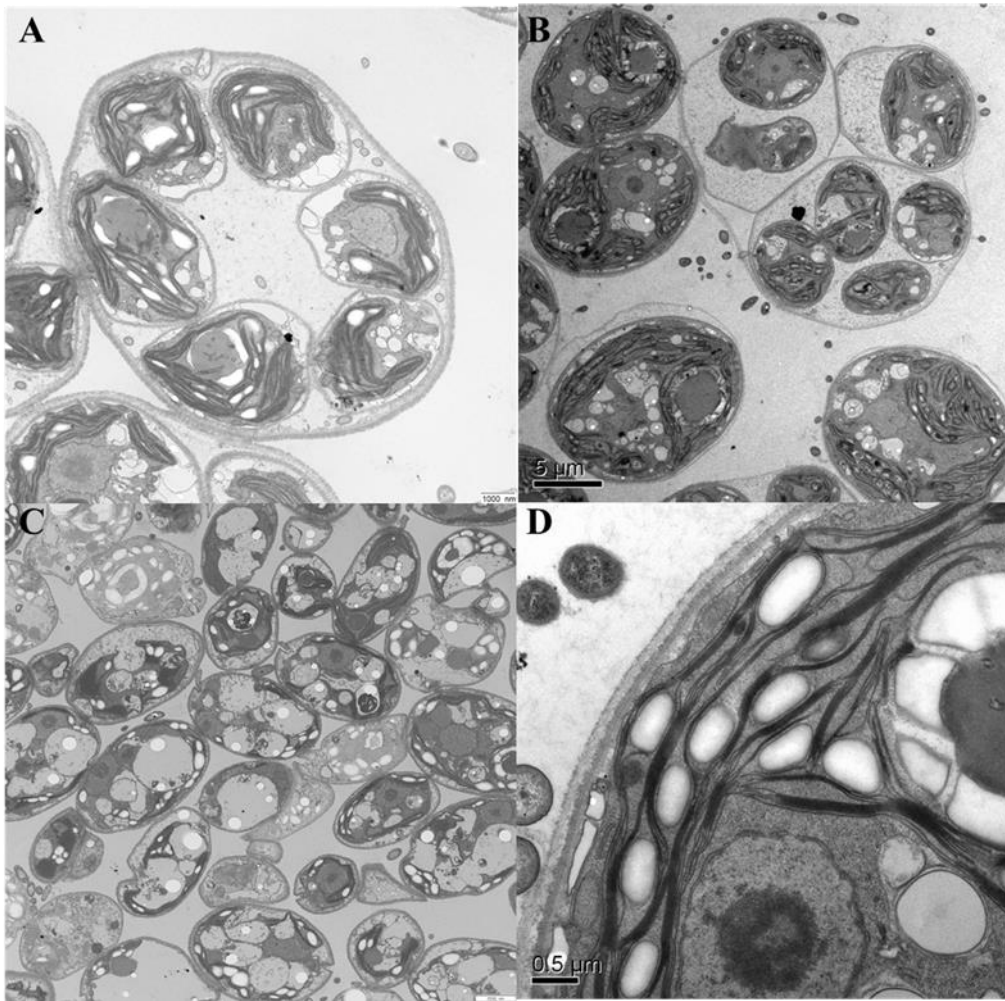
Supplemental Figure 1. Cell morphology. A, palmelloid formation in CC124 after 24h of HL. B, *npq4* cells after 4h of HL containing large starch bodies and forming palmelloids. C, non-functional *kdPsbS(4A+)* cells in the HL-acclimated state. D, starch bodies in *npq4* after 4h of HL at higher magnification. Zeiss CEM 902, CCD Camera Controller Sharp:eye (B,D) and H600 TEM Gatan Camera system and Digital Micrograph Software; Hitachi (A, C) were used.

6 Concluding Remarks

Chlamydomonas clearly has a biotechnological potential as sustainable machinery to convert light energy into biomass. The theoretical maximal photon energy conversion (PCE) rate into biomass is about 10%, while natural outdoor conditions only allow a rate of 2%, suggesting that PCE is the limiting factor (Kruse et al., 2005). An increase of the light use efficiency at the level of light-harvesting or energy dissipation can thus be a promising tool to optimize the PCE rate. Detailed understanding of the function of the individual components involved in light utilization is thus important to achieve this goal. Indeed, modification of the light-harvesting antenna size has been successfully applied to improve the conversion of solar energy to biomass in microalgae (Ort et al., 2011). Moreover, fine-tuning of the NPQ dynamics has recently been shown to result in improved photosynthetic efficiency and hence crop productivity (Kromdijk et al., 2016). In this work, the PsbS protein in *C. reinhardtii* was characterized at the physiological and biochemical level, with emphasis on the impact of different PsbS amounts on HL sensitivity. The most important results of this work give rise to three major aspects, which also raise the need for further investigation: 1. The transient expression of PsbS alongside with NPQ induction and LHCSR protein accumulation suggests an indirect role of PsbS in the activation of the NPQ capacity during HL acclimation. 2. The increased HL resistance of cells with increased PsbS without changed NPQ properties suggests a specific NPQ-independent photoprotective function of PsbS. 3. The demand for degradation of PsbS at longer HL acclimation time, even in PsbS over-expressing mutants implies a negative impact of permanently high PsbS amounts on photosynthetic performance.

1. Transient expression of PsbS

The PsbS protein in *C. reinhardtii* accumulates to maximum levels after about 4-6h of HL exposure and disappears with prolonged HL exposure (Correa-Galvis, Redekop et al., 2016, manuscript 2). Hence, peaking amounts of PsbS occur shortly before maximum NPQ levels and maximum LHCSR3 amounts are reached, indicating a differential regulation of PsbS and LHCSR3 expression. The HL-induced expression of LHCSR3 is predominantly facilitated by blue light (420-480 nm) under control of the blue light photoreceptor phototropin (PHOT) (Petroutsos et al., 2016), but further shows a response to limiting CO_2 conditions in the absence of HL due to the EEC motif (enhancer element of low CO_2-inducible genes) in the promoter region of *LHCSR3* (Maruyama et al., 2014). In contrast, LHCSR1 expression is mainly induced by UV-B light (Allorent et al., 2016) under control of the UV-B photoreceptor UV RESISTANCE LOCUS 8 (UVR8) and the E3 ubiquitin ligase CONSTITUTIVELY PHOTOMORPHOGENIC 1 (COP1) (Rizzini et al., 2013). The induction of PsbS expression was recently found to be rather regulated like the LHCSR1, by UV-B light and

UVR8/COP1, than like the LHCSR3 by HL and the PHOT receptor (Allorent et al., 2016). However, like LHCSR3, PsbS expression is also regulated in response to limiting CO_2 conditions and hence by photosynthetic efficiency (Correa-Galvis, Redekop et al., 2016). Future work on different mutants and various growth conditions (light quality and intensity, CO_2 availability) are therefore required to unravel the signaling network involved in PsbS expression. The UV-B controlled co-expression of LHCSR1 and PsbS could be understood as more rapid response to light stress, early on after LL to HL transition to provide LHCSR3 independent photoprotection.

2. NPQ-independent photoprotective function of PsbS

Higher amounts of PsbS do not result in a higher NPQ capacity, while a down-regulation of the PsbS amount leads to decreased LHCSR levels as well as a lower NPQ capacity, indicating that PsbS is indirectly required for NPQ establishment (Correa-Galvis, Redekop et al., 2016). Further experiments concerning the localization of PsbS in *C. reinhardtii* have been conducted to determine the dynamics of PsbS localization during HL acclimation (Fig. A). These analyses revealed that a small fraction of PsbS associates with PSII-LHCII supercomplexes (in accordance with Correa-Galvis, Redekop et al., 2016), but that the PSII-bound PsbS is less susceptible to degradation than the fraction migrating with free LHCII trimers (Fig. A).
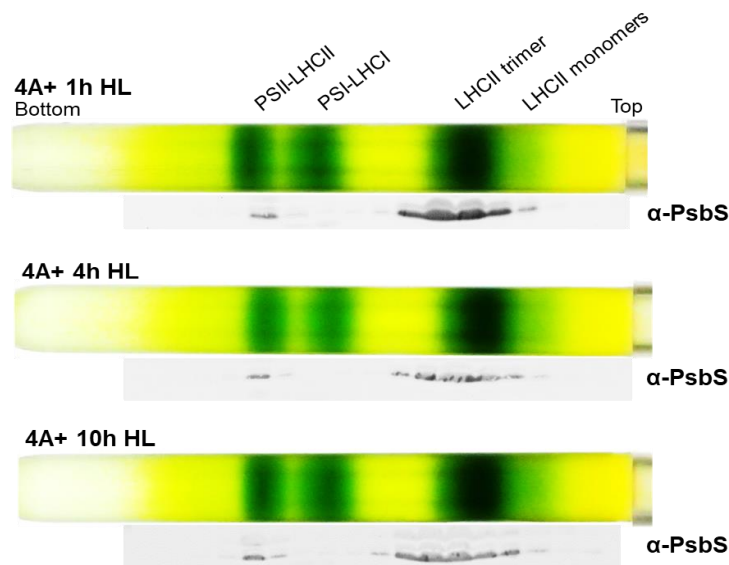
Figure A: Immunoblot analysis and localization of PsbS after sucrose density gradient fractionation after (Tokutsu and Minagawa, 2013) of thylakoid membranes (0.4mg Chl) of 4A+ WT cells exposed to HL (350µmol photons m^{-2}s^{-1}) for 1, 4 and 10h. Anti-PsbS antibody (α-PsbS) was used to determine the distribution of PsbS in the different fractions.

This interaction of PsbS with PSII-LHCII SC could be related to the proposed role of PsbS in reorganization of the PSII antenna upon establishment of NPQ during HL acclimation (Correa-Galvis, Redekop et al., 2016), while the major PsbS pool with weaker affinity to

PSII and PSI might serve other, NPQ-independent functions. Further preliminary experiments indicated that LHCSR1 proteins interact with PSI-LHCI SC and that this interaction is dependent on the HL illumination time and the PsbS amount (not documented). These observations are indicative of a regulatory role of PsbS for LHCSR1 functioning. LHCSR1 is supposed to contribute to NPQ by energy transfer to either LHCII (Dinc et al., 2016) or PSI (Kosuge et al., 2018), which explains the low NPQ in the LHCSR3 lacking *npq4* mutant (manuscript 2). Increasing the PsbS amount in *npq4* does not increase the NPQ capacity, but leads to earlier NPQ induction (manuscript 2), which might result from an interference of PsbS with LHCSR1-PSII and/or LHCSR1-PSI interactions. Increased levels of PsbS further alter thylakoid membrane dynamics and electron transfer at the level of PSI (manuscript 2). The latter could thus result from interactions of LHCSR1 with PSI that might depend on the PsbS amount. Hence, further research should clarify the dynamics of the interactions of PsbS and LHCSR proteins with PSI and PSII during HL acclimation to understand the function of PsbS in thylakoid membrane organization.

3. PsbS degradation at longer HL acclimation time

Strikingly, even constitutively over-expressed PsbS becomes degraded after prolonged HL exposure, suggesting an active rapid degradation of PsbS at later stages of HL acclimation. So far, studies on the role of PsbS in *C. reinhardtii* focused rather on accumulation kinetics than the subsequent degradation. It is thus unclear by which proteases PsbS is degraded and how this process is regulated. To obtain some preliminary information, five *C. reinhardtii* mutants defective in Deg and FtsH, proteases known to be involved in the repair of PSII during photoinhibition, have been analyzed regarding PsbS abundance (Fig. B).
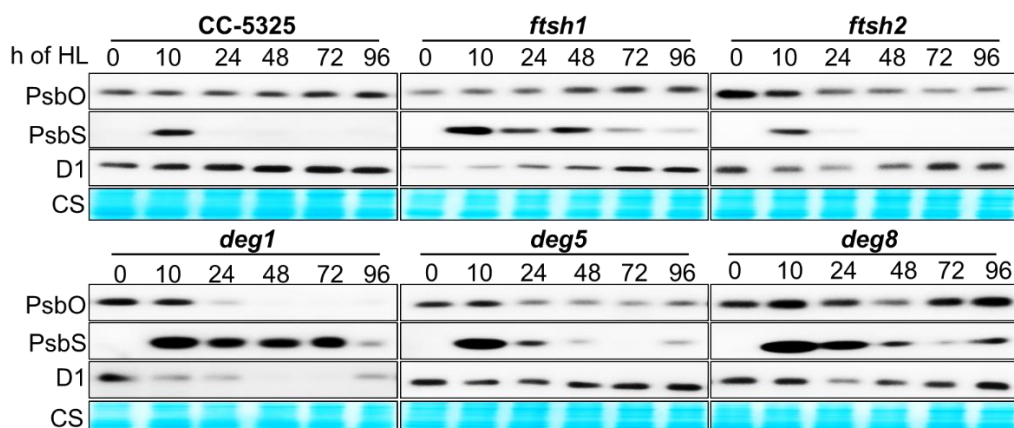

Figure B: Protein expression in WT (CC5325) and protease mutants *deg1, deg5, deg8, ftsh1* and *ftsh2*. For immunoblot analysis of PsbS, 40µg of total protein was loaded, whereas 5µg were used for PsbO and D1. WT and mutant cells were grown at 35µmol photons $m^{-2}s^{-1}$ and then illuminated for up to 96h of HL (350µmol photons $m^{-2}s^{-1}$). Samples for protein analysis were taken after 10, 24, 48, 72 and 96h in HL. Representative immunoblots from 3 biological replicates are shown. CS, coomassie stained gels (apparent molecular mass in the range between 20 and 30 kDa) served as loading control.

PsbS accumulation and degradation was characterized in *ftsh1* and *ftsh2* as well as in *deg1*, *deg5* and *deg8* mutants. Unlike WT stains, which accumulate PsbS after 10h of HL exposure only, PsbS abundance remains rather stable in strains lacking the proteases Deg1, Deg5, Deg8 and FtsH1, whereas absence of FtsH2 has no effect on PsbS degradation (Fig. B). The more stable accumulation of PsbS after prolonged HL exposure in the mutants *deg1*, *deg5*, *deg8* and *ftsh1* suggests impaired PsbS degradation. In particular the *deg1* mutant was found to be highly sensitive to HL, as this mutant strain exhibited strong bleaching and a diminished PSII efficiency after prolonged HL exposure. The stable accumulation of PsbS during HL exposure in this strain thus allows to hypothesize that Deg1 might contribute to PsbS degradation in *C. reinhardtii.* These findings are in line with the HL-induced cleavage of Arabidopsis PsbS by recombinant Deg1 (Zienkiewicz et al., 2012). Since PsbS abundancies remain high in *deg5*, *deg8* and *ftsh1* after prolonged HL as well, Deg1 might not act alone in PsbS degradation, but rather could be involved in cooperative interaction of several proteases that endorse degradation of PsbS. Future work will thus be important to study in detail the interaction of the different proteases with PsbS in *C. reinhardtii*.

7 Summary

Solar energy is the ultimate energy source for photosynthesis and thus for life on earth. In natural environments, light intensities often vary rapidly (seconds to minutes) in orders of magnitude. Photosynthetic organisms must therefore be able to utilize efficiently low light (LL) intensities and to minimize photo-oxidative damage resulting from high light (HL) intensities due to the formation of reactive oxygen species. Plants and algae have evolved mechanisms, collectively termed non-photochemical quenching (NPQ) to dissipate excessive light energy as heat. NPQ comprises several quenching mechanisms, with the most important being the rapidly adjustable pH-dependent quenching component qE. In vascular plants, qE is well described as a constitutively active mechanism that is regulated by the constantly present PsbS protein. PsbS controls pH-regulated conformational changes in the antenna of photosystem II which allows the rapid molecular switch of the antenna between the light-harvesting and the energy dissipating state. In the green alga *C. reinhardtii*, qE is regulated in a similar way, but by the LHCSR3 protein and not by PsbS. Furthermore, activation of qE requires a longer period of HL acclimation and the synthesis of LHCSR3. Although the PsbS protein exists in green microalgae like *C. reinhardtii* as well, its function in these algae is largely unknown. This work addresses (i) the PsbS expression patterns during HL acclimation along with LHCSR3 expression and qE activation, and (ii) the impact of different PsbS levels on the qE capacity, the photosynthetic performance and vitality of *C. reinhardtii* during HL acclimation. The experimental data provide evidence that PsbS in *C. reinhardtii* accumulates only transiently during HL acclimation along with the activation of qE and the expression of LHCSR3, but PsbS is degraded before the maximal qE capacity is reached. PsbS expression patterns depend on the CO_2 availability suggesting that PsbS expression is increased at higher stress conditions when photosynthetic activity is limited. However, PsbS does not compensate for the function of LHCSR3, which is essential for qE. Analyses of the impact of different PsbS amounts in comparison with the wild type revealed that lower PsbS levels result in (1) reduced qE capacity, (2) an increase of PSII antenna in HL, (3) a faster P700 oxidation in HL when LHCSR3 is already present, but slower in LL when LHCSR3 does not accumulate, (4) an increased cyclic electron transport in HL, (5) altered thylakoid membrane organization and (6) a reduced cell viability. Analyses of PsbS over-expressing cells suggest that (1) PsbS is actively degraded at later stages of HL acclimation, (2) more PsbS does not result in a higher qE capacity and (3) more PsbS improves the HL resistance and hence the fitness of the cells during HL acclimation. These results underline that PsbS in *C. reinhardtii* is not crucial for the qE capacity – in contrast to the situation in vascular plants – but essentially contributes to photoprotection upon HL acclimation (i) by re-organization of the thylakoid membrane during activation of qE and (ii) in qE-independent mechanisms.

8 Zusammenfassung

Das Sonnenlicht liefert die Energie für die Photosynthese und damit für das Leben auf der Erde. Unter natürlichen Bedingungen kann die Lichtintensität schnell (Sekunden bis Minuten) um mehrere Größenordnungen variieren. Photosynthetische Organismen müssen daher in der Lage sein, sowohl sehr niedrige (LL) Lichtintensitäten effizient zu nutzen, zugleich aber auch photo-oxidative Schädigungen, die bei sehr hohen (HL) Intensitäten durch reaktive Sauerstoff-Spezies verursacht werden, zu minimieren. Pflanzen und Algen haben Mechanismen entwickelt, die unter dem Begriff nicht-photochemische Löschung (*engl.* non-photochemical quenching, NPQ) zusammengefasst werden, und welche überschüssige Lichtenergie in Form von Wärme ableiten. NPQ umfasst verschiedene Mechanismen der Energielöschung, wobei die wichtigste Komponente die schnell regulierbare, pH- abhängige qE Komponente ist. Der qE Mechanismus ist in Gefäßpflanzen als konstitutiv aktiver Mechanismus beschrieben, der durch das PsbS Protein reguliert wird. PsbS kontrolliert pH-regulierte Konformationsänderungen in der Antenne von Photosystem II (PSII), die eine Schaltung der Antenne zwischen einem Licht-sammelnden und einem Energie-löschenden Zustand ermöglichen. In der Grünalge *C. reinhardtii* wird qE ähnlich reguliert, allerdings durch das LHCSR3 Protein und nicht durch PsbS. Darüber hinaus erfordert die Aktivierung des qE eine längere HL Akklimatisation und die Synthese von LHCSR3. Obwohl das PsbS Protein auch in Grünalgen wie *C. reinhardtii* vorkommt, ist dessen Funktion in diesen Algen völlig unklar. Die vorliegende Arbeit befasst sich mit (i) der Charakterisierung des PsbS Expressionsmusters während der HL-Akklimatisation im Vergleich mit der LHCSR3 Expression und der qE-Aktivierung (ii) die Wirkung unterschiedlicher PsbS Mengen auf die qE-Kapazität, die photosynthetische Leistungsfähigkeit, sowie die Vitalität von *C. reinhardtii* während der HL-Akklimatisation. Die Ergebnisse zeigen, dass PsbS in *C. reinhardtii* während der HL-Akklimatisation nur transient akkumuliert, und zwar parallel mit der Aktivierung von qE und der Expression von LHCSR3, aber wieder abgebaut wird bevor die maximale qE-Kapazität erreicht ist. Die PsbS Expression hängt von der CO_2 Verfügbarkeit ab, sodass bei Beeinträchtigung der Photosynthese und damit verbundenem höheren Stress die PsbS Expression verstärkt wird. Jedoch kann PsbS nicht die für das qE essentielle Funktion des LHCSR3 ersetzen. Die Analysen zur Wirkung verschiedener PsbS-Mengen im Vergleich mit dem Wildtyp zeigten folgende Änderungen bei erniedrigtem PsbS-Gehalt: (1) eine reduzierte qE-Kapazität, (2) eine vergrößerte PSII-Antenne im HL, (3) eine schnellere P700 Oxidation im HL, wenn LHCSR3 vorhanden ist, während die P700 Oxidation im LL verlangsamt ist, wenn LHCSR3 nicht vorhanden ist, (4) einen verstärkten zyklischen Elektronentransport in HL, (5) eine veränderte Organisation der Thylakoidmembran und (6) eine reduziert Fitness der Zellen in HL. Untersuchungen der Zellen mit einer Überexpression von PsbS zeigten, dass (1) PsbS während der HL-Akklimatisation verstärkt abgebaut wird, (2) mehr PsbS nicht zu einem höheren qE führt und (3) dass mehr PsbS die HL Resistenz und damit die allgemeine Fitness der Zellen unter HL-Bedingungen fördert. Diese Ergebnisse belegen, dass PsbS in *C. reinhardtii* nicht essentiell für die qE Kapazität ist – im Gegensatz zur Situation in Gefäßpflanzen – aber wesentlich zur Photoprotektion bei der HL-Akklimatisation beiträgt, (i) durch Reorganisation der Thylakoidmembran während der Aktivierung von qE und (ii) durch qE-unabhängige Mechanismen.

9 References

Adams III WW, Zarter CR, Mueh KE, Amiard V, Demmig-Adams B (2006) Energy Dissipation and Photoinhibition: A Continuum of Photoprotection. Photoprotection, Photoinhibition, Gene Regul Environ. doi: 10.1007/1-4020-3579-9_5

Alboresi A, Gerotto C, Giacometti GM, Bassi R, Morosinotto T (2010) *Physcomitrella patens* mutants affected on heat dissipation clarify the evolution of photoprotection mechanisms upon land colonization, Proc Natl Acad Sci, 201002873.

Allen JF (2017) Why we need to know the structure of phosphorylated chloroplast light-harvesting complex II. Physiol Plant **161**: 28–44

Allen JF, de Paula WBM, Puthiyaveetil S, Nield J (2011) A structural phylogenetic map for chloroplast photosynthesis. Trends Plant Sci **16**: 645–655

Allorent G, Lefebvre-legendre L, Chappuis R, Kuntz M, Truong TB (2016) UV-B photoreceptor-mediated protection of the photosynthetic machinery in Chlamydomonas reinhardtii. 1–6

Allorent G, Tokutsu R, Roach T, Peers G, Cardol P, Girard-Bascou J, Seigneurin-Berny D, Petroutsos D, Kuntz M, Breyton C, et al (2013) A Dual Strategy to Cope with High Light in Chlamydomonas reinhardtii. Plant Cell **25**: 545–557

Anderson JM (1992) Cytochrome b6f complex: Dynamic molecular organization, function and acclimation. Photosynth Res **34**: 341–357

Andersson B, Anderson JM (1980) Lateral heterogeneity in the distribution of chlorophyll-protein complexes of the thylakoid membranes of spinach chloroplasts. BBA - Bioenerg **593**: 427–440

Anwaruzzaman M, Chin BL, Li XP, Lohr M, Martinez DA, Niyogi KK (2004) Genomic analysis of mutants affecting xanthophyll biosynthesis and regulation of photosynthetic light harvesting in Chlamydomonas reinhardtii. Photosynth Res **82**: 265–276

Asada K (2006) Production and Scavenging of Reactive Oxygen Species in Chloroplasts and Their Functions. Plant Physiol **141**: 391–396

Avenson TJ, Cruz JA, Kanazawa A, Kramer DM (2005) Regulating the proton budget of higher plant photosynthesis. Proc Natl Acad Sci **102**: 9709–9713

Bailey S, Walters RG, Jansson S, Horton P (2001) Acclimation of Arabidopsis thaliana to the light environment: The existence of separate low light and high light responses. Planta **213**: 794–801

Ballottari M, Truong TB, Re De E, Erickson E, Stella GR, Fleming GR, Bassi R, Niyogi KK (2016) Identification of ph-sensing sites in the light harvesting complex stress-related 3 protein essential for triggering non-photochemical quenching in chlamydomonas reinhardtii. J Biol Chem **291**: 7334–7346

Barber J (2012) Photosystem II: The Water-Splitting Enzyme of Photosynthesis. Cold Spring Harb Symp Quant Biol **77**: 295–307

Bergantino E, Segalla A, Brunetta A, Teardo E, Rigoni F, Giacometti GM, Szabo I (2003) Light- and pH-dependent structural changes in the PsbS subunit of photosystem II. Proc Natl Acad Sci **100**: 15265–15270

Bonente G, Ballottari M, Truong TB, Morosinotto T, Ahn TK, Fleming GR, Niyogi KK, Bassi R (2011) Analysis of LHcSR3, a protein essential for feedback de-excitation in the green alga Chlamydomonas reinhardtii. PLoS Biol. doi: 10.1371/journal.pbio.1000577

Briantais JM, Vernotte C, Picaud M, Krause GH (1979) A quantitative study of the slow decline of chlorophyll a fluorescence in isolated chloroplasts. BBA - Bioenerg **548**: 128–138

Cardol P, Forti G, Finazzi G (2011) Regulation of electron transport in microalgae. Biochim Biophys Acta - Bioenerg **1807**: 912–918

Cavalier-Smith T (2000) Membrane heredity and early chloroplast evolution. Trends Plant Sci **5**: 174–182

Chaux F, Johnson X, Auroy P, Beyly-Adriano A, Te I, Cuiné S, Peltier G (2017) PGRL1 and LHCSR3 Compensate for Each Other in Controlling Photosynthesis and Avoiding

Photosystem I Photoinhibition during High Light Acclimation of Chlamydomonas Cells. Mol Plant **10**: 216–218

Choquet Y, Vallon O (2000) Synthesis, assembly and degradation of thylakoid membrane proteins. Biochimie **82**: 615–634

Correa-Galvis V, Poschmann G, Melzer M, Stühler K, Jahns P (2016) PsbS interactions involved in the activation of energy dissipation in Arabidopsis. Nat Plants **2**: 15225

Correa-Galvis V, Redekop P, Guan K, Griess A, Truong TB, Wakao S, Niyogi KK, Jahns P (2016) Photosystem II Subunit PsbS Is involved in the induction of LHCSR Protein-dependent energy dissipation in chlamydomonas reinhardtii. J Biol Chem **291**: 17478–17487

Danielsson R, Albertsson PÅ, Mamedov F, Styring S (2004) Quantification of photosystem I and II in different parts of the thylakoid membrane from spinach. Biochim Biophys Acta - Bioenerg **1608**: 53–61

Dekker JP, Boekema EJ (2005) Supramolecular organization of photosystem II in green plants. Biochim Biophys Acta - Bioenerg **1706**: 12–39

Demmig-Adams B (1990) Carotenoids and photoprotection in plants: A role for the xanthophyll zeaxanthin. BBA - Bioenerg **1020**: 1–24

Dinc E, Tian L, Roy LM, Roth R, Goodenough U, Croce R (2016) LHCSR1 induces a fast and reversible pH-dependent fluorescence quenching in LHCII in *Chlamydomonas reinhardtii* cells. Proc Natl Acad Sci **113**: 7673–7678

Drop B, Webber-Birungi M, Yadav SKN, Filipowicz-Szymanska A, Fusetti F, Boekema EJ, Croce R (2014) Light-harvesting complex II (LHCII) and its supramolecular organization in Chlamydomonas reinhardtii. Biochim Biophys Acta - Bioenerg **1837**: 63–72

Elrad D, Grossman AR (2004) A genome's eye view of the light-harvesting polypeptides of Chlamydomonas reinhardtii. Curr Genet **45**: 61–75

Engelken J, Brinkmann H, Adamska I (2010) Taxonomic distribution and origins of the extended LHC (light-harvesting complex) antenna protein superfamily. BMC Evol Biol. doi: 10.1186/1471-2148-10-233

Erickson E, Wakao S, Niyogi KK (2015) Light stress and photoprotection in Chlamydomonas reinhardtii. Plant J **82**: 449–465

Fan M, Li M, Liu Z, Cao P, Pan X, Zhang H, Zhao X, Zhang J, Chang W (2015) Crystal structures of the PsbS protein essential for photoprotection in plants. Nat Struct Mol Biol **22**: 729–735

Ferreira KN, Iverson TM, Karim M, Barber J, Iwata So (2004) Architecture of the Photosynthetic Oxygen-Evolving Center. **303**: 1831–1839

Green B, Pichersky E, Kloppstech K (1991) Chlorophyll a/b-binding proteins: an extended family. 181–186

Gururani MA, Venkatesh J, Tran LSP (2015) Regulation of photosynthesis during abiotic stress-induced photoinhibition. Mol Plant **8**: 1304–1320

Guskov A, Kern J, Gabdulkhakov A, Broser M, Zouni A, Saenger W (2009) Cyanobacterial photosystem II at 2.9-Å resolution and the role of quinones, lipids, channels and chloride. Nat Struct Mol Biol **16**: 334–342

Harris EH (2001) Chlamydomonas as a model Organism. Annu Rev Plant Biol **52**: 363–406

Havaux M, Porfirova S, Rey P, Do P, Eymery F, Porfirova S, Rey P, Dörmann P (2005) Vitamin E protects against photoinhibition and photooxidative stress in Arabidopsis thaliana. Plant Cell **17**: 3451–3469

Hervás M, Navarro JA, De La Rosa MA (2003) Electron Transfer between Membrane Complexes and Soluble Proteins in Photosynthesis. Acc Chem Res **36**: 798–805

Holzwarth AR, Miloslavina Y, Nilkens M, Jahns P (2009) Identification of two quenching sites active in the regulation of photosynthetic light-harvesting studied by time-resolved fluorescence. Chem Phys Lett **483**: 262–267

Horton P, Johnson MP, Perez-Bueno ML, Kiss AZ, Ruban A V. (2008) Photosynthetic acclimation: Does the dynamic structure and macro-organisation of photosystem II in higher plant grana membranes regulate light harvesting states? FEBS J **275**: 1069–1079

Hummel E, Guttmann P, Werner S, Tarek B, Schneider G, Kunz M, Frangakis AS, Westermann B (2012) 3D Ultrastructural Organization of Whole Chlamydomonas reinhardtii Cells Studied by Nanoscale Soft X-Ray Tomography. PLoS One. doi: 10.1371/journal.pone.0053293

Jahns P, Latowski D, Strzalka K (2009) Mechanism and regulation of the violaxanthin cycle: The role of antenna proteins and membrane lipids. Biochim Biophys Acta - Bioenerg **1787**: 3–14

Johnson X, Steinbeck J, Dent RM, Takahashi H, Richaud P, Ozawa S-I, Houille-Vernes L, Petroutsos D, Rappaport F, Grossman AR, et al (2014) Proton Gradient Regulation 5-Mediated Cyclic Electron Flow under ATP- or Redox-Limited Conditions: A Study of ATPase pgr5 and rbcL pgr5 Mutants in the Green Alga Chlamydomonas reinhardtii. Plant Physiol **165**: 438–452

Joliot P, Johnson GN (2011) Regulation of cyclic and linear electron flow in higher plants. Proc Natl Acad Sci **108**: 13317–13322

Kargul J, Nield J, Barber J (2003) Three-dimensional reconstruction of a light-harvesting complex I-photosystem I (LHCI-PSI) supercomplex from the green alga Chlamydomonas reinhardtii: Insights into light harvesting for PSI. J Biol Chem **278**: 16135–16141

Kosuge K, Tokutsu R, Kim E, Akimoto S, Yokono M, Ueno Y, Minagawa J (2018) LHCSR1-dependent fluorescence quenching is mediated by excitation energy transfer from LHCII to photosystem I in Chlamydomonas reinhardtii. Proc Natl Acad Sci **I**: 201720574

Kouřil R, Nosek L, Bartoš J, Boekema EJ, Ilík P (2016) Evolutionary loss of light-harvesting proteins Lhcb6 and Lhcb3 in major land plant groups - break-up of current dogma. New Phytol **210**: 808–814

Krause GH (1988) Photoinhibition of photosynthesis. An evaluation of damaging and protective mechanisms. Physiol Plant **74**: 566–574

Krause GH, Jahns P (2004). Non-photochemical Energy Dissipation Determined by Chlorophyll Fluorescence Quenching: Characterization and Function. In Chlorophyll a Fluorescence, G. Papageorgiou, and Govindjee, eds. (Springer Netherlands), pp. 463-495.

Krauß N, Schubert W-D, Klukas O, Fromme P, Witt HT, Saenger W (1996) Photosystem I at 4 A resolution represents the first structural model of a joint photosynthetic reaction centre and core antenna system. Nat Struct Biol **3**: 965–973

Kromdijk J, Katarzyna GL, Stéphane L, Masakazu TG, Niyogi I, Krishna K, Stephen P. L (2016) Improving photosynthesis and crop productivity by accelerating recovery from photoprotection. Science (80-) **354**: 857–861

Kruse O, Rupprecht J, Mussgnug JH, Dismukes GC, Hankamer B (2005) Photosynthesis: A blueprint for solar energy capture and biohydrogen production technologies. Photochem Photobiol Sci **4**: 957–970

Kubota-Kawai H, Burton-Smith RN, Tokutsu R, Song C, Akimoto S, Yokono M, Ueno Y, Kim E, Watanabe A, Murata K, et al (2019) Ten antenna proteins are associated with the core in the supramolecular organization of the photosystem I supercomplex in *Chlamydomonas reinhardtii*. J Biol Chem jbc.RA118.006536

Kühlbrandt W, Wang DN, Fujiyoshi Y (1994) © 19 9 4 Nature Publishing Group. Nature **367**: 532–8

Kukuczka B, Magneschi L, Petroutsos D, Steinbeck J, Bald T, Powikrowska M, Fufezan C, Finazzi G, Hippler M (2014) Proton Gradient Regulation5-Like1-Mediated Cyclic Electron Flow Is Crucial for Acclimation to Anoxia and Complementary to Nonphotochemical Quenching in Stress Adaptation. Plant Physiol **165**: 1604–1617

Li XP, Björkman O, Shih C, Grossman AR, Rosenquist M, Jansson S, Niyogi KK (2000) A pigment-binding protein essential for regulation of photosynthetic light harvesting. Nature **403**: 391–395

Li XP, Gilmore AM, Caffarri S, Bassi R, Golan T, Kramer D, Niyogi KK (2004) Regulation of photosynthetic light harvesting involves intrathylakoid lumen pH sensing by the PsbS protein. J Biol Chem **279**: 22866–22874

Li Z, Wakao S, Fischer BB, Niyogi KK (2009) Sensing and Responding to Excess Light. Annu Rev Plant Biol **60**: 239–260

Liguori N, Roy LM, Opacic M, Durand G, Croce R (2013) Regulation of light harvesting in the green alga chlamydomonas reinhardtii: The c-terminus of lhcsr is the knob of a dimmer switch. J Am Chem Soc **135**: 18339–18342

Malnoë A (2018) Photoinhibition or photoprotection of photosynthesis? Update on the (newly termed) sustained quenching component qH. Environ Exp Bot **154**: 123–133

Malnoë A, Schultink A, Shahrasbi S, Rumeau D, Havaux M, Niyogi KK (2018) The Plastid Lipocalin LCNP is Required for Sustained Photoprotective Energy Dissipation in Arabidopsis. Plant Cell **30**: tpc.00536.2017

Maruyama S, Tokutsu R, Minagawa J (2014) Transcriptional regulation of the stress-responsive light harvesting complex genes in Chlamydomonas reinhardtii. Plant Cell Physiol **55**: 1304–1310

McFadden G, Gilson P (1995) Something borrowed, something green: lateral transfer of chloroplasts by secondary endosymbiosis. Trends Ecol Evol **10**: 12–17

Mehler AH (1951) Studies on reactions of illuminated chloroplasts. II. Stimulation and inhibition of the reaction with molecular oxygen. Arch Biochem Biophys **34**: 339–351

Minagawa J, Takahashi Y (2004) Structure, function and assembly of Photosystem II and its light-harvesting proteins. Photosynth Res **82**: 241–263

Minagawa J, Tokutsu R (2015) Dynamic regulation of photosynthesis in Chlamydomonas reinhardtii. Plant J **82**: 413–428

Møller IM, Jensen PE, Hansson A (2007) Oxidative Modifications to Cellular Components in Plants. Annu Rev Plant Biol **58**: 459–481

Moseley JL, Allinger T, Herzog S, Hoerth P, Wehinger E, Merchant S, Hippler M (2002) Adaptation to Fe-deficiency requires remodeling of the photosynthetic apparatus. EMBO J **21**: 6709–6720

Nawrocki WJ, Santabarbara S, Mosebach L, Wollman F-A, Rappaport F (2016) State transitions redistribute rather than dissipate energy between the two photosystems in Chlamydomonas. Nat Plants **2**: 16031

Nelson N, Junge W (2015) Structure and Energy Transfer in Photosystems of Oxygenic Photosynthesis. Annu Rev Biochem **84**: 659–683

Nilkens M, Kress E, Lambrev P, Miloslavina Y, Müller M, Holzwarth AR, Jahns P (2010) Identification of a slowly inducible zeaxanthin-dependent component of non-photochemical quenching of chlorophyll fluorescence generated under steady-state conditions in Arabidopsis. Biochim Biophys Acta - Bioenerg **1797**: 466–475

Niyogi KK (1999) PHOTOPROTECTION REVISITED: *Genetic and Molecular Approaches*. Annu Rev Plant Physiol Plant Mol Biol **50**: 333–359

Ort DR, Zhu X, Melis A (2011) Optimizing Antenna Size to Maximize Photosynthetic Efficiency. Plant Physiol **155**: 79–85

Ozawa S, Bald T, Onishi T, Xue H, Matsumura T, Kubo R, Takahashi H, Hippler M, Takahashi Y (2018) Configuration of ten light-harvesting chlorophyll a/b complex I subunits in Chlamydomonas reinhardtii photosystem I. Plant Physiol pp.00749.2018

Ozawa SI, Onishi T, Takahashi Y (2010) Identification and characterization of an assembly intermediate subcomplex of photosystem I in the green alga Chlamydomonas reinhardtii. J Biol Chem **285**: 20072–20079

Pagliano C, Nield J, Marsano F, Pape T, Barera S, Saracco G, Barber J (2014) Proteomic characterization and three-dimensional electron microscopy study of PSII-LHCII supercomplexes from higher plants. Biochim Biophys Acta - Bioenerg **1837**: 1454–1462

Park Y II, Karlsson J, Rojdestvenski I, Pronina N, Klimov V, Öquist G, Samuelsson G (1999) Role of a novel photosystem II-associated carbonic anhydrase in photosynthetic carbon assimilation in Chlamydomonas reinhardtii. FEBS Lett **444**: 102–105

Peers G, Truong TB, Ostendorf E, Busch A, Elrad D, Grossman AR, Hippler M, Niyogi KK (2009) An ancient light-harvesting protein is critical for the regulation of algal photosynthesis. Nature **462**: 518–21

Petroutsos D, Tokutsu R, Maruyama S, Flori S, Greiner A, Magneschi L, Cusant L, Kottke T, Mittag M, Hegemann P, et al (2016) A blue-light photoreceptor mediates the feedback regulation of photosynthesis. Nature **537**: 563–566

Polukhina I, Fristedt R, Dinc E, Cardol P, Croce R (2016) Carbon Supply and

Photoacclimation Cross Talk in the Green Alga *Chlamydomonas reinhardtii*. Plant Physiol **172**: 1494–1505

Pospíšil P, Arató A, Krieger-Liszkay A, Rutherford AW (2004) Hydroxyl radical generation by photosystem II. Biochemistry **43**: 6783–6792

Puthiyaveetil S, Van Oort B, Kirchhoff H (2017) Surface charge dynamics in photosynthetic membranes and the structural consequences. Nat Plants **3**: 1–9

Rizzini L, Favory J-J, Cloix C, Faggionato D, O´Hara A, Kaiserli E, Baumeister R, Schäfer E, Nagy F, Jenkins GI, et al (2013) Perception of UV-B by the Arabidopsis UVR8 Protein. Science (80-) **332**: 9–12

Rochaix J-D (2001) Assembly, Function, and Dynamics of the Photosynthetic Machinery in Chlamydomonas reinhardtii. Plant Physiol **127 (4)**: 1394–1398

Rochaix J-D (2014) Regulation and Dynamics of the Light-Harvesting System. Annu Rev Plant Biol **65**: 287–309

Rochaix J (1995) CHLAMYDOMONAS REINHARDTII AS THE PHOTOSYNTHETIC YEAST.

Sacharz J, Giovagnetti V, Ungerer P, Mastroianni G, Ruban A V. (2017) The xanthophyll cycle affects reversible interactions between PsbS and light-harvesting complex II to control non-photochemical quenching. Nat Plants **3**: 1–9

Schleiff E, Becker T (2011) Common ground for protein translocation: Access control for mitochondria and chloroplasts. Nat Rev Mol Cell Biol **12**: 48–59

Schöttler MA, Toth SZ (2014) Photosynthetic complex stoichiometry dynamics in higher plants: environmental acclimation and photosynthetic flux control. Front Plant Sci **5**: 1–15

Shapiguzov A, Ingelsson B, Samol I, Andres C, Kessler F, Rochaix J-D, Vener A V., Goldschmidt-Clermont M (2010) The PPH1 phosphatase is specifically involved in LHCII dephosphorylation and state transitions in Arabidopsis. Proc Natl Acad Sci **107**: 4782–4787

Steinbeck J, Ross IL, Rothnagel R, Gäbelein P, Schulze S, Giles N, Ali R, Drysdale R, Sierecki E, Gambin Y, et al (2018) Structure of a PSI–LHCI–cyt b$_6$f supercomplex in *Chlamydomonas reinhardtii* promoting cyclic electron flow under anaerobic conditions. Proc Natl Acad Sci **115**: 201809973

Suorsa M, Jarvi S, Grieco M, Nurmi M, Pietrzykowska M, Rantala M, Kangasjarvi S, Paakkarinen V, Tikkanen M, Jansson S, Aro EM (2012) Proton Gradient Regulation5 Is Essential for Proper Acclimation of Arabidopsis Photosystem I to Naturally and Artificially Fluctuating Light Conditions. Plant Cell **24:** 2934-2948

Takahashi H, Clowez S, Wollman FA, Vallon O, Rappaport F (2013) Cyclic electron flow is redox-controlled but independent of state transition. Nat Commun. doi: 10.1038/ncomms2954

Takahashi H, Iwai M, Takahashi Y, Minagawa J (2006) Identification of the mobile light-harvesting complex II polypeptides for state transitions in Chlamydomonas reinhardtii. Proc Natl Acad Sci U S A **103**: 477–482

Telfer A (2002) What is β-carotene doing in the photosystem II reaction centre? Philos Trans R Soc B Biol Sci **357**: 1431–1440

Teramoto H, Ono T, Nakamori A, Minagawa J (2002) Light-Intensity-Dependent Expression of lhc Gene Family Encoding Light- Harvesting Chlorophyll-a/b Proteins of Photosystem II in Chlamydomonas reinhardtii. Plant Physiol **130**: 325–333

Tibiletti T, Auroy P, Peltier G, Caffarri S (2016) Chlamydomonas reinhardtii PsbS protein is functional and accumulates rapidly and transiently under high light. Plant Physiol **171**: pp.00572.2016

Tokutsu R, Minagawa J (2013) Energy-dissipative supercomplex of photosystem II associated with LHCSR3 in Chlamydomonas reinhardtii. Proc Natl Acad Sci U S A **110**: 10016–21

Triantaphylides C, Krischke M, Hoeberichts FA, Ksas B, Gresser G, Havaux M, Van Breusegem F, Mueller MJ (2008) Singlet Oxygen Is the Major Reactive Oxygen Species Involved in Photooxidative Damage to Plants. Plant Physiol **148**: 960–968

Umena Y, Kawakami K, Shen J-R, Kamiya N (2011) Crystal structure of oxygen-evolving photosystem II at 1.9 Å resolution. Nature **473**: 55–60

Vass I, Styring S (1993) Characterization of Chlorophyll Triplet Promoting States in

Photosystem II Sequentially Induced during Photoinhibition. Biochemistry **32**: 3334–3341

Wang Y, Stessman DJ, Spalding MH (2015) The CO_2 concentrating mechanism and photosynthetic carbon assimilation in limiting CO_2: How Chlamydomonas works against the gradient. Plant J **82**: 429–448

Weston E, Thorogood K, Vinti G, López-Juez E (2000) Light quantity controls leaf-cell and chloroplast development in Arabidopsis thaliana wild type and blue-light-perception mutants. Planta **211**: 807–815

Wood WHJ, MacGregor-Chatwin C, Barnett SFH, Mayneord GE, Huang X, Hobbs JK, Hunter CN, Johnson MP (2018) Dynamic thylakoid stacking regulates the balance between linear and cyclic photosynthetic electron transfer. Nat Plants **4**: 116–127

Yamamoto Y (2016) Quality Control of Photosystem II: The Mechanisms for Avoidance and Tolerance of Light and Heat Stresses are Closely Linked to Membrane Fluidity of the Thylakoids. Front Plant Sci **7**: 1–13

Zienkiewicz M, Ferenc A, Wasilewska W, Romanowska E (2012) High light stimulates Deg1-dependent cleavage of the minor LHCII antenna proteins CP26 and CP29 and the PsbS protein in Arabidopsis thaliana. Planta **235**: 279–288

Zones MJ, Blaby IK, Merchant SS, Umen JG (2015) High-Resolution Profiling of a Synchronized Diurnal Transcriptome from Chlamydomonas reinhardtii Reveals Continuous Cell and Metabolic Differentiation. Plant Cell **27**: 2743–2769

10 Acknowledgements